The development of a method to predict ship-bank interaction in real-time

A thesis presented for obtaining the degree:
"Master of Science in Marine Technology"
Specialisation: Ship Hydromechanics

Torben Helsloot

Graduation Commitee

Prof.dr.ir. R.H.M. Huijsmans
Dr.ir. H.J. de Koning Gans
Dr.ir. A.M. Talmon
Ir. E. Rotteveel
Ir. E. Bolt

Maritime and Transport Technology
Delft Univerisity of Technology
September 8, 2016

with the cooperation of
Deltares Rijkswaterstaat

ABSTRACT

Due to increasing marine traffic intensity on inland waterways the interaction between ships and banks is becoming more of a problem. Bank effects make ship manoeuvring more difficult and rivers need to be protected against ship-induced currents and waves. This thesis contributes to the development of a new method that simulates these ship-bank interaction effects in real-time. Such predictions are useful in for example manoeuvring simulation and navigation channel design.

The developed method represents a ship as a moving pressure field in a numerical model that solves the two-dimensional non-linear shallow water equations in the horizontal plane. An approximation for skin friction is included. The method passes numerical verification.

The computed flow field and interaction forces are compared with experimental results in various conditions, showing that the method performs well enough to be useful in the design of navigation channels and to make initial computations on flow fields beneath ships.

Modelling errors limit the applicable range of the method so that it is not ready to be used in a general manoeuvring simulator. Recommendations are made to improve the model so that in the future this can be achieved.

SUMMARY

The subject of investigation for this thesis is the interaction between ships and banks in shallow and confined waterways such as rivers and channels. This interaction occurs because the water that a ship displaces flows asymmetrically through the confined spaces between ship and bank. The asymmetry causes external forces and moments upon the ship, and the confined flow causes increased pressure and shear on banks and bed. External forces and moments complicate the manoeuvring of ships, which can lead to dangerous situations. Pressure and shear can speed up natural changes in morphology of rivers, which is often not desirable.

Because of increasing traffic intensity on inland waterways the adverse effects of interaction are becoming more of a problem. Real-time simulations are a valuable tool to assess this. For example real-time simulation of the external interaction forces can be used in manoeuvring simulators to test the capability of helmsman to safely navigate closely to river banks and at small under keel clearances.

Although there are multiple secondary effects that also influence manoeuvring in shallow and confined water, the objective of this thesis is to find a prediction method that can be used to assess the external sway force and yaw moment.

The development of the method begins with an investigation of the physics behind ship-bank interaction effects after which a review of possible methods that can predict them is done. During this review it becomes apparent that numerical methods that have previously been used to compute ship-bank interaction forces are either too computationally demanding to do real-time simulations, or cannot capture all the physical mechanisms (including free surface and viscous effects) that are required.

It is therefore decided to work on the development of a new method that is expected to provide a better assessment of interaction effects than the available ones. The method is 'new' in the sense that it has never been applied before to compute forces on a sailing ship.

The starting point of the development is an existing numerical solver called D-FLOW FM in which a rudimentary subroutine that represents a ship is already available. This solver solves the two-dimensional non-linear shallow water equations in the horizontal plane in which a ship is represented as a moving pressure field. The advantage of this model is that large scale viscous effects and the effect of free surface can be included while keeping computational requirements low.

The subroutine is improved and extended with an approximation of skin friction, so that lift and flow blockage, which are expected to be relevant, can be simulated. The subroutine is also verified by performing a convergence analysis on the sway force and yaw moment that it predicts. The verified method is then used to perform a validation study. During this validation study it is determined to what extent the developed modelling method is able to provide an accurate representation of the real world values that it is designed to predict. The study indicates in which cases the developed method is usable, and points out modelling errors in cases where it

is not. The performance of the model is not only studied for the interaction force and moment, but also for ship-induced velocity and pressure on bed and banks. In addition to experimental results, predicted interaction force and moment are also compared to the solution of an existing potential flow solver.

The method that has been developed in this thesis has passed numerical verification. To compute the interaction force and moment with sufficient numerical accuracy approximately 3400 grid cells are needed to represent the ship. The recommended time step is such that the ship crosses a grid cell in two steps at nominal speed.

The interaction effects predicted by the new method are equivalent to those predicted by the potential flow method in cases where free surface and viscous effects are not important to ship-bank interaction. This shows that the developed method is well usable as an alternative to time-domain potential flow codes. By taking into account the flow blockage between ship bottom and river bed in the NLSW model, the prediction of sway force at small under keel clearance has significantly improved. Besides performing better at small under keel clearances the new method is better suited to model complex river/harbour geometries, it can therefore be useful in the design of entrance and navigation channels. It can also be used to make initial computations on flow fields beneath ships sailing in narrow and confined waterways, which is useful to investigate ship induced erosion on river beds. Furthermore the results of the validation study indicate that the model predicts far field velocity and pressure with acceptable accuracy.

The model is simple enough to be suitable for real-time computations, depending on the size of the domain, requirements on numerical accuracy and available computation power.

Despite efforts to include skin friction at the sides of the ship, both the developed method and potential flow code fail to predict the right magnitude of yaw moment. In addition to the yaw moment it is found that other results do not always agree with experimental observations. In those cases the modelling errors that are most likely responsible for this discrepancy are pointed out.

In general the model does not perform well enough to be used in a manoeuvring simulation loop, the aforementioned modelling errors limit the applicable range and the ship-bank interaction moment cannot be predicted. Moreover requirements on the grid make it impossible for a ship to navigate a domain freely. However if the modelling errors that were addressed in this thesis can be resolved then the applicable range can be extended, and when the computational domains of ship and surroundings can be decomposed the requirements on the grid are lifted. It is therefore recommended to continue the development of the method so that in the future a coupling with a manoeuvring simulator can be achieved.

CONTENTS

on the cover: the official seal of the Delft University of Technology

LIST OF TABLES

LIST OF FIGURES

NOMENCLATURE

$\boldsymbol{\Delta}$	-	Laplace operator
$\boldsymbol{\nabla}$	-	Del operator
ν	m^2/s	Kinematic viscosity
ρ	kg/m^3	(Water) density
ζ	m	Local surface elevation
B	m	Ship breath
C_B	-	Ship block coefficient
Cf	-	Average skin friction factor
CF_{skin}	-	Uniform skin friction factor (D-FLOW FM parameter)
c_s	1/m	Ship bottom friction factor
d	m	Total local draught of a ship
dt	s	Time step
$Elder$	-	Elder's turbulence factor (D-FLOW FM parameter)
$\boldsymbol{f}$	m/s^2	3D external force vector
$\boldsymbol{F}$	m/s^2	Two dimensional body force vector
Fr_h	-	Froude depth number
Fr_{ukc}	-	Froude number based on under keel clearance
g	m/s^2	Gravitational field strength
h	m	Water depth
L	m	Ship length
$\boldsymbol{M}$	m/s^2	Two dimensional external force vector
N	Nm	Yaw moment due to ship-bank interaction
p	Pa	Local pressure
P	Pa	Hydrostatic pressure
p_a	Pa	Atmospheric pressure
r	rad/s	Yaw rate

Re_x	-	Reynolds number of flow beneath ship
$Smagorinksy$	-	Smagorinsky's horizontal turbulence factor (D-FLOW FM parameter)
T	m	Ship draught
t	s	Time
T_e	s	The time in which a moving pressure field passes over one grid cell
u	m/s	Local x-velocity component
$\boldsymbol{u}$	m/s	Local velocity vector
$\boldsymbol{u'}$	m/s	Local fluctuation of velocity around mean velocity
U_0	m/s	Ambient current velocity
ukc	m	Under keel clearance
$UniFrictCoef$	-	Uniform (Manning) bed friction coefficient (D-FLOW FM parameter)
v	m/s	Local y-velocity component
V_s	m/s	Ship forward speed
$Vicouv$	m^2/s	Uniform horizontal eddy viscosity (D-FLOW FM parameter)
$Vicuship$	m^2/s	Uniform viscosity beneath ship only (D-FLOW FM parameter)
$wall\_ks$	m	Wall roughness factor for partial slip (D-FLOW FM parameter)
X	N	Force in x-direction
Y	N	Sway force due to ship-bank interaction
y_b	-	Non-dimensional inverse distance to bank
y_{port}	m	Distance from midship to channel wall on port side
y_{star}	m	Distance from midship to channel wall on starboard side

PREFACE

With this report I conclude my Master of Science in Marine Technology at the Delft University of Technology. I would like to thank my professors, fellow students and employees at the TU Delft because they have enabled me to obtain this degree smoothly and have guided me away from problems. I also wish to express my thanks to all volunteers at S.G. "William Froude" and SMT, the student associations of Marine Technology that have fulfilled a valuable role during my studies.

The acid test for the MSc degree is of course writing a graduation thesis, a goal unattainable without outside help. Therefore I need to acknowledge the role of the members of my graduation committee, who have provided guidance, advice and were open to questions during the past months. Their presence on the front page of this report is well deserved.

I also wish to acknowledge Deltares, the research institute that provided not only a more than comfortable place for me to work, but also a financial contribution and a wealth of information. The employees and fellow graduate students at Deltares have been challenging and inspiring, and I owe some of them a word of thanks. Without Herman Kernkamp this thesis could not have been written; he has done all of the programming for me and has come up with valuable ideas on the ship implementation in the numerical model. Herman has also patiently corrected me every time my understanding of the flow model was wrong. Sander van der Pijl and Arthur van Dam have also helped me with the numerical model. As one of the few marine engineers at Deltares, Arne van der Hout was always open to questions and has provided useful input for my thesis. Lastly I would like to thank my supervisor Jurjen de Jong for arranging a place for me at Deltares and helping me throughout the graduation process.

Torben Helsloot

1 INTRODUCTION INTO SHIP-BANK INTERACTION

1.1 PROBLEM DESCRIPTION AND MOTIVE

This thesis treats the interaction between ships and banks in shallow and confined waterways. A sailing ship and a neighbouring bank interact because a flow of water accelerates in the confined spaces between ship, bed and bank. The asymmetric flow causes interaction forces and moments upon the ship that complicate manoeuvring. Moreover the bank and bed undergo the effects of waves and shear stresses induced by this flow.

The motivation to study this subject now is that the capacity of inland waterways to facilitate transport is becoming a bottleneck in the transport chain. Due to the ever-increasing demand for transport in the modern age, more and larger ships are navigating rivers and channels. It is hardly feasible to expand the navigable width, so that vessels will have to sail closer to the boundaries of waterways. Moreover larger ships will be sailing at small under keel clearances to maximise their loading capacity. Both these trends aggravate interaction effects. As a result interaction effects are becoming more of a problem both from the perspective of the marine engineer as well as the river engineer.

Another reason to investigate these effects now is simply because the possibilities are there to do it. In the past the making of sound predictions concerning the complex interaction flow between ship and bank was unattainable. In recent times scientific progress and ever-growing computation power have created better means to analyse complex problems like this and in this thesis these means are going to be investigated.

The presence of river banks and channel walls induces a time-varying external force and moment on vessels, which have to be counteracted by rudder action. This complicates manoeuvring and can lead to dangerous situations when the magnitude or sign of the external force and moment suddenly changes. In channels that have a more or less constant cross section an equilibrium rudder and drift angle are needed to keep the ship moving parallel to the channel wall. Most commonly a suction force occurs which pulls the ship closer to the bank, in combination with a bow-away moment. These effects are counteracted by a small drift angle directed toward the centre of the channel, so that lift neutralises the suction force. Additionally a relatively large rudder force is needed to compensate the bow-away moment induced by both the drift angle and bank effect.

The use of rudder just to keep a straight coarse means that less steering ability is available for manoeuvring. Real problems can occur when a ship encounters variations in waterway geometry and correspondingly changing interaction forces. A well documented example was found in [15] from which the following paragraph is quoted:

"A medium sized vessel with good manoeuvring qualities and strong engine power was approaching the port at a speed of 15 mph in quiet weather, calm sea, good visibility and an ebb current of 2 mph.

The draught was 6.5 metres. Sailing favourably with lights in line, the vessel suddenly started to yaw to starboard. In spite of the fact that strong port side rudder action was taken and an immediate manoeuvre was carried out with the propellers, the ship sailed further and further to starboard until she was right along the starboard harbour pier. Here the suction effect was felt again but this time from starboard, so that the ship veered to port, and, as this movement could not be changed, she finally became grounded."

Accidents and near accidents that can be attributed completely or partly to bank interaction are quite common. Either the ship's master misjudges or cannot account for the interaction effect because of its erratic nature combined with a loss of manoeuvring capacity.

Marine traffic is not the only party that undergoes adverse effects due to interaction. Rivers and channels also experience the influence of ships through waves and flow. Ship induced flow can lead to bed material being picked up and redistributed, affecting the navigable depth of the waterway. Waves caused by navigation can harm the stability of banks and be a potential threat to fishermen and other lifeforms that find themselves near the water. An extreme example is a fatal accident along the Nieuwe Waterweg in the Port of Rotterdam where two anglers were swept off their feet by the stern wave of a vessel [13].

The problem owner is Rijkswaterstaat. As the responsible institution for the main waterways of the Netherlands, Rijkswaterstaat is trying to improve the accessibility of waterways while keeping them safe. A long-term research project has therefore been set up in which Rijkswaterstaat, the TU Delft and Deltares[1] work together to provide practical solutions to current or anticipated problems by performing measurements, model tests and other research. The research program is called KPP (Knowledge of Primary Processes in) River Engineering. Within this project the subproject 'Durable Navigable Depth' aims towards predicting the dynamics of a waterway, innovating dredging and maintenance, and predicting the interaction between waterways and the vessels that navigate them. This research program does therefore not only encompass the effect that the presence of bank and bottom has on a ship, but also the reverse: how does the presence of ships affect the bank and bottom. The incentive behind predicting the aforementioned interaction between river and ship is that it will enable Rijkswaterstaat to make a better forecast of navigable depths and to predict the influence of adaptations in river geometry. It will also enable the assessment of navigability and safety for ships sailing in existing and hypothetical river topologies.

A good way of assessing safety is to determine the capability of helmsmen to navigate in real-life situations. This is preferably done in a simulation environment in which any kind of topology can be virtually created, and where the limits of what is safe and what is not can be looked for without causing actual accidents. In such a manoeuvring simulator many physical effects need to be modelled in real-time. Modern manoeuvring simulators are well capable of predicting the behaviour of ships in open water. In shallow and confined water however, many more physical mechanisms begin to play a role, which make the simulation a lot more complex.

[1]Deltares is an independent institute for applied research in the field of water, subsurface and infrastructure.

1.2 BACKGROUND ON MANOEUVRING IN CONFINED WATERS

A manoeuvring simulator in its simplest form assesses all the forces that act upon a single ship performing a manoeuvre, and predicts its future motion. These forces can be hydrodynamic forces but also external forces such as wind. The way a ship responds to the forces applied to it is expressed in manoeuvring coefficients, also known as hydrodynamic derivatives. These derivatives express the relation between a (time rate of) change of one of the ship's degrees of freedom, and the force or moment needed to achieve it. For example the manoeuvring coefficient $X_r = \frac{\partial X}{\partial r}$ expresses how the force in x-direction X changes when the yaw rate r becomes different.

In open water the hydrodynamic derivatives are not a function of position or water depth. A manoeuvring ship in confined water however, has a different behaviour than one in open water. The confinement of a waterway has several effects on a manoeuvring ship:

- The hydrodynamic derivatives are different in shallow water.

  Shallow water effects occur when the flow around a ship's hull is restricted by the presence of the bed. This causes squat[2] to increase resulting in a change in the submerged part of the hull, causing changes in manoeuvring behaviour. The influence of added mass, which plays an important role during manoeuvring, also changes. In shallow water induced acceleration of the fluid surrounding the ship is much different from deep water, simply because the bed restricts the flow.

- The hydrodynamic derivatives are affected by the narrowness of a channel.

  When a channel is narrow enough compared to the width of the ship it affects the hydrodynamic derivatives with respect to drift angle and angular velocity, as well as added mass and added mass moment of inertia. These effects were found to be non-negligible for channel widths smaller than 6 times the breath of a ship [10]. In [16] it was found that the lateral forces and yawing moments due to drift increased by a factor 2 in a narrow canal compared to open (shallow) water. In addition these coefficients show dependency on the off-centreline displacement within the same narrow channel. Which according to [27] can not always be neglected.

- Squat is aggravated and the ship is drawn towards shallower sections of the bed.

  Squat is of influence to a manoeuvring ship because it reduces the under keel clearance which has an effect on the interaction force and moment. It also changes the shape of the submerged part of the hull which influences the manoeuvring behaviour adversely, because the pivot point[3] moves backwards. [4]

- The presence of banks will introduce external forces and moments due to asymmetric flow.

  As mentioned earlier in this chapter the interaction forces and moments do not influence the manoeuvring characteristics of the ship itself, but they do have to be counteracted by

[2] Squat is the combination of sinkage, trim and heel caused by the flow around a vessel due to its own motion.

[3] The pivot point is the instantaneous point on the ship that has no sideways motion during turning. It is therefore the point about which a ship appears to pivot.

the rudder so that less manoeuvring capacity is left to steer the ship.

All of this implies that for a comprehensive description of hull forces in an inland manoeuvring simulator all the aforementioned phenomena need to be described. The hydrodynamic derivatives will need to be expressed as a function of local water depth and confinement, and the external ship-bank interaction forces will have to be known at any given time. These external forces become a dominant influence when a ship sails close to a river bank and/or at small under keel clearances. Therefore they will be the main interest during this study.

1.3 OBJECTIVES AND SCOPE

The objective of this thesis is to develop a method to predict ship-bank interaction phenomena fast enough for real-time simulation. The main goal is to predict the external sway force and yaw moment on a bare hull caused by ship-bank interaction. Additionally the influence of a ship on the banks will be assessed by predicting the flow field at the bed directly underneath a ship, and waves and currents around the vessel. In order to achieve this a number of sub-objectives have been formulated:

- Report on gained knowledge and insight in ship manoeuvring in shallow and confined water.
- Collect relevant experimental data.
- Investigate different options that are available to predict ship-bank interaction.
- Select the most promising prediction technique and develop a method based upon it.
- Apply the developed method and assess its effectiveness.

In this thesis the scope will be limited to only a subsection of the confined water effects mentioned in the previous section. In the remainder of this document only the sway force and yaw moment caused by interaction with the boundaries of the waterway will be investigated. The changes in manoeuvring characteristics of a ship as a function of the shallowness and narrowness of a waterway as well as squat effects will not be considered.

Ship-bank interaction forces are caused by a very complex interplay of physical processes which compels the need to make further limitations to the scope of this study. Heel, sinkage and trim (i.e. squat) will not be predicted nor be explicitly taken into account. All ships under consideration are towed, no propellers are present in any of the computations and their effect on the flow field is not accounted for. Moreover the ships under consideration do not have rudders or other lifting surfaces so their influence is absent. The effect of drift angles will also be left out of the investigation.

1.4 RESEARCH METHODOLOGY

The research that is reported in this document has been done in different phases, which are listed below:

- Literature research on shallow water manoeuvring
- Development of approach
- Literature research on approach
- Model development
- Verification
- Data collection
- Validation

The first literature study aims to provide insight in manoeuvring in shallow and confined waters. From this literature study it will become clear that ship-bank interaction forces are an important part of the many mechanisms that affect manoeuvring in shallow and confined water. A general insight on the processes involved in ship-bank interaction is obtained and several existing methods to predict them are looked into.

In order to develop an approach the existing methods are compared and discussed, during which it will become apparent that all of the existing methods have their shortcomings. It is therefore decided to work on the development of a new method that is expected to provide a better assessment of interaction effects than the available ones. This method is 'new' in the sense that it has never been used before to compute forces on a sailing ship. The method involves solving the depth averaged non-linear shallow water equations to compute ship-bank interaction effects.

A second literature research is done to get familiar with the method. The governing equations are derived and discussed as well as the simplifications that this method makes. Relevant publications are reviewed so that lessons can be learned from them.

Model development means that the method that has been chosen is applied to solve for ship-bank interaction. It is not feasible to develop an entirely new numerical model, such a project can take years. Therefore an existing numerical solver is adapted in such a way that it becomes usable for computing ship-bank interaction.

Verification is needed because during the model development phase changes were made to a numerical solver. The application of the solver has also changed so that now it solves for solution functionals that were not evaluated before. A new verification study makes sure that the computations can be trusted on numerical grounds, and if not, points in the direction of errors.

After the model has been developed and verified its validity should be demonstrated. A large amount of simplifications are made so that the solver is fast enough for simulation purposes, and all of those simplifications can harm the accuracy and applicability of the model. In this last phase of the research experimentally measured values are compared with outcomes of computation. The measured values have to be collected and interpreted before the comparison can take place, this happens during the data collection phase that precedes validation.

The structure of the report follows the listed order of research phases. In Chapter 2 the first iteration of literature study is described. Chapter 3 describes the development of approach. A second literature review on the non-linear shallow water equations and its application is done in

Chapter 4, which also encompasses model development. Verification of the developed method is performed in Chapter 5. In Chapter 6 the reader can find a description and analysis of the collected data upon which the validation is based which is described in Chapter 7. Conclusions and recommendations can be found in Chapter 8.

2 STATE OF THE ART

In this chapter the findings of publications relevant to ship-bank interaction will be discussed. The first section of this chapter will provide a general insight in ship-bank interaction. The second section discusses prediction methods. That section is divided into subsections for experimental research, mathematical formulations and numerical methods. These are the three main ways in which ship-bank interaction can be investigated.

Research so far has mainly focussed on manoeuvring in shallow water only, with bank effects neglected. Even though most towing tanks are itself a narrow channel very few studies have been done that actually investigate the influence of the narrowness of the channel. The ones that have sometimes only address the sway and yaw force induced by the presence of side walls, and sometimes take into account also the influence of channel walls on manoeuvring coefficients/hydrodynamic derivatives. That towing tank walls do affect manoeuvring comes forward for example when attempting to validate open water CFD results with manoeuvring coefficients found in a towing tank [31].

2.1 THE NATURE OF SHIP-BANK INTERACTION

The findings from earlier research are that a ship sailing off the (hydrodynamic) centre of a channel undergoes a sway force that is normally directed towards the nearest bank and a yaw moment that turns the bow away from that bank. Relevant parameters to ship-bank interaction effects are: [34]

- ship geometry
- draught
- water depth to draught ratio
- bank characteristics
- lateral ship-bank distance
- forward speed
- drift angle
- propeller loading
- rudder angle

The closer a ship is to the bank, the larger the forces are, this relationship is approximately proportional to the inverse of the distance between the ship and the bank [18]. In some previous

publications this distance is reported as the non-dimensional y_b.

$$y_b = \frac{1}{2}B\left(\frac{1}{y_{port}} + \frac{1}{y_{star}}\right) \tag{2.1}$$

Where y_{port} and y_{star} are the distances from midship to the port and starboard bank respectively. Note that they are opposite in sign.

There exists a distance called 'horizontal reach' at which the influence of a bank is no longer detectable. The distance at which no significant influence of the banks can be found shows dependency on the Froude depth number and was found to lie in between 6 and 8 times the breadth of a ship for Froude depth numbers between 0.15 and 0.7 [17].

When the distance to the bank is very small however, bank suction will turn into repulsion. This happens sooner when the under keel clearance is small.

Aside from the distance to the bank there are two more non-dimensional parameters that play a role in ship-bank interaction. The three parameters that play a role in the severity of interaction effects are:

- $Fr_h = \frac{V_s - U_0}{\sqrt{gh}}$ Froude depth number, larger is more severe.
- $y_b = \frac{B}{2}\left(\frac{1}{y_{port}} + \frac{1}{y_{star}}\right)$ Inverse distance from ship to bank, larger is more severe.
- h/T Under keel clearance, smaller is more severe.

In the more severe cases the behaviour of the external forces is highly non-linear [35]. This is already apparent from the earlier statement that bank suction can turn into repulsion. The interaction force and moment cannot be considered to be purely proportional to the square of forward speed, but tends to follow a higher power.

When the speed of the ship is near-critical a heavily non-linear behaviour is observed. The critical speed of the ship is the group velocity of waves in shallow water $\sqrt{gh}$. Near critical effects start at a Froude depth number of 0.85. At (near) critical speeds it has been observed in towing tanks that forces acting on a ship fail to reach a steady state, but rather oscillate periodically in time while the ship model generates solitary waves [5].

A prediction method is preferably based on the physics behind the problem. In the following paragraphs the physical mechanisms behind ship-bank interaction will be discussed. Insight in these mechanisms was distilled from literature but cannot be attributed to a specific publication. Because there is insufficient proof that these mechanisms are in fact the main cause of ship-bank interaction the following paragraphs should be considered as a working hypothesis.

The working hypothesis is that there are four main contributions to the ship-bank interaction effect:

- Bernoulli wave asymmetry
- Lift induced moment
- Flow blockage
- Bow wave asymmetry

Bernoulli wave asymmetry

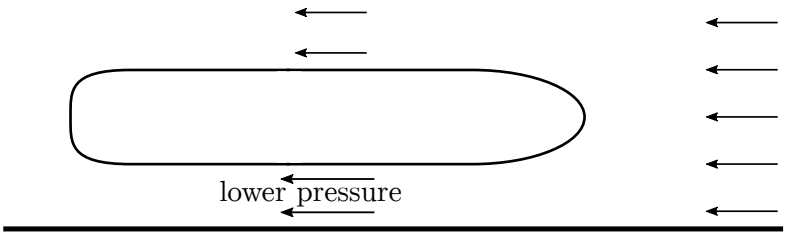

Figure 2.1: A sketch of the Bernoulli wave asymmetry

The Bernoulli wave is the name of the water level draw down that occurs due to the Venturi effect. As the ship moves through the water the fluid is set in motion travelling from bow to stern. This is called the return flow. The water that goes around the ship flows faster through the confined space between ship and bank. The higher velocity in that area results in a decrease in pressure causing a long wave along the length of the ship. The low pressure area causes suction towards the bank. Depending on the point of application this mechanism may also induce a moment. In Figure 2.1 the frame of reference moves along with the ship so that a uniform flow appears to approach the ship.

Lift induced moment

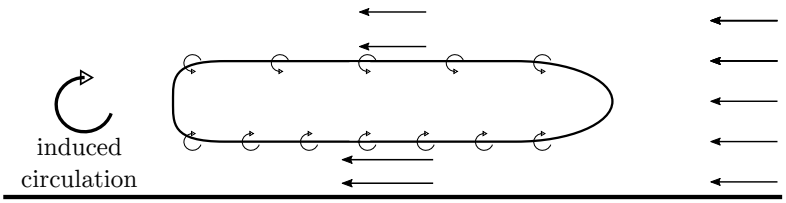

Figure 2.2: A sketch of the lift induced moment

Figure 2.2 shows a sketch of the lift induced moment, in this figure the frame of reference moves along with the ship. Along both sides of the ship skin friction induces vorticity into the flow. The flow is asymmetric so that the vorticity created at the bank side will be greater than at the channel side, creating circulation. This means that a moment has to have been applied to the flow, directed opposite to the direction of circulation. This is a bow-away moment.

A boundary layer forms along the sides of the ship due to the influence of friction. This layer will separate forming a turbulent wake behind the ship. The separated region is a low pressure area located at the aft ship and will probably lie slightly towards the side at which the velocity is higher, as is the case with wings. This separated region will contribute to the bow away moment as well.

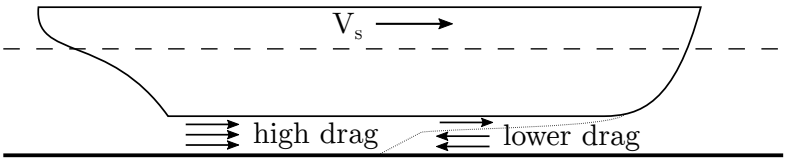

Figure 2.3: A sketch of the drag caused when the boundary layer of a ship hits the bed

Flow Blockage

In Figure 2.3 the ship moves with a velocity V_s through the water. Because of skin friction the ship experiences drag resistance. Water applies a force on the hull of the ship and the hull reacts with a force on the water. This causes some of the flow to be dragged along with the hull, slowing the return flow underneath and beside the ship down. At very small under keel clearances it may happen that the boundary layer underneath the ship touches the bed. In this case the flow beneath the ship becomes increasingly blocked causing flow speeds to reduce especially in the confined area between ship and bank. This may result in faster flow velocities and lower pressure at the channel side of the ship where the fluid can flow more freely. This explains why at small under keel clearances a repulsive force is observed.

The same thing may happen between the side of the hull and a channel wall, though it is less likely that a ship will sail close enough to a wall for the boundary layer to grow large enough.

Bow wave asymmetry

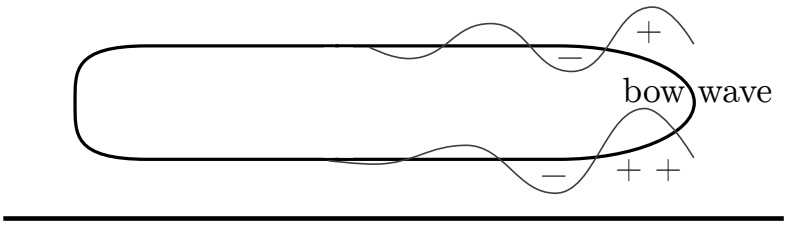

Figure 2.4: A sketch of bow wave asymmetry

In Figure 2.4 a sailing ship pushes a high pressure area in front of its bow which results in a bow wave. This high pressure area can act as a cushion when a ship is approaching a bank, turning the bow away. This is known as the bow cushioning effect.

When a ship sails parallel to a channel wall the bow may also be turned away by the bow wave. This happens because the bow wave needs to squeeze through the confined space between ship and bank. To do this it needs to become longer and/or higher in amplitude. The wave will also dissipate more quickly in the region between ship and bank.

The difference between the bow waves on either side will create a bow-away moment and possibly a force directed away from the bank. The smaller the confinement the greater this effect will be, and because the bow wave is greater at higher speeds and smaller under keel clearances these parameters might aggravate the effect.

When the effect of bow wave asymmetry becomes larger than the Bernoulli wave effect suction may turn into repulsion. This would explain the observed dependency on the distance to the bank, where initially suction increases linearly with the inverse of the ship to bank distance, but turns into repulsion for very small bank distances.

2.2 PREDICTING SHIP-BANK INTERACTION

2.2.1 EXPERIMENTAL FORMULATIONS

There are a small number of experimental formulations available to investigate the sway force and yaw moment caused by ship-bank interaction. Norrbin suggested expressions for a specific tanker model for vertical, sloping and flooded banks. Ch'ng proposed formulations based on tests with 2 ships for sloping banks. Li et al. published graphs showing the results for a tanker, ferry and catamaran. Their findings are summarised in [6].

A comprehensive test program of more than 10000 model test runs was performed by Flanders Hydraulics Research and the Ghent university with the purpose of obtaining more insight in ship-bank interaction. This enormous dataset has led to many papers discussing the forces and moments caused by the presence of banks as a function of many parameters. A preliminary regression model based on these test can be found in [35].

A more sophisticated model was developed in [17], in this paper the complex interrelation of bank and ship characteristics has been simplified to two parameters that exhibit an approximately linear relation to the resulting force and moment. The two parameters are an equivalent distance to bank, and an equivalent blockage parameter. These two parameters are expressed in influence functions, which assign a level of influence to the water between ship and bank. If water close to the ship is blocked the influence value will be larger than when water far away from the ship is blocked. In doing so a formulation is found that will work for arbitrary bank geometries, rather than having different formulations for sloped, straight, flooded and surface piercing banks. Furthermore it results in an unambiguous definition of 'distance to bank' that works equally well for straight banks as for sloped banks and does not depend on discrete points as was the case for other formulations.

Using the newly developed formulation, forces and moments caused by an arbitrary bank only need to be fitted using three ship dependent coefficients. This result is very satisfying because it implies that model tests done with one bank geometry can be extended to apply to any bank geometry. The model that was thus obtained is applicable when blockages are not too large (say, not in locks), and only works for sub-critical speeds. As mentioned earlier heavily non-linear effects start taking over at near-critical ship speeds.

Experimentally determined transient effects are rarely considered in literature when it regards simulation. In [16] it was found that transient effects while sailing through bend sections generate interaction forces up to 5 times the mean value found for standard cross sections. This influence was accounted for in a simulation by tabulating the moments and forces as a function of drift angle and position in the canal. This meant ship models had to be towed through a recreated version of the channel multiple times for each drift angle, direction of passage and then again for each ship model.

2.2.2 MATHEMATICAL FORMULATIONS

An alternative method to performing model tests is to model the physical problem theoretically and find analytical solutions. Theoreticians have previously had success within the field of ship manoeuvrability as the slender body theory has proven to be a good method to assess some of the manoeuvring coefficients of arbitrary hull shapes.

The problem of a ship sailing in a channel is interesting to solve analytically. However the impact of theory on this subject has so far been minimal [32]. For vertical canal walls the problem is mathematically equivalent to a mirrored image of the same ship. If then the free surface is also modelled as a rigid surface the ship can be mirrored along the horizontal plane as well. The latter assumption is often referred to as the double-body method and is valid as long as wave making effects are insignificant.

Two and three-dimensional solutions to slender and full bodies close to banks or in shallow and wide canals are given in [26]. To this end the method of matched asymptotic expansions is applied to a potential flow problem. The same method can also be applied to non-linear partial differential equations that describe wave motion such as the Korteweg-deVries or Kadomtsev-Petviashvili equations. These have been used in [5] to obtain forces and moments on a slender ship moving in a shallow canal at near-critical speed. Results showed good agreement to experimental results of calculated wave resistance. The force and moment however were not measured during those experiments.

In [3] a qualitative agreement with experimental data is found for the side force and yaw moment on a slender ship sailing in a canal with a linearised shallow-water solution.

2.2.3 NUMERICAL METHODS

Rather than finding analytical expressions for flow problems the differential equations and boundary conditions chosen to model the problem can also be solved with a numerical technique. Of course analytical and numerical methods are not mutually exclusive because every numerical method always has mathematical theory behind it, and any analytical solution must end in computations. What distinguishes this section from the previous is that here the literature is discussed that uses established numerical techniques or software to simulate ship-bank interaction problems. The methods that are discussed are solvers of potential flow and the Reynolds Averaged Navier-Stokes (RANS) equations.

Potential Flow

Because ship manoeuvring is a problem in which viscosity plays an important role it seems odd to compute with an idealised flow. However potential flow methods can be extended to comply with the Kutta condition by adding a vortex distribution or modelling the wake by imposing streamlines as in [25]. At low Froude numbers (when wave making is insignificant) good results can be obtained by modelling the free surface as rigid. The near-field interaction effect without a free surface is in many cases the dominant factor, which is illustrated by successful applications of double-body potential flow methods to compute interaction effects [19], [37]. These kinds of methods are fast enough to perform real-time computations, at least when accuracy requirements

are eased and the amount of panels reduced [22]. An interesting development here is the moving panelled patch method that can be used to keep the computational domain small by dynamically meshing the surroundings of the manoeuvring ship [39], [40]. Potential flow can also be applied in combination with free-surface computations, in [21] it was found that in cases with complex harbour geometries taking the free-surface into account was desirable.

RANS

Viscous effects can be accounted for by solving averaged forms of the Navier-Stokes equations. Doing this is computationally very demanding, but can also be very accurate[1]. Because of the computation power they require these kind of viscous solvers however are not, and will not be in the foreseeable future, able to make real-time calculations. However they have been successfully applied in the field of manoeuvrability by functioning as a numerical towing tank. It has been demonstrated that for deep water manoeuvring the results from RANS can compete in accuracy with model tests [30]. These RANS calculations can then be used to determine coefficients and trends that are usable in simulation software.

In [9] viscous and potential flow solvers with and without the effect of a free surface were applied to a ship-ship interaction problem in shallow water. This problem shows resemblance to the ship-bank interaction problem. The viscous results were promising but did not substantially differ from the potential flow solver. It was concluded that in this case the effect of free surface was more important than the effect of viscosity.

Experimental ship-bank interaction data for a standard hull (KVLCC2) was collected and this data has been used to validate results of Computational Fluid Dynamics (CFD) [33]. The conclusions are that viscous flow solvers perform much better than potential flow solvers when keel and bank clearance become small and speeds high. It was found that in many cases viscous effects can not be neglected. While in [41] the CFD calculations did not pass the formal verification and validation tests and modelling errors were reported, recent research [33] showed better results. Although computing bank effects with RANS calculations is challenging these papers show that viscous flow solvers can possibly achieve towing tank accuracy in the future.

[1] Relative to many other numerical methods. In some cases even relative to scale model tests.

3 DEVELOPMENT OF APPROACH

3.1 COMPARISON OF PREDICTION METHODS

In Chapter 2 many methods that have already been applied to evaluate interaction effects of ships in confined waters were discussed. Some of these methods might be more suitable than others to apply in a real-time manoeuvring simulation. In this chapter the methods will be compared and the most promising method will be chosen to be the subject of further investigation.

To be able to include a prediction method in the manoeuvring simulation loop the method must be fast. To some extent speed can be gained by increasing computing power, however there are limitations to this. Another requirement is that the prediction should be applicable to a wide range of situations, preferably any ship in any river or channel. Moreover a method that performs well at mild (small flow blockage, low speeds) as well as severe conditions is desirable.

A method that solves the flow field is valuable because it can be used to examine the related interaction effects such as erosion, which is of secondary interest in this thesis. These requirements are quite demanding, so concessions will inevitably have to be made.

3.1.1 EXPERIMENTAL PREDICTION

One of the options to predict ship-bank interaction is done by performing model experiments on which regression formulations can be based. This has two big advantages, firstly in such an experiment the physics can be reliably captured (set aside from scale effects) because all physical mechanisms will be present in a towing tank. Secondly the regression formulations are very suitable to be used in real-time simulation as they are easily computed.

Disadvantages of empirical approximations are that they can only cover the range of conditions that were experimentally tested, and transient effects are very hard to generalise. As a result developing such formulations asks for a very elaborate experimental program with hundreds of test conditions, which is costly and time consuming and therefore not a viable option for this thesis.

3.1.2 MATHEMATICAL PREDICTION

The second category of prediction methods mentioned in Chapter 2 are mathematical formulations. Although not many theoreticians have attempted to solve interaction problems analytically the ones that have were moderately successful especially those that used non-linear wave equations. However the mathematical assumptions that are made in these methods are too specific to allow for usage in a manoeuvring simulator. There are no mathematical models available that are able to predict all four mechanisms that were discussed in Section 2.1.

3.1.3 NUMERICAL: 3D VISCOUS FLOW

The remaining option to compute interaction forces is to use a numerical method. The big advantage of numerical simulation is that generalisation is very easy (although not necessarily always valid), any flow domain can in principle be discretised and computed. Another advantage of numerical methods is that they produce information about the flow field so that not only the forces on the ship can be determined, but also pressures and velocities that can be used to compute erosion.

The governing equations of fluid flow are so heavily non-linear that direct computation of a manoeuvring simulation problem is impossible even for the largest supercomputers in existence. To make the problem computable a popular approach is to use a RANS method, but even these solvers are not nearly fast enough to compute in real-time. Although detailed 3D viscous solvers should be able to capture all physical mechanisms discussed in Section 2.1 it appears from previous publications that predicting ship-bank interaction flows with RANS is very challenging even for CFD experts [41], [33]. Because of the high difficulty and slow computation speed it is not a realistic option to use a RANS solver during this thesis.

3.1.4 NUMERICAL: POTENTIAL FLOW

It is therefore preferred to look for a faster numerical method that is able to compute in real-time. This means that more drastic simplifications have to be made regarding the nature of the flow around a manoeuvring ship.

A possible simplification is to assume the flow to be irrotational and inviscid. Under this assumption the flow field can be described by a potential function, which is why the class of methods using this assumption are called potential flow methods. It is a widely used simplification in ship hydromechanics which has proven its value in predicting interaction forces and has already been applied successfully in real-time simulations [22].

Many potential flow solvers are based on the Boundary Element Method (BEM). The entire flow can be computed by solving only for elements on the boundary of the domain. Usually these elements are placed only on the hull of the ship, and the rest of the boundaries are incorporated using boundary conditions. This is the main reason why these solvers are so fast. In this thesis however, manoeuvring in shallow and confined water is considered, in which case the characteristics of bed and banks as well as the envelope of the free surface will be important. As a result these surfaces will also have to be covered in boundary elements (panels) which will significantly increase computation time.

Another reason why a potential flow method may not be as effective in solving ship-bank interaction problems is that it cannot capture all the physics behind it. The viscous effects of lift, separation and drag are probably going to be of influence at least in the more severe interaction cases. Although lift can be approximated by making use of the Kutta condition, the other two effects cannot be reproduced in an irrotational inviscid flow.

3.1.5 NUMERICAL: NON-LINEAR SHALLOW WATER FLOW

From the comparison of different methods so far it can be concluded that, within the scope of this thesis, a numerical method is preferable over an analytical or experimental method, but that the available methods of RANS and potential flow are respectively too slow or cannot capture the relevant physics. This is why in this thesis a new approach is suggested. This approach is based on the Non-Linear Shallow Water (NLSW) equations.

The most successful analytical predictions of ship-bank interaction were based on equations that are able to describe non-linear waves. Non-linear waves are likely to occur in shallow and confined water such as inland waterways. In the field of hydraulic engineering numerical solvers based on the NLSW equations are widely used to solve river flow. It might therefore be a good option to look for numerical solutions of this type.

As mentioned before it is inevitable to make far-going simplifications to the problem in order to be able to compute within real-time. In this case the assumptions will be that the water is shallow, and that the flow can be described in two dimensions. The first assumption is reasonable for flow in rivers, the second assumption can be justified by noting that when a ship sails with an increasingly small keel clearance the flow around the ship will increasingly become two-dimensional in nature. A two-dimensional flow is thus expected to provide a better approximation as the ship sails in shallower water.

There have been studies in the past that demonstrate the capability of this type of solver to compute ship induced waves as well as forces on berthed ships, more on this can be found in Section 4.1.

An advantage of the NLSW equations with respect to double-body flow is that free-surface effects are not neglected. Viscous terms also remain in the equations so that some large scale viscous effects may be modelled using this approach. There are multiple open-source solvers available that solve the NLSW equations, in which a river geometry can be easily modelled. This has the big advantage that a realistic inland waterway flow field can be included in the analysis. For these reasons a solver based on the numerical approximation of solutions to the NLSW equations may have the edge over a potential flow calculations especially in the more complex ship-bank interaction scenarios.

3.2 APPROACH: SOLVING THE NLSW EQUATIONS

Since the suggested method is novel, the current investigation will be explorative in nature. It may not be feasible to create a finished method within the scope of this thesis. However it should be possible to indicate whether using the NLSW equations to compute ship-bank interaction is potentially a good method, what the opportunities of it are and if further improvements are needed. This section describes the approach that is taken to investigate the modelling of ship-bank interaction using the NLSW equations.

The first step in the study will be to create a set-up with which a ship hull can be reliably included in an existing NLSW solver. The solver that is going to be used in this thesis is called D-FLOW FM, a new software engine for hydrodynamical simulations on unstructured grids which is

currently being developed by Deltares. Currently D-FLOW FM has a rudimentary implementation for ship induced flow.

The approach is to test, improve and verify this subroutine in order to create a simulation technique that can outperform existing potential flow codes. One part of this is adopting the right flow parameters and making the right modelling choices such as grid structure and time step. Another part of it is simulating the appropriate physical phenomena in the subroutine, for which the help of the programming department of Deltares is needed. Because the subroutine has not been extensively tested before and untested additions will be made to the code, it is necessary to perform verification of D-FLOW FM for this particular implementation.

Firstly a literature study is done concerning shallow water flow models and their governing equations in general and ship related implementations in particular to find out about previous attempts to model ship-induced flow in shallow water flow solvers. This study will provide insight in the difficulties and opportunities that were found by other authors using other numerical solvers. The lessons learned by these predecessors can be used to speed up the modelling process.

The most important physical phenomena that play a role in ship-bank interaction need to be included in D-FLOW FM in order to get the right solution. In Section 2.1 it was discussed which of them are expected to play are role. A big part of the model development is to try and simulate the physical mechanisms behind ship-bank interaction.

An iterative process of testing, trouble shooting and verification will lead to a properly working subroutine. The most important indicator for a working model is a convergent behaviour both in time and space.

When a sufficiently well working model is obtained it can be put to the test. Comparison with experimental data will show how effective the developed method is in predicting ship-bank interaction. The results from D-FLOW FM will also be compared with potential flow calculations. These calculations will be done using the ROPES package, a time-domain double-body potential flow solver designed to compute forces on berthed ships due to passing vessels [20].

Based on the outcomes of the comparison with experimental data and ROPES conclusions are drawn about the ability of the developed method to predict ship-bank interaction effects. It is established in which situations the developed method works well. Where numerical results deviate from experimental results it should be invesigated which modelling errors are responsible for it. Recommendations can then be made on how these modelling errors may be removed in the future.

4 MODELLING A SHIP IN THE NON-LINEAR SHALLOW WATER EQUATIONS

In this chapter the modelling of a ship in the NLSW equations is discussed. These equations are based on the Navier-Stokes equations, which are simplified by assuming that the characteristic horizontal length scale is much larger than the characteristic vertical length scale and that the characteristic vertical velocity is small in comparison to the characteristic horizontal velocity. There are several types of mathematical models available that are based on the NLSW equations. There are one, two and three-dimensional formulations which may use different coordinate systems depending on the type of problem and the geometry of the domain. The pressure in these equations is hydrostatic, however some models implement a correction to reconstruct a dynamic pressure.

The assumptions of shallow water as given in the previous paragraph have as a consequence that the momentum equation in the vertical direction reduces to the hydrostatic pressure distribution. This implies that vertical flow acceleration is small, which is true only for waves that are long in comparison to the water depth. Under the shallow water assumption the smaller flow structures around the hull of which the vertical scale is of the same order as the horizontal scale cannot be resolved. However, the main contribution to the interaction forces and moments is expected to originate from the large scale features of the flow for which the assumptions do hold. This justifies an attempt to solve the problem using a simplified model that is not going to be able to resolve the details of flow in the immediate vicinity of the ship.

Within this chapter an overview of previous attempts to model ships within the NLSW equations is presented in Section 4.1, a discussion of the governing equations for the mathematical model is given in Section 4.2 and the implementation of a ship within the mathematical model is treated in section 4.3. The simplified mathematical model that is going to be used in this thesis is a two-dimensional formulation in the horizontal plane (2DH).

4.1 PRIOR ART

In the past many studies have been performed to compute ship induced wave systems using the NLSW equations. Almost all of these methods model a ship by imposing a moving pressure field. In this section results from prior art will be presented along with the difficulties that were encountered during those studies.

The earliest implementations aimed at solving primary waves and currents induced by ships. In [14] a moving pressure field representation of a push-tow unit was implemented in a 2DH

model to investigate the effect of navigation induced currents on groyne fields. This study used an early version of the computational model DELFT3D-FLOW. A pressure correction iteration was applied near the shoulders of the vessel, this iteration makes sure that the water level at those locations stays equal to the draught of the ship even when waves interfere. To keep the representation of the vessel equal in each time step the ship was moved only one grid cell at a time, accordingly the time step needed to be adjusted to the vessel speed. The pressure field was gradually lowered into the water to avoid start-up waves, but they could not be avoided altogether. The vessel needed to be accelerated slowly to avoid large waves. In the ship's wake wiggles were observed which were reportedly damped out by supplying a very high eddy viscosity. Qualitative agreement was found between the moving pressure field method, other models and available data.

In another study a finite element method (FEM) scheme specifically designed to cope with flow fields with large gradients was applied to compute vessel-generated currents using the numerical solver HIVEL2D [28]. Reportedly a component was added to the FEM basis functions to control oscillations. Good agreement with experimental data was found except near the river banks.

The adaptive mesh flow solver ADH is also capable of computing vessel induced waves and currents [11]. This model automatically refines the mesh surrounding the vessel regardless of the path it takes. The time step is set such that the vessel moves a distance of one finite element length per time step.

In other publications the resolved wave field is used to compute forces on other vessels. In [38] the non-hydrostatic XBEACH model is used to predict ship-ship interactions. XBEACH uses a fine rectangular grid to represent the ship. The fine ship grid is interpolated to the coarser computational grid. An initial condition is used to prevent start-up waves as the pressure field is imposed. Inaccurate small scale oscillations were reported, but have not been filtered, as they were not expected to have an influence on the resulting forces. Computed interaction forces on a non-moving ship agreed well with experimental data.

In [8] a 2D hydrostatic finite difference model called VH-LU was used to evaluate passing vessel effects. The model works on a domain with moving boundaries that sail along with the vessel in order to reduce computation time. The moving vessel introduces ripples on the surface which are filtered by applying a mask throughout the domain at each time step. The model is able to represent measured ship induced water level fluctuations well, and reasonably estimates forces on berthed ships.

The aforementioned models have successfully demonstrated their ability to predict far field effects, i.e. the waves and currents at some distance from the moving pressure field. Computing forces on the moving vessel itself has proved to be more difficult. This may be because the assumptions of shallow water in the direct vicinity of the vessel become a bit shaky. In [2] a case study is presented in which current forces are computed on a non-moving moored ship using DELFT3D-FLOW. The method is the result of an elaborate capability study at Delft Hydraulics[1]. The numerical model solves a three-dimensional representation of the shallow water equations

[1]The former name of Deltares

using sigma layer modelling with hydrostatic pressure. Because flow separation is of importance an advanced (Horizontal) Large Eddy Simulation ((H)LES) turbulence model is applied to capture the large scale turbulent structures. The pressure loss due to the sudden expansion in flow area that occurs when the fluid has passed underneath the ship cannot be resolved accurately on a coarse flow mesh and is therefore accounted for by a correction based on the Borda-Carnot equation. The computational mesh was boundary fitted to the upstream side of the hull shape to achieve an accurate representation of its shape. The forces computed by this method were compared with experimentally determined force coefficients, but the method could not be validated.

In a continuation of this capability study it was shown that computed forces from a 3D model did not differ much from 2DH results, except for cases in which vortex merging took place. The study concluded also that the Borda-Carnot correction was superfluous. Using a barge to model an actual ship a good agreement with experimental results was found for larger under keel clearances, but the method significantly overpredicted the current forces at small under keel clearances.

A different approach to modelling a vessel is proposed in [23]. Rather than using a pressure field a non-moving barge is modelled by prescribing a water height at its location. This divides the flow field in an area with free surface flow and an area with pressurised flow. On these two domains a non-hydrostatic 2DH solution is found that agrees well with semi-analytical and experimental results, even in the near field of the non-moving barge. Because wave heights close to the barge were well predicted it is to be expected that interaction forces can be predicted using this method as well.

A number of difficulties were encountered in previous attempts to model ship related flow using the NLSW equations.

- Imposing a pressure field while the simulation is running will induce a large disturbance. The solution to this seems to be to include the ship in the initial conditions of the flow. Related to this is the acceleration of the ship hull, this needs to be done gradually to avoid large start-up waves.
- While the pressure field moves through the grid the discretisation changes in time if the ship is not displaced with a whole number of cells per timestep. This will cause slight changes in the discretised hull shape which can cause oscillations in the flow field. Some papers report using countermeasures to reduce spurious oscillations such as imposing a very high viscosity locally or special filters.
- It is difficult to model the right hull shape. Several techniques have been applied to get a better discretisation of a ship such as local mesh refinement, boundary fitting a curvilinear mesh to the hull shape and fine interpolation.

It has been shown that using a 2DH formulation can lead to good predictions regarding ship-induced waves and forces on berthed vessels. However computing forces on the sailing vessel itself has not been demonstrated convincingly yet. In the rest of this thesis an attempt will be made to calculate these forces using a two-dimensional model.

4.2 GOVERNING EQUATIONS

In this thesis the NLSW equations are used to solve the flow and waves in ship-bank interaction problems. The formulation that is used is a two-dimensional formulation in the horizontal plane (2DH model). The governing equations to such a mathematical model will be given in this section. Starting point for the derivation are the Navier-Stokes equations under the Boussinesq approximation[2].

$$\boldsymbol{\nabla} \cdot \boldsymbol{u} = \mathbf{0} \tag{4.1}$$

$$\frac{\partial \boldsymbol{u}}{\partial t} + (\boldsymbol{u} \cdot \boldsymbol{\nabla})\, \boldsymbol{u} = -\frac{1}{\rho_0} \boldsymbol{\nabla} p + \nu \boldsymbol{\Delta} \boldsymbol{u} + \boldsymbol{f} \tag{4.2}$$

Where in the absence of Coriolis force the external force vector $\boldsymbol{f}$ contains only the gravitational force $f_z = -\frac{\rho}{\rho_0} g$

The next step is to filter these equations either using a transient Reynolds averaging procedure or performing an LES filtering. This filtering is often done only implicitly due to numerical discretisation. The approaches differ conceptually but yield the same low-pass filtered equations (4.3).

$$\frac{\partial \overline{\boldsymbol{u}}}{\partial t} + (\overline{\boldsymbol{u}} \cdot \boldsymbol{\nabla})\, \overline{\boldsymbol{u}} + \left(\boldsymbol{\nabla} \cdot \overline{\boldsymbol{u}' \boldsymbol{u}'} \right)^{\mathsf{T}} = -\frac{1}{\rho_0} \boldsymbol{\nabla} \overline{p} + \nu \boldsymbol{\Delta} \overline{\boldsymbol{u}} + \boldsymbol{f} \tag{4.3}$$

An overline is used to distinguish a filtered quantity from a non-filtered one. The term $\overline{\boldsymbol{u}' \boldsymbol{u}'}$ contains an implicit transpose to yield a 3 by 3 matrix containing residual terms, which have to be closed by modelling turbulence. Depending on the type of model they are called either Reynolds stress or sub-grid scale stress.

In the following steps the assumption of shallow water is made. This assumption allows the momentum equation in the vertical direction to reduce to the hydrostatic pressure distribution, which can be integrated to Equation 4.4.

$$\overline{p} = g \int_z^{\zeta} \rho \, \mathrm{d}z + p_a \tag{4.4}$$

Substituting a hydrostatic pressure term P into the filtered Navier-Stokes equations reduces the system of three equations to Equation 4.5 and 4.6. In these equations the term containing molecular viscosity has been neglected because it is much smaller than the influence of residual stresses.

$$\frac{\partial \overline{u}}{\partial t} + \overline{u} \frac{\partial \overline{u}}{\partial x} + \overline{v} \frac{\partial \overline{u}}{\partial y} + \overline{w} \frac{\partial \overline{u}}{\partial z} = -\frac{1}{\rho_0} \frac{\partial P}{\partial x} + F_x + \frac{\partial}{\partial z} \left(\nu_V \frac{\partial \overline{u}}{\partial z} \right) \tag{4.5}$$

$$\frac{\partial \overline{v}}{\partial t} + \overline{u} \frac{\partial \overline{v}}{\partial x} + \overline{v} \frac{\partial \overline{v}}{\partial y} + \overline{w} \frac{\partial \overline{v}}{\partial z} = -\frac{1}{\rho_0} \frac{\partial P}{\partial y} + F_y + \frac{\partial}{\partial z} \left(\nu_V \frac{\partial \overline{u}}{\partial z} \right) \tag{4.6}$$

[2]The Boussinesq approximation states that if density variations are small it may be assumed constant except in the gravitational term.

The residual terms have been split into a horizontal and a vertical contribution. The scale of horizontal turbulent mixing is much larger than the vertical one, which induces the quasi-2D nature of turbulence in shallow water flow so that a distinction like this is justifiable. The parameter ν_V is the vertical eddy viscosity parameter. The vector $\boldsymbol{F}$ contains terms accounting for the horizontal residual stresses. These are filled by a turbulence model and could follow the eddy viscosity concept adopting a different eddy viscosity in the horizontal direction, but this depends on the chosen model. P is the hydrostatic pressure not necessarily[3] according to Equation 4.4. This term depends on the modelling choices. For a constant density and neglecting atmospheric pressure gradient it is $P = \rho g \zeta$.

The three-dimensional equations 4.5 and 4.6 are depth averaged resulting in the 2DH formulation. Averaging is done by integrating through depth, applying relevant boundary conditions at the free surface and bed.

$$\frac{\partial \overline{\zeta}}{\partial t} + \frac{\partial h \widetilde{\overline{u}}}{\partial x} + \frac{\partial h \widetilde{\overline{v}}}{\partial y} = 0 \tag{4.7}$$

$$\frac{\partial \widetilde{\overline{u}}}{\partial t} + \widetilde{\overline{u}} \frac{\partial \widetilde{\overline{u}}}{\partial x} + \widetilde{\overline{v}} \frac{\partial \widetilde{\overline{u}}}{\partial y} = -\frac{1}{\rho_0} \frac{\partial P}{\partial x} + F_x + M_x \tag{4.8}$$

$$\frac{\partial \widetilde{\overline{v}}}{\partial t} + \widetilde{\overline{u}} \frac{\partial \widetilde{\overline{v}}}{\partial x} + \widetilde{\overline{v}} \frac{\partial \widetilde{\overline{v}}}{\partial y} = -\frac{1}{\rho_0} \frac{\partial P}{\partial y} + F_y + M_y \tag{4.9}$$

Just as in Equation 4.5 and 4.6 these equations contain a vector of body forces that model the influence of viscosity and small scale turbulent motion ($\boldsymbol{F}$). Note that in the depth averaged equations this vector needs to be modelled differently than in the three-dimensional equations. Additional external forces have entered the equation via integration constants from the depth integration ($\boldsymbol{M}$). Examples of such forces are bed friction and wind stresses. The unknowns in Equation 4.7 to 4.9 are filtered depth averaged x-velocity $\widetilde{\overline{u}}$, filtered depth averaged y-velocity $\widetilde{\overline{v}}$ and filtered water level $\overline{\zeta}$.

4.3 MODEL IMPLEMENTATION

This section will discuss the way in which a ship is represented in the numerical model D-FLOW FM. The goal is to model the large scale effects that play a role in ship-bank interaction. Those effects were discussed in Section 2.1 and are repeated here:

- Bernoulli wave asymmetry
- Lift induced moment
- Flow blockage
- Bow wave asymmetry

[3] To model a ship for example, an additional moving pressure field will be imposed.

4.3.1 PRESSURE FIELD

To obtain the bow wave and Bernoulli wave the presence of the ship in the flow field needs to be modelled. A hull is modelled in D-FLOW FM by imposing a pressure field of magnitude $\rho g d(x, y)$ with d the local draught of the structure. In quiescent water this pressure field results in an indentation of the surface equal to the shape of the submerged part of the structure.

The pressure field is supplied to the program via a sample file that contains a grid of draughts that is preferably finer than the grid to which it is interpolated. Figure 4.1 shows the draught of a ship on a coarse grid coded by colour. Figure 4.2 shows a side view of the same ship in D-FLOW FM, the vertical lines divide grid cells, the horizontal lines can be seen as buttock lines. The provided pressure field can be given a time dependent position, simulating the movement of a hull through the water.

Because only one draught can be prescribed per grid cell, features such as a bulbous bow cannot be represented. There are a couple of possibilities to deal with this. One of them is to use the projection from above the ship, which removes the bulb all together. Another option is to use the projection from below the ship, so that the maximum draught is prescribed. Probably the best answer will be obtained if at each position the total amount of ship volume is removed from the flow by the pressure field. This method is applied during this study because it reduces the flow area in the 2D flow field by the right amount.

Figure 4.1: Pressure contours of a coarse pressure field.

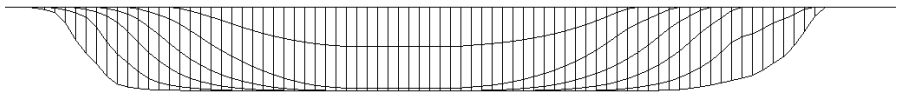

Figure 4.2: Side view of water indentation caused by pressure field.

Figure 4.3 shows a mesh plot of a sample file of a ships draught at high resolution. This ship has been smoothed in horizontal direction so that the moving pressure field in D-FLOW FM will not have any discontinuities in its direction of propagation. This makes sure that instabilities do not occur and consequently do not have to be damped.

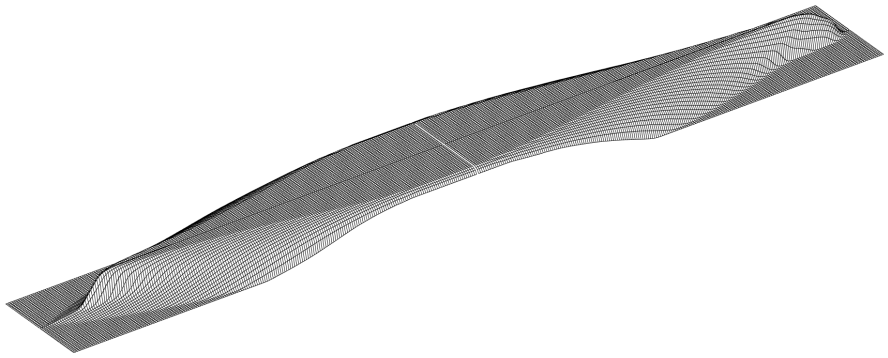

Figure 4.3: Mesh plot of ship definition file

4.3.2 SKIN FRICTION

An important mechanism that contributes to the bow away moment is lift. Lift is created because the side of the hull along which water flows fastest induces more vorticity than the other side. Vorticity is induced by skin friction creating a velocity gradient in the boundary layer. It is impossible to resolve the boundary layer given the time constraints in manoeuvring simulation, therefore the effect of friction is estimated directly by using a friction factor. Skin friction also exerts a drag force upon the flow which can cause a flow blockage beneath the ship when the under keel clearance becomes small. These effects are expected to be relevant to the ship-bank interaction problem and therefore D-FLOW FM is extended with a skin friction estimation.

There are two ways in which skin friction has been implemented in D-FLOW FM. Either a mean uniform friction factor is imposed over the whole hull, or a variable friction estimate is made. The uniform factor can be based on resistance estimates such as the ITTC 1957 correlation line [1]. Variable friction is implemented in D-FLOW FM by estimating the total shear stress per grid cell. This is done by using idealised analytical solutions for flat plates in a uniform flow. For each grid cell the local Reynolds number is used to determine a local friction factor that decides the amount of shear force that has to be applied to the flow. This formulation is a very rough estimate because the real flow conditions only weakly resemble a flat plate in a uniform flow.

The crude estimation is done as follows. The flow conditions beneath the ship are divided into four categories; laminar or turbulent unconfined flow and laminar or turbulent confined flow. When the local Reynolds number is lower than a predetermined transition number the flow is modelled as fully laminar, when it exceeds this number the flow is assumed turbulent. When the boundary layer thickness is smaller than the under keel clearance the flow is unconfined, when the boundary layer touches the bed the confined flow model is used. The boundary layer thickness is estimated based on the Blasius solution for a flat plate boundary layer.

In Figure 4.4 the described flow conditions are schematically depicted. In this figure the laminar unconfined flow corresponds to Region 1. To model the transition from laminar to turbulent flow the transition Reynolds number has to be supplied. When the local Reynolds number is

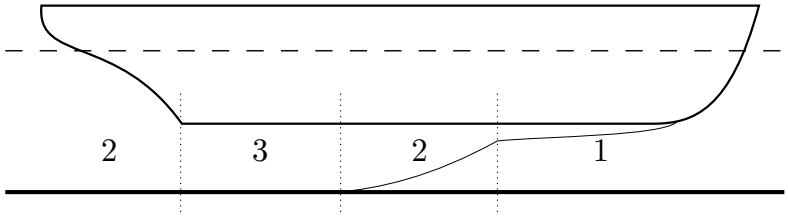

Figure 4.4: A sketch to illustrate the flow regions

lower than the transition point the laminar friction factor is applied, when it is higher the friction factor is based on the solution for turbulent flow. Region 2 is the turbulent unconfined flow which, as soon as the boundary layer comes in contact with the bed, turns into confined turbulent flow; Region 3. Laminar confined flow only takes place at very small keel clearances when the laminar boundary layer touches the bed. In the aft region of the ship where the clearance becomes larger the friction estimation switches back to turbulent unconfined flow.

For Region 1 the friction factor is estimated based on Blasius' solution for a laminar flat plate boundary layer, see Equation 4.10

$$c_s = 0.664 Re_x^{-\frac{1}{2}} \tag{4.10}$$

For Region 2 the friction factor is based on von Kármán's momentum integral theory for a flat plate boundary layer, see Equation 4.11

$$c_s = 0.027 Re_x^{-\frac{1}{7}} \tag{4.11}$$

In Figure 4.5 a validation of this approach is shown where the Schoenherr mean line for the resistance coefficient of flat plates is used for comparison. The numerical results where obtained with D-FLOW FM's ship subroutine by prescribing a rectangular plate with a 1 cm draught that is towed at different Reynolds numbers. The transition Reynolds number is between $3 * 10^5$ and $5 * 10^5$ for flat plates.

When the boundary layer coming from the bottom of the ship touches the river bed the flow conditions between keel and river bed become very different from the Blasius case. In this region the fully developed turbulent flow will probably show more resemblance to pipe flow. In this region therefore the estimation of the friction factor that is applied on the hull is based on flow between parallel plates. Analytical and experimental results for this case are given by [36]. Their formulations for laminar and turbulent flow between flat plates have been used, displayed in Equation 4.12 and 4.13 (Region 3) respectively.

$$c_s = \frac{24}{Re_x} \tag{4.12}$$

$$c_s = \frac{0.079}{Re_x^{0.25}} \tag{4.13}$$

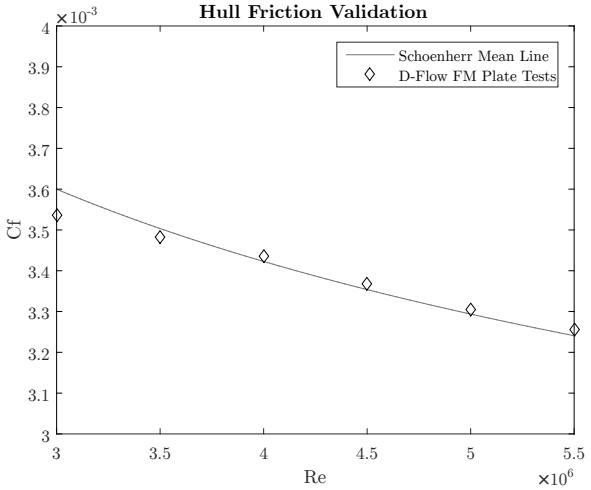

Figure 4.5: Validation of friction implementation against Schoenherr Mean Line

The four estimates for different types of flow are used to assign an estimated local Fanning friction factor to each grid cell below the ship's hull. An example of the friction distribution is displayed in Figure 4.6. In the displayed case a 3.8 m long 8000 TEU container carrier model sails with an under keel clearance of 4.5 cm at a speed of 0.25 m/s.

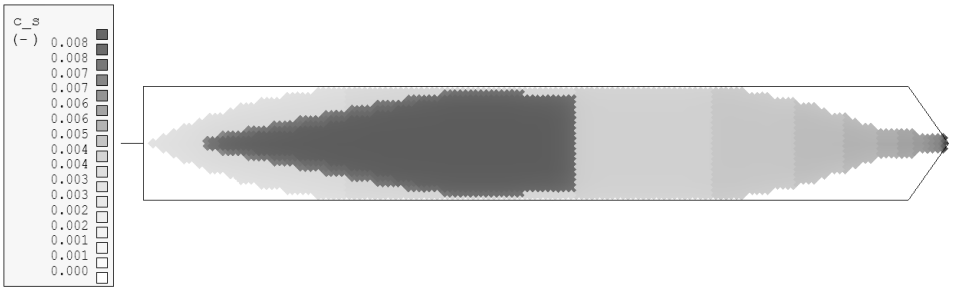

Figure 4.6: Local friction factor estimation

Note again that this is a very rough estimate, the flow conditions beneath the ship's hull will in reality be a lot more complex than the idealised flow between two flat plates. Moreover the hard transition between fully laminar and fully turbulent flow is unrealistic. The rough estimate however approximates the blockage of flow at small under keel clearances within the right order of magnitude so that the effect of this blockage on interaction can be simulated.

For each grid cell that belongs to the ship a friction factor is estimated based on the local Reynolds number. Also the hull area that this grid cell represents is calculated. The velocity at the previous time step is then used to determine the amount of friction that has to be applied to the flow, and the amount of friction resistance that this grid cell contributes. At the sides of the ship the hull area per grid cell is very high, so on these grid cells a larger friction is applied to the

flow. The high friction of the side walls brings the flow in circulation and thereby simulates the lift induced moment.

An example of vorticity created due to skin friction is displayed by means of a screenshot from D-FLOW FM in Figure 4.7. The black outline is a bounding box that only very schematically indicates the position of the ship and does not represent its shape.

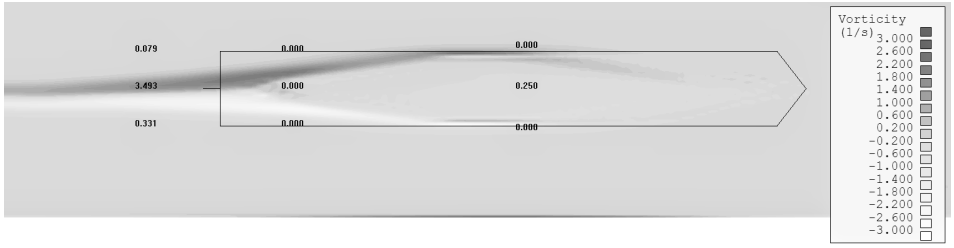

Figure 4.7: Vorticity introduced due to skin friction.

4.3.3 TURBULENCE MODELLING AND BED FRICTION

Aside from skin friction there are other viscous effects that play a role when modelling a ship sailing in shallow and confined water. Bed friction in D-FLOW FM is accounted for by empirical friction formulations. By using these formulations it is implicitly assumed that there is a fully developed velocity profile in the vertical. The Manning friction formulation that is used in the current implementation of the ship subroutine assumes a velocity profile that is a one-sixth power function of the water depth. This is invalid especially in the region near the ship.

In the case of a towing tank there are side walls that enclose the flow domain. In this thesis side walls have been present in every computation because the computations have to be compared to towing tank results. Side walls are closed boundaries in D-FLOW FM, for which a no slip or partial slip condition can be applied. The partial slip condition needs a specified Nikuradse roughness value to compute with. The shear stress is then calculated based on a logarithmic law of the wall.

The nature of turbulence in shallow water flows is quasi two-dimensional. This means that although the most important turbulent motion happens in the horizontal plane, the effect that vertical fluid motions have in reality cannot be disregarded. According to [29] the residual terms that result from the combination of filtering and depth averaging the Navier-Stokes equations can be divided into three parts. The mean horizontal flow experiences the effects of horizontal sub grid flow fluctuations, 3D mean motion and 3D sub grid turbulence. The effect of 2D sub grid flow fluctuations is preferably closed with an horizontal LES model, in D-FLOW FM currently only a Smagorinsky-type sub grid model is implemented.

The effect that unresolved 3D mean motion has on the flow is modelled with a constant background eddy viscosity. The last effect, that of small scale 3D turbulent motion is accounted for by Elder's term. This term accounts for the physical phenomenon of the reverse energy cascade that can be observed in shallow water flows, in other words, it transports energy back from small scale turbulence to larger scales.

Underneath the ship a uniform eddy viscosity can be applied, which is designed to suppress spurious oscillations caused by sudden changes in the moving pressure field. If possible this option should not be used.

5 VERIFICATION

5.1 INTRODUCTION

In this chapter it is verified that the developed model is able to provide a consistent output when given a certain input. This is done because the implementation of ships in D-FLOW FM is new. Changes have been made to the code to enable a ship to be represented, and computing forces on a pressure field which models a ship has not been demonstrated before. Therefore both the application of the moving pressure field method as well as the new parts of the code will have to be verified.

Verification is done to show that the results that are computed can be trusted on numerical grounds. D-FLOW FM has been used at Deltares for several years so the velocities and wave heights computed by it are assumed to have passed verification. In this section the computation of the interaction force and moment that act upon the ship will be verified by studying the temporal and spatial discretisation errors. Ideally the computed result is compared with an analytical solution, this cannot be done because such a solution is not readily available. Instead the solution of the potential flow solver ROPES is used. ROPES has been previously verified and validated so that when given the same problem under the same boundary conditions and assumptions, both models should arrive at the same answer.

The verification study will also provide information about numerical accuracy as a function of spatial and temporal step size. This information can be used to make a trade-off between computation speed and accuracy. This chapter will make clear that the developed model can solve the equations properly and show which numerical resolution is needed to provide an acceptable level of accuracy.

Computed Case

The case that is used for the grid refinement study is described in this section. In this case a model of a container carrier sails along a straight wall at a distance of 1 meter. The ship sails in 0.234 meter deep water with a speed of 0.3 m/s. The scenario is sketched in Figure 5.1.

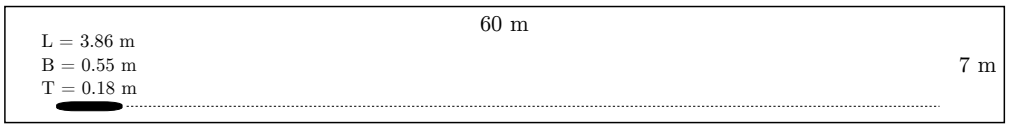

Figure 5.1: Plan view of the computed case

Property	Value
y_b (-)	0.314
Fr_h (-)	0.198
h/T (-)	1.30

This case is chosen because it is known that in these conditions ROPES is able to find a good answer for the interaction force, see Appendix A. In other words, in these conditions viscous effects do not play an important role[1]. These are rather mild conditions and therefore probably not the worst case for finding convergence. When less temperate cases are computed by D-FLOW FM and when viscous effects are going to be included, it should be kept in mind that the discretisation errors found in this chapter were determined for mild conditions. The numerical uncertainty of more complex calculations is probably going to be larger.

5.2 GRID REFINEMENT STUDY

5.2.1 INTRODUCTION

In this section a grid convergence study is done to determine an estimate of the discretisation error of the applied numerical method. The type of method that is used is a 2DH shallow water flow solver, often used within the field of hydraulic engineering. Convergence studies in general for 2DH solvers are not often done. This is because these codes adopt a high level of calibration to make up for the simplifications that the model applies. In practice coarse grids can provide acceptable answers with the right calibration parameters. The quality of the model is thus judged based on the correspondence with calibration data rather than verification and validation.

In hydraulic engineering practice, the whole procedure of creating the right grid with an appropriate fineness relies a lot on human insight and experience. This is another reason grid convergence is rarely studied, each refinement involves a lot of hand work. For the applications that 2DH solvers are traditionally used for however, there is some experience on how fine a grid should be in order to be able to generalise the results after calibration. This is not so much the case for the moving pressure field method. Therefore a convergence study is valuable.

As a grid is refined further and further the spatial discretisation error should approach zero. For manoeuvring simulation it will be necessary to do computations on a coarse grid, for which it is important to have an estimate of the numerical uncertainty. Knowing the uncertainty as a function of grid size enables a rational choice between numerical accuracy and speed.

The solution functionals for which the convergence study is done are the steady state interaction force and moment that is found when a ship sails in a straight line at a constant velocity along a bank with a constant cross-section. This is the time average of force and moment during a period of time in which the ship sails at stable conditions and transient effects have passed. These forces may still oscillate in time but their mean value around which they do is what is of interest.

5.2.2 FOLLOWED PROCEDURE

A coarse cartesian grid is refined in steps by halving the grid spacing each time. The coarsest grid used has a spacing of 0.1 m which means there are 212 grid cells to describe the ship. This grid is

[1]Except from lift related effects which will influence the yawing moment, as will be addressed in the remainder of this chapter

cumulatively refined locally in the region where the ship sails. To justify using a local refinement first the solution on a locally refined grid was compared to the one on a fully refined grid. The deviation between these two is negligible. This can be seen in Figure 5.2. In this figure the diamonds represent the solution on a grid that is refined throughout the entire domain, whereas the solid line is the solution on a grid that is only refined in vicinity of the ship. Judging from this result refining the grid only in the region around the ship is sufficient.

It can be observed from the graph that the measured force fluctuates. To get a good estimation of the mean value the average is taken over a whole amount of periods.

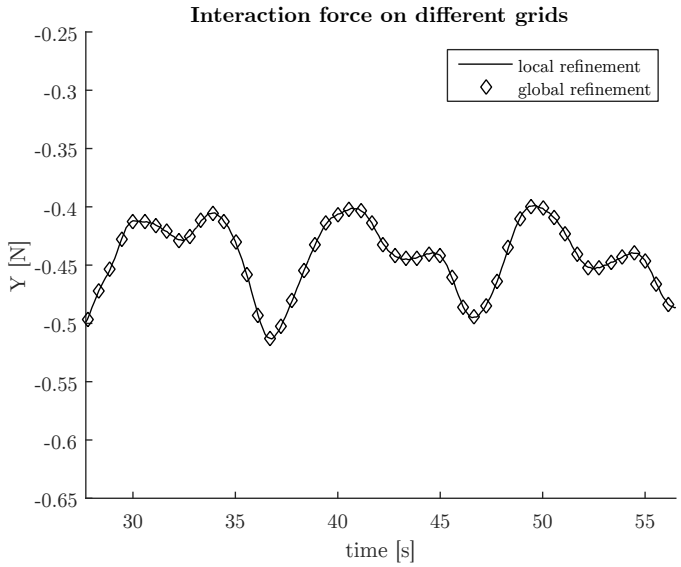

Figure 5.2: The solutions on a locally and a globally refined grid are identical

Parameter	Value	Description
dt (s)	$\frac{1}{36}$	Time step
$Vicouv$ (m/s)	0	Uniform horizontal eddy viscosity
$Smagorinsky$ (-)	0	Smagorinsky horizontal turbulence factor
CF_{skin} (-)	0.004	Hull skin friction coefficient

Table 5.1: Fixed parameters during grid convergence study

As was mentioned in the introduction there are a few numerical parameters that might hamper convergence because they are grid dependent. One of them is background viscosity, which gets a larger influence as the grid size decreases. Background viscosity has been set to zero for the convergence study. In fact, almost all of the turbulent influences have been disabled in the model.

On top of making sure that none of the modelling parameters are grid dependent, turning off viscous influences also causes the problem to become similar to the potential flow model in ROPES, which is going to be used for comparison.

The same level of hull smoothing was applied to all of the grids, even though more smoothing may be helpful for the coarser grids. The time step has been kept equal in all of the computations as well, the influence of the time increment is separately considered in Section 5.3. The important parameters used in the convergence study are displayed in Table 5.1

The coarsest grid is not refined locally. For the finest grid four cumulative levels of refinement have been applied, so that the grid spacing ranges from 10 cm to 0.625 cm. In Figure 5.3 an overview of the tank with a 1.25 cm grid spacing is displayed. For this calculation three levels of refinement are applied. Only half of the tank length is refined, this is because transient effects after acceleration are gone after the ship has travelled a relatively short distance. Therefore the ship needs to travel less than half a tank length to reach steady state. The tank itself cannot be much shorter however because otherwise the soliton wave created during the acceleration phase will reflect too soon and disturb the ship.

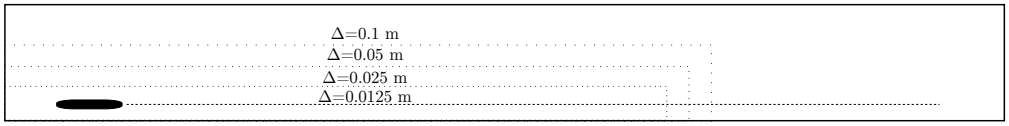

Figure 5.3: Three levels of refinement

To obtain convergence it is important that the ship is always interpolated symmetrically with respect to each of the grids. If this is not the case the asymmetry of the interpolated hull will pollute the results. The hull shape is provided on a very fine mesh which is interpolated to the coarser computational grid. The provided hull shape is smoothed by three accumulative moving average filters with a small span. This type of smoothing makes sure that discontinuities are removed while retaining the important features of the ship.

In Figure 5.4 the computed instantaneous suction force is plotted for different grid spacings. During the acceleration phase there are wiggles present. These wiggles have a period of $\frac{3}{8}$th of a second which is equal to the sample rate of the file in which the ships velocity is specified. They are caused by the discontinuities in the prescribed velocity.

After the acceleration phase has passed a smoother curve is obtained that still contains oscillations. The wiggles that occur with a 0.05 m grid spacing have a period of $\frac{1}{3}$rd of a second, which is twice the period at which the ship encounters grid cells. These wiggles are probably related to coarse pressure field interpolation. This theory is strengthened by the fact that the coarsest mesh (0.1 m) has very high amplitude wiggles with the same frequency. This is not displayed in the graph because it would obfuscate the other lines.

5.2.3 GRID CONVERGENCE: INTERACTION FORCE

As is apparent from Figure 5.4 the force in y-direction converges. This can better be seen in Figure 5.5, which shows the convergence behaviour of the mean side force. The result of the largest grid spacing falls outside the asymptotic range. The three finest grids fall within the asymptotic range

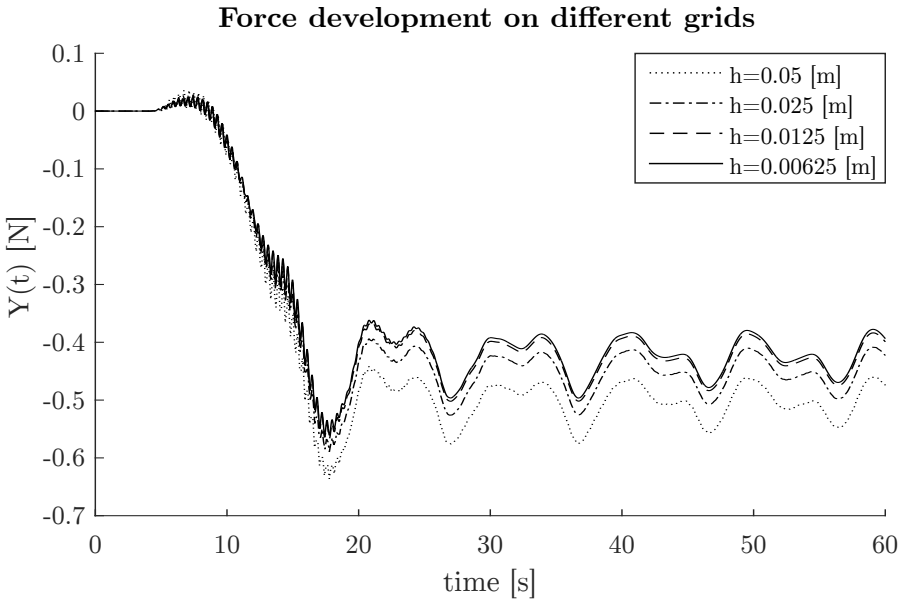

Figure 5.4: Development of Y computed on coarse and fine grids

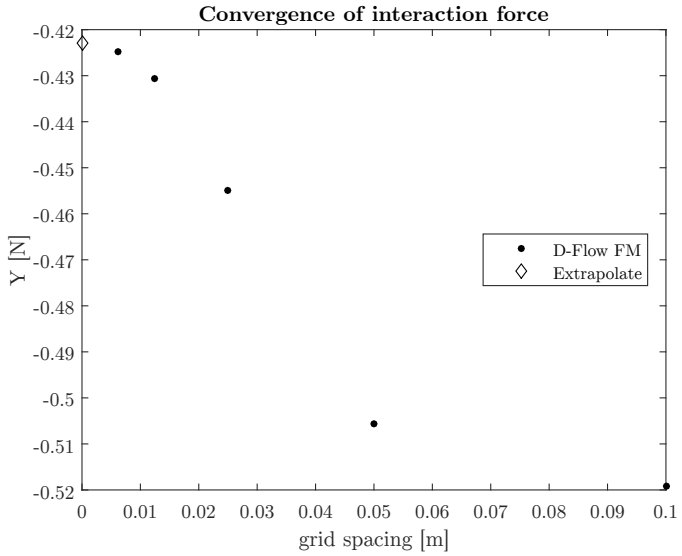

Figure 5.5: Convergence behaviour of Y

and are used to find an improved estimate of the analytical result to the problem. This is done by using Richardson Extrapolation.

The errors shown in Table 5.2 are calculated with respect to the extrapolated value because there is no analytical solution to compare with. The reported errors are an estimate for the actual spatial discretisation error.

The variance of the force is reported in the table as well, it is meant to provide an indication

Grid Spacing [m]	Cells for ship	Mean [N]	Variance [N]	Error [%]
0.1	212	-0.5191	$4.493E-2$	22.7
0.05	850	-0.5055	$1.247E-3$	19.5
0.025	3400	-0.4549	$1.006E-3$	7.54
0.0125	13601	-0.4307	$1.008E-3$	1.82
0.00625	54405	-0.4248	$1.022E-3$	0.42

Table 5.2: Convergence details for Y

Method:	Vantorre's Regression	ROPES	D-FLOW FM
$\boldsymbol{Y}$ **[N]:**	-0.400	-0.418	-0.423

Table 5.3: Predicted values of Y

as to how well the periodic behaviour converges. The coarsest grids have a very high variance which indicates the solution is polluted by wiggles. The finer grids have almost equal variance caused by the physical oscillations in suction force.

The extrapolated value to which the other results are compared is -0.423 Newton. When it is assumed that D-FLOW FM solves the problem without any other error than the discretisation error then this extrapolated value is an estimate to the analytical result of the problem that is being modelled. The problem that was modelled is very similar to one of the problems solved with ROPES in Appendix A. However there are a number of differences between the two models that may cause the results to differ:

- D-FLOW FM calculates with free surface effects included where ROPES adopts the double-body simplification.
- D-FLOW FM is unable to enforce the same no penetration boundary condition that ROPES does at the ship's hull.
- D-FLOW FM calculates with a small skin friction where ROPES neglects all friction.

It has already been established that the viscous and free surface effect are small in this case because ROPES provides a good answer compared to experimental results. It would be nice if the inability to properly enforce the boundary condition only has a small effect on the solution. When this is the case, the solution from the potential flow calculation and from D-FLOW FM will be very similar.

It appears that this is the case. ROPES predicts an interaction force of -0.418 Newton. This only differs 1.12% from the extrapolated result found by D-FLOW FM, which allows the conclusion that the method of modelling is valid, at least for the case considered here. It should be noted that the discretisation error for the ROPES calculation has not been formally considered, though it should be small. Table 5.3 summarises the predicted interaction force for this case by experimentally determined regression (see Section 6.3), the potential flow calculation and the moving pressure field method in the 2DH shallow water model.

Grid Spacing [m]	Cells for ship	Mean [Nm]	Variance [Nm]	Error [%]
0.1	212	0.1466	$2.258E-3$	17.8
0.05	850	0.1578	$1.351E-3$	11.5
0.025	3400	0.1768	$1.561E-3$	0.90
0.0125	13601	0.1803	$1.682E-3$	1.06
0.00625	54405	0.1761	$1.716E-3$	1.29

Table 5.4: Convergence details for N

5.2.4 GRID CONVERGENCE: INTERACTION MOMENT

Figure 5.6 shows the computed interaction moment on grids of different sizes. The largest grid size is too large for the solution to be within the asymptotic range. The finer grids seem to converge, however the answer on the finest grid deviates from the expected monotonically increasing behaviour. This may indicate that something is wrong, however the differences between the three finest grids are only 2.5 percent, so probably it is something small. It can possibly be attributed to differences in numerical diffusivity on different grids, the artificial viscosity is likely to have some influence on the lifting moment.

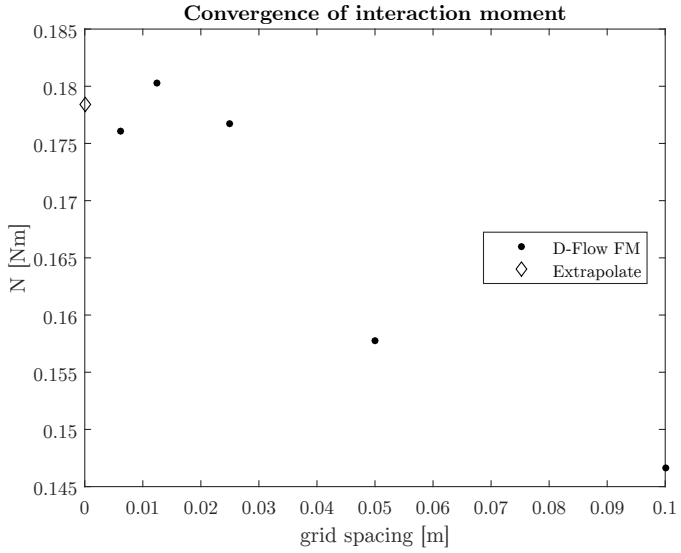

Figure 5.6: Convergence behaviour of N

The same procedure is followed as with the side force to get to the Richardson Extrapolate, although it is not strictly applicable because the points are not monotonically increasing. Table 5.4 summarises the results. The fact that the middle grid has received the lowest error is counter intuitive, it is due to the fact that the estimation of the answer at 'zero grid spacing' is bad.

It was mentioned in the previous section that the simplifications made in ROPES (and in D-FLOW FM for this particular calculation) still allow for a somewhat accurate calculation of the side

Method:	Vantorre's Regression	ROPES	D-FLOW FM
***N* [Nm]:**	1.713	0.135	0.178

Table 5.5: Predicted values of N

force. For the yawing moment this is not true as can be deduced from Table 5.5. The yawing moment in the tested case is expected to be influenced by the point of application of the Bernoulli wave and the lift induced moment. Lift is a viscous effect that is created by friction at the sides of the ship's hull.

In the current calculation viscous effects have been deliberately excluded, this is probably the reason why the moment is not predicted well. That D-FLOW FM predicts some 30% more lift might be explained by the skin friction that was applied and may partly be because the solver has more numerical diffusion.

5.2.5 GRID CONVERGENCE: RESISTANCE

Although not of primary interest of this report, the pressure force in x-direction is interesting to consider. It will be of help to verify the solution technique. In Figure 5.7 it can be seen that the pressure resistance converges only very slowly. The order of convergence is only a little under 1.25, which is too small for the computed resistance to be reliable.

This indicates that something is wrong with the model. In the next section the problem will be exposed when time step convergence is considered.

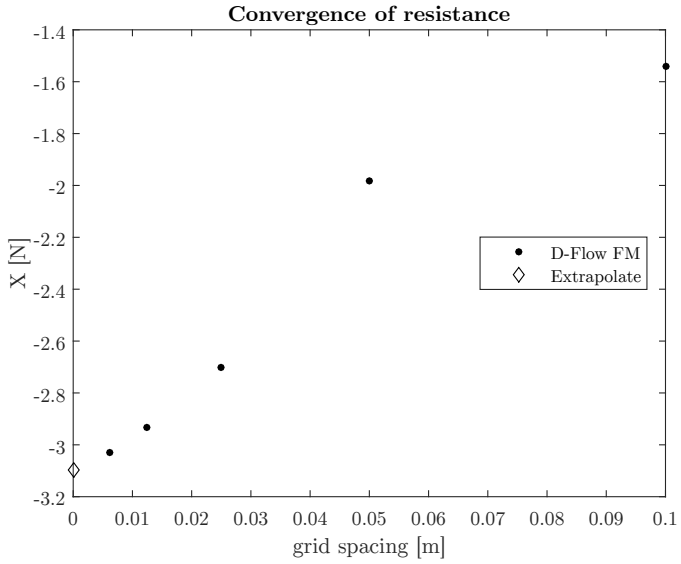

Figure 5.7: Convergence behaviour of the pressure resistance

5.3 TIME STEP CONVERGENCE

The discretisation error consists of two components; the spatial discretisation error was discussed in the previous section, while this section investigates the numerical error arising from the discreteness of the time step. The procedure to do this is simple, the same calculation is run several times with decreasing time step and the way the results change says something about the accuracy of the numerics. The calculations are done with a grid spacing of 2.5 centimetres, the middle grid size from Section 5.2.

For a fair comparison it is made sure that each of the time steps are chosen such that they are a whole fraction of the frequency at which the ship encounters grid cells. In the largest time step the ship moves a whole grid cell per step. Since the grid size is 2.5 centimetres and the ship sails at 0.3 metres per second, this amounts to a time step of $\frac{1}{12}$th of a second. The smallest time step is $\frac{1}{96}$th of a second, so that the ship needs exactly 8 steps to move to the next grid cell.

The reason that this is done is because of interpolation. The shape of the hull is prescribed at a high resolution (see Figure 4.3), but approximated by interpolating it to the coarser grid at a lower resolution. As a result the pressure field approximates the hull shape as closely as possible at any given time, but also differently depending on the relative position to the grid. This is illustrated in Figure 5.8 where a coarse grid is used to exemplify the difference in interpolation when the pressure field moves across a grid.

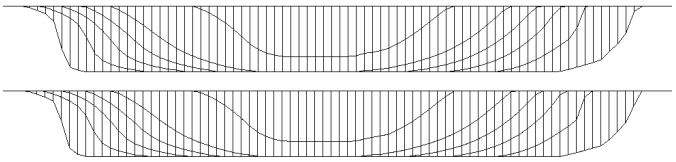

Figure 5.8: A ship interpolated slightly differently because it moved along a grid cell

When the ship moves an entire grid cell each time step this problem does not occur. The interpolation is the same each time. When the ship takes 8 steps to cross a cell there will be 8 slightly different versions of the ship which cycle at a frequency of $\frac{1}{12}$th of a second. If the time step is not a whole fraction of the grid cell encounter frequency, the greatest common divisor between them will be larger which induces lower frequency oscillations in the shape of the ship.

The oscillations in ship shape will cause oscillation in the flow field, and therefore oscillations in the pressure distribution. It will be shown in the rest of this section that this affects the computed forces.

Figure 5.9 and 5.10 show the convergence in the time domain of the interaction force and moment respectively. The graphs show the computed time average quantity as a function of time step. The time scale has been non-dimensionalised with respect to the period at which the ship encounters new grid cells, which is $\frac{1}{12}$th of a second in this case. The difference between the largest and smallest time increment does not exceed one percent in both these graphs. The relative independence of the solution on the time step is satisfying.

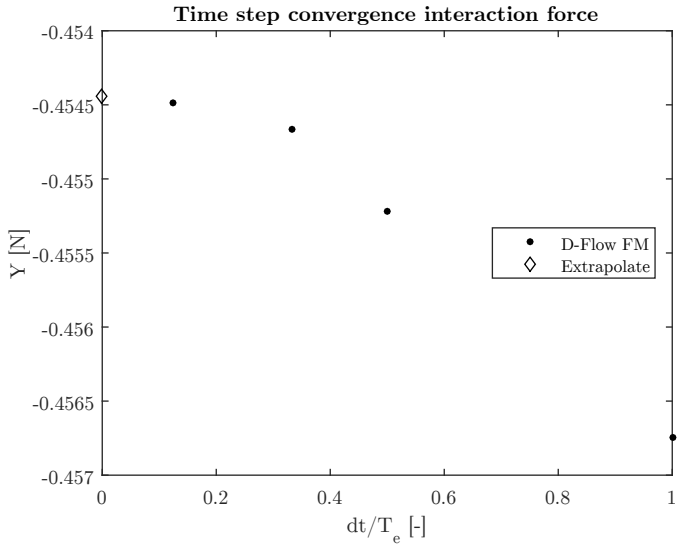

Figure 5.9: Convergence of the interaction force as a function of time increment

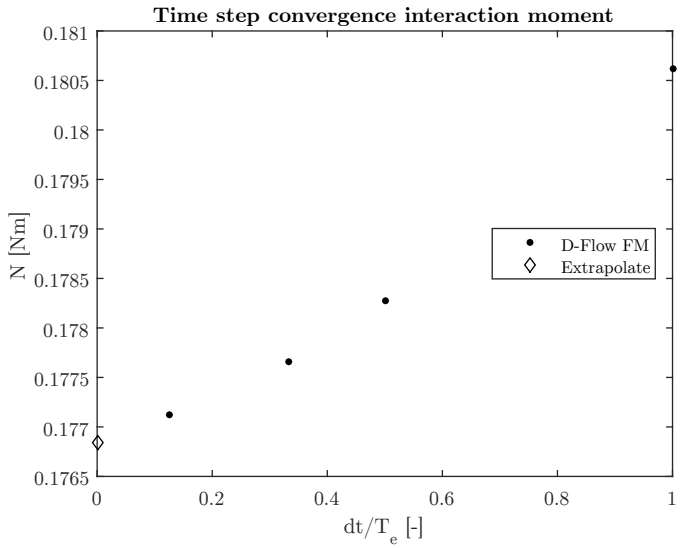

Figure 5.10: Convergence of the interaction moment as a function of time increment

When a closer look is taken on the time domain output of the calculations some more differences can be spotted. The results acquired with the largest time step have a small phase shift compared with the other three.

What is also striking is that the smallest time steps cause high frequency oscillations to appear that would otherwise have been filtered. The hypothesis is that these oscillations are caused by the slight differences in the interpolated pressure field.

These oscillations are caused by slight differences in water level that result from the forcing

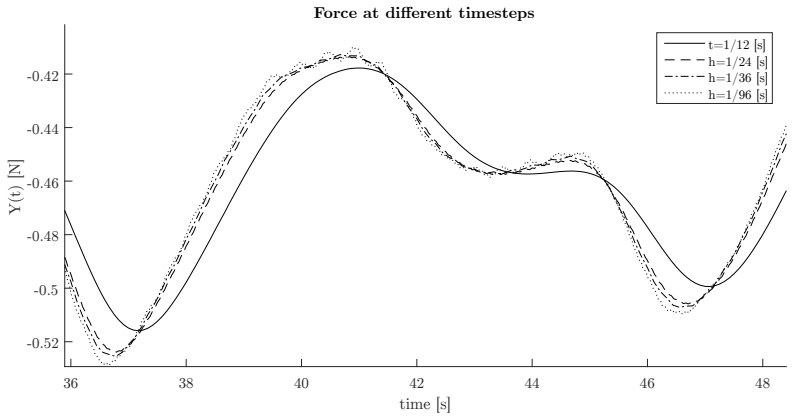

Figure 5.11: The development of force at different time steps

that is applied to the flow by the moving pressure field. Think of them as ripples. These ripples die out quickly when the grid spacing and or time step are large, because those things act as a filter. Normally the ripples do not exist long enough for them to cause oscillatory behaviour at the sampling frequency of forces. But because a very small time step is used and there is no background viscosity present to filter them the ripples can travel to the side wall of the towing tank and back, causing an asymmetric disturbance in the pressure underneath the ship, which shows up in the plots.

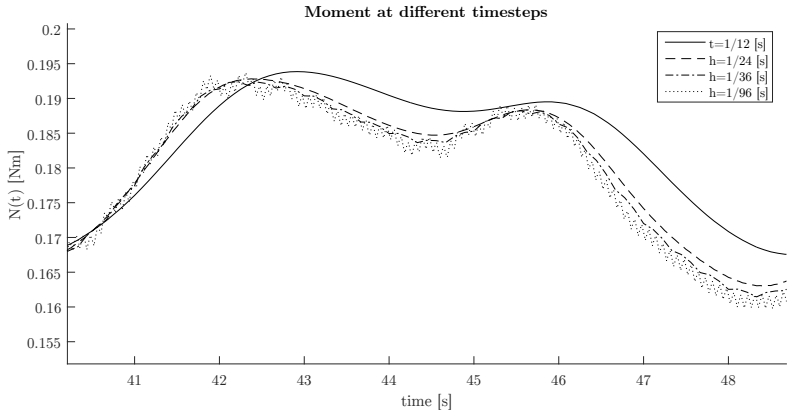

Figure 5.12: The development of moment at different time steps

If those ripples do not reflect back their contribution to the side force is zero, because they are symmetric. However their contribution to resistance is always present because the ship itself has a forward speed. As a result the ripples become asymmetric with respect to the ship in the direction of propagation (x-direction). The main difference in pressure in front and behind the ship as it sails across the ripples is due to the asymmetry of the ripples itself.

This explains the behaviour of the pressure resistance as the time step is decreased as dis-

played in Figure 5.13. The computed resistance is almost exactly linear with the chosen time step. Therefore the computation of resistance with the moving pressure field method is not reliable. The effect of the ripples can be mitigated by choosing high values for the eddy viscosity or choosing extremely small time steps, both are not ideal and will not get rid of the ripples all together. The real solution would be to not move the pressure field with respect to the grid.

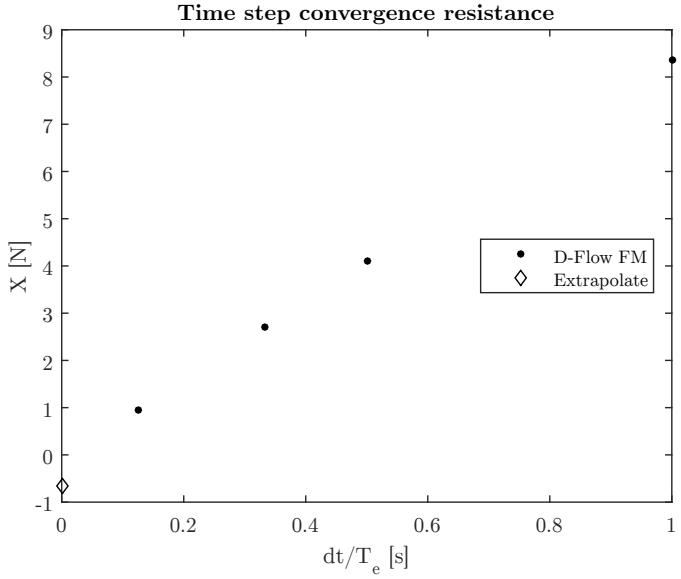

Figure 5.13: Convergence of pressure resistance as a function of time increment

5.4 CONCLUSIONS

The verification study has shown that the interaction force and moment that D-FLOW FM computes can be trusted on numerical grounds. Both converge in space and time to a value that is close to what ROPES computes.

The computed side force is a realistic value. It is not far from what experimental regression predicts it should be. The computed interaction moment however converges to a value that does not correspond to the regression prediction. This could be because viscous effects, that were neglected during the verification study, play a large role in the yawing moment. To get this yawing moment right therefore it will be needed to model viscous effects in D-FLOW FM.

The study has also shown that the pressure resistance cannot be computed using the moving pressure field method. The unsteady forcing that is applied to the flow while moving the pressure field across the grid causes small ripples in the fluid directly underneath the hull which are asymmetric with respect to the moving ship.

The smaller the time step is the smaller in magnitude and higher in frequency the disturbances are that the pressure field creates. This causes the computed force in x-direction to be directly correlated to the time step that is chosen. Hence it does not converge.

The computations during the remainder of this thesis will be done on a grid that is comparable to the middle grid size from Section 5.2. This means that the ship will be covered by approximately 3400 cells. An estimated numerical error of 7.5% applies to this grid size.

The time step will be such that the ship crosses a grid cell in 2 steps. Although a larger step size only marginally decreases the accuracy of the mean result it was noticed in Figures 5.11 and 5.12 that the larger time step introduced a phase shift.

Using the aforementioned numerical resolution the CORE I7-4700MQ laptop computer with which the computations were done needs approximately 4 minutes of computation to simulate a minute of real time at model scale. Full scale computations can likely be done in real-time, and with a more powerful processing unit the real-time simulation of a ship sailing in more complex surroundings than a towing tank is expected to be feasible.

6 COLLECTED DATA

6.1 INTRODUCTION

This chapter provides an overview of all the experimental data that is used during the research. Some background information is provided in the text itself and references are made to the original publications. Where applicable a short analysis is done. A large amount of data raw data that is available needs some preprocessing and an uncertainty analysis, for this reference is made to the appendices. There are three types of measurements that are going to be used:

- The sway force and yaw moment induced on a ship due to the presence of a bank
- The flow field underneath a ship in shallow and confined water
- Pressures and flow velocities on bed and banks caused by ships

All of the measurements have been done at model scale with ships that were towed as opposed to self propelled. This chapter will list the sources of experimental data and give a short description of the conditions under which they were obtained.

6.2 FLOW BENEATH VESSELS IN RESTRICTED WATERS

Measurements on the flow field beneath a model of an inland navigation vessel were done in [24]. The ship model had a length of 3 and a width of 0.56 meters. It was rigidly connected to the towing construction, fixed in all its 6 degrees of freedom. It was towed through a measurement section which was 9 meters long and 2.4 meters wide. The measurement section was located on a false bottom which was preceded by a ramp. See Figure 6.1 for an overview of the towing tank.

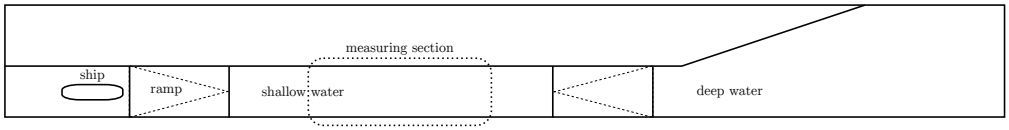

Figure 6.1: Overview of the towing tank layout used in [24]

Most of the experiments were done with an ambient flow present. The tests that are used were done with a ship sailing without a drift angle in the centreline over a flat bed. The variables were under keel clearance, ship speed and water depth. Flow velocities were measured at the bed beneath the ship. For some experiments velocity measurements were also done at different depths beneath the ship, giving an indication about the shape of the velocity field near the bow and stern of the vessel.

On the measuring section there were three velocity sensors placed flush with the bed. The height at which the velocity was measured is not exactly known, it is estimated to have been 5

millimetres. The three measurement devices were placed below midship, 10 and 20 centimetres to port. Because the conditions in the towing tank were supposed to be symmetrical the outer two velocity measurements have been mirrored from port to starboard. However in reality the flow pattern beneath the vessel was not so nicely symmetrical, which causes the mirroring to yield strange velocity fields. It would have been better if sensors had been placed at both the port and starboard sides of the ship.

The asymmetric flow field is probably in part introduced because an ambient flow passes along the skewed wall before entering the confined section, and may be in part attributed to misplacement of the ship or the instruments. Viscous effects may also introduce some asymmetry in the flow field.

Velocity sensors have measured the flow at several moments in time beneath the ship as it passed over the devices. This information can be reconfigured to a velocity distribution underneath a ship assuming that the measurements were done in steady conditions. However transient effects caused by the ramp only have three ship lengths to disappear, so that those transient effects might still have been present at the time the ship passed the sensors. No uncertainty analysis has been done for these measurements.

6.3 INTERACTION FORCE AND MOMENT ON SHIPS

Several sources of experimental data on the interaction force and moment have been used. Two regression formulations were found that are applicable to towed ships. One of them is by Vantorre [35]. It is based upon experimental results that were found for three ships; two bulk carriers and a container carrier. The ship models were towed alongside a vertical wall. Twelve regression coefficients that rely on non-dimensional hull form parameters are used to model the influence of under keel clearance, distance to bank and forward speed. The effect of squat is taken into account by including it into an 'effective' under keel clearance parameter.

An alternative to the trend lines by Vantorre is cited in [6], originally proposed by Ch'ng et al. This formulation relies on model tests from two MarAd Series hull forms and a container carrier. The models were towed along sloping banks. The formulas include the effects of under keel clearance, Froude number and distance to bank. The effect of squat is included within the Froude number dependency. Of both formulations the uncertainty is unknown.

More data about ship-bank interaction forces was produced at Deltares recently. These experiments have been performed and were analysed in part by Exer [7] and further in [12]. Still a large part of the data has not been analysed thoroughly yet. The experimental conditions include the presence of small banks in a channel, inducing asymmetrical hydrodynamic interaction effects between bank and ship. A part of the experimental data that has not yet been analysed are ship-bank interaction effects that were measured by force transducers in the model ship. What is unique about these measurements is that the measured interaction force and moments are time-varying. This makes the data suitable to compare with a time-domain numerical solver.

The new set of data is meant as an extension on the data produced earlier about the flow field beneath inland ships. The same set up is used as in those experiments, see Figure 6.1. In this new set of experiments however, the conditions are much more severe in terms of Froude numbers,

flow blockage and drift angles. The experiments that were performed were done at critical and near-critical flow conditions. Earlier research has indicated that in these circumstances strongly non-linear effects start dominating, the current dataset focusses especially on these conditions. The experiments have been performed with relatively short banks ($\frac{1}{2}$ $\frac{1}{4}$ and $\frac{1}{20}$ times the ship length) so that transient effects can be investigated. Furthermore the experiments are intended as validation and or calibration material for numerical simulations. A presentation and discussion of the experimental results will be given in Appendix B.2. A treatment of uncertainty and credibility will be given in Appendix B.3

6.4 PRESSURE AND VELOCITY ON BED AND BANKS

The dataset produced at Deltares that was mentioned in the previous section also contains a large amount of data on the flow field, measured by velocity meters and pressure sensors. Velocity meters were placed on the keel of the ship and above the bed beneath the sailing line. Some velocity meters were placed outside the sailing line of the ship which give extra information about induced velocities on the bed. Different kinds of pressure sensors at multiple locations provide additional information about the flow field. See Figure 6.2 for an overview of the layout of the experiments and the location of instruments. The area in between the vertical lines at 0 and 16 meters is the shallow water section from Figure 6.1

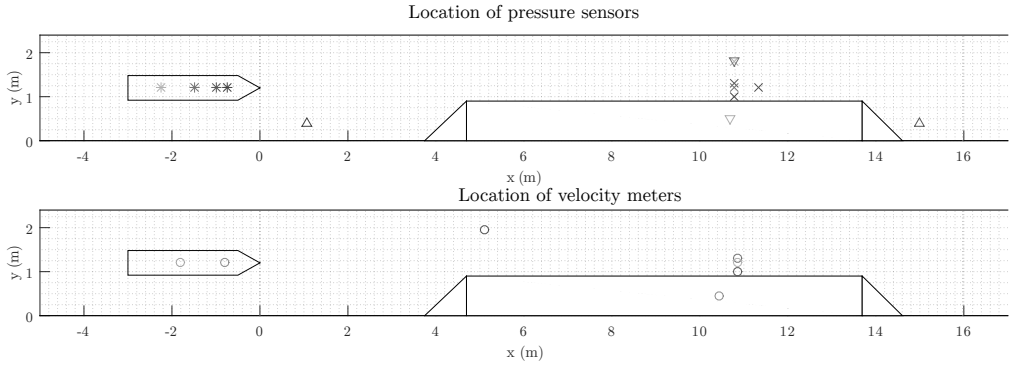

Figure 6.2: Location of pressure and velocity measurements

The dataset from FHR that was mentioned in the previous section also contains the output of three wave gauges in the region between ship and bank. These values can be translated to a pressure on the bank under the assumption that hydrostatic pressure is the main contribution.

7 VALIDATION

7.1 INTRODUCTION

In this chapter a validation study is done to determine to what extent the developed modelling method in D-FLOW FM is able to provide an accurate representation of the real world values that it is designed to predict. This is done by comparing computational simulations with experimental observations.

If the uncertainty of experimental results and of the numerical computation are known it is possible to quantify error. Unfortunately most of the experimental datasets that are available have unknown uncertainties which makes it impossible to put a number on the modelling error. In this chapter experimental uncertainties will be displayed if they are known. However this chapter will not contain a very formal validation procedure of the modelling method. Instead a qualitative indication will be given of the suitability of the model in different scenarios.

The goal of this chapter is to indicate in which cases the developed method is usable, and to point out modelling errors in cases where it is not. In future developments the modelling errors may then be addressed, and possibly fixed.

7.2 MODELLING APPROACH AND PARAMETER SENSITIVITY

In each of the simulations that are done in this chapter the same set of modelling parameters is used. The relevant physical parameters all have to do with viscous effects, settings for the numerical solving process itself will not be treated within this thesis. The values for the parameters have been picked based partly on experience with the model and partly on physical arguments. This means that no calibration has been done in between the validation cases. The settings that have been used can be found in Table 7.1.

Parameter	Value	Description
$Smagorinsky$ (-)	0.15	Smagorinsky horizontal turbulence factor
$Elder$ (-)	0.30	Elder factor in horizontal turbulence
$Vicouv$ (m/s)	0.00	Uniform horizontal eddy viscosity
$UnifFrictCoef$ (-)	0.00	Uniform Manning bed friction coefficient
$wall\_ks$ (m)	0.02	Wall roughness factor for partial slip

Table 7.1: Fixed parameters during validation assessment

In the next few paragraphs the choice of these parameters will be discussed and it will be indicated whether the mean interaction forces are sensitive to them. In general the interaction forces are a lot more sensitive to a change in the turbulence parameters than water level and

velocities around the ship. A formal sensitivity analysis has not been performed, only a few test runs have been done per parameter to provide an indication.

The Smagorinsky model is a well known formulation to take into account the apparent viscosity caused by sub grid scale turbulent motion. The range of values between which this parameter is usually chosen is from 0.10 to 0.15. Because viscous effects are expected to be large in the area around the ship the parameter has been chosen high. The mean interaction forces are not very sensitive to the choice of this parameter.

The Elder factor estimates the effect of depth averaging the flow by taking into account an assumed parabolic profile for the horizontal eddy viscosity. Values are commonly chosen between 0.3 and 1.0. A low value for the Elder factor was found to result in a more realistic looking wake behind the ship, when compared to footage from the experiments at Deltares. Therefore its value has been set to 0.3. The mean interaction forces are moderately sensitive to the choice of this parameter.

A uniform horizontal eddy viscosity can be added to the flow field, this is commonly applied for flows with very large grid sizes such as ocean models. It is preferred to let the Elder and Smagorinsky models handle the turbulent influences because they have a better physical background and therefore $Vicouv$ has been set to 0. The mean interaction forces are not very sensitive to reasonable values of background viscosity.

The parameter for uniform bed friction has proven to have a very large influence on the flow field when the under keel clearance is small. The Manning formulation upon which it is based implies a one-sixth power law flow profile which is unrealistic in the area beneath and around the ship. Because the flow assumption is wrong and because it has such a large influence on the result it was decided to disable it completely for the time being.

Along the channel walls a partial slip boundary condition has been applied which depends on a roughness factor. This factor has been kept at the default value of 0.02. The mean interaction forces are insensitive to the value of $wall\_ks$ and also switching to a no slip condition barely influences the results.

During all of the simulations the resolution in time and space will be as decided in Section 5.4 after the verification study. This means there will be approximately 3400 grid cells to represent the hull and the time step is chosen such that a ship crosses a grid cell in two steps, except if it needs to be decreased to avoid violating the Courant condition for numerical stability. The chosen resolution is expected to provide sufficient numerical accuracy for the intended purpose.

The turbulence parameters are kept equal in all the types of calculation because a generally applicable method is desirable. There is one parameter however that had to be changed in some calculations in order to obtain sensible results, this parameter is called $Vicuship$ and it is used to add a constant horizontal eddy viscosity directly underneath the moving pressure field. This parameter is a trick that has to be applied to keep the ship hull stable at larger speeds.

At large speeds the moving pressure field creates gradients that are too steep, causing spurious oscillations in the flow field. The $Vicuship$ parameter removes these oscillations but also influences the flow as a side effect. Admittedly this isn't very pretty, but it enables calculations

to be run that normally would have been unstable. $Vicuship$ is only applied when it is needed, and when it is the lowest possible value is chosen that keeps the calculation stable.

7.3 FLOW BENEATH VESSELS

7.3.1 PROBLEM DESCRIPTION

Ships sailing in shallow and confined water induce flow velocities near the bed of the waterways they are sailing in. This induced flow leads to high velocity gradients which in turn causes a large shear so that loose-lying bed material may be picked up and redistributed due to the influence of the ship. The long term change in bathymetry due to the passing of many vessels is of key interest because it influences the navigable depth of inland waterways. A fast computation of the flow field beneath a ship is a first step in simulating this.

7.3.2 METHOD

The depth averaged flow field under and around a moving pressure field that is computed by D-FLOW FM might be usable to estimate the flow velocities that occur at the bed due to a passing vessel. To put this to the test experimental data from model scale tests done at Deltares will be used [24]. During these experiments velocities were measured underneath a towed ship of which the relative under keel clearance and Froude depth number have been varied. The experiments are a bit more elaborately described in Section 6.2.

Velocity meters were placed on a fixed position within a towing tank so that velocity vectors were measured beneath the ship as it passed over the devices. This information can be reconfigured to a velocity distribution underneath a ship assuming that the measurements were done in steady conditions.

There were three instruments placed, one at midship and two in between midship and full breath. As a result only velocities at the port side of the ship were measured. The ship sailed in the middle of a narrow canal, therefore the flow field was expected to be symmetrical which would allow the outer two measurements to be mirrored. Unfortunately the actual measured velocities show that the flow field cannot have been symmetrical. To distinguish the real measurements from the mirrored ones the vector plots such as Figure 7.1 show the mirrored vectors with a lighter colour.

To replicate the experiments the experimental conditions were modelled in D-FLOW FM. The most notable differences between the model and the experiments are briefly discussed in the following paragraphs.

The towing tank that was used during the experiments is shown in Figure 6.1, but it differs from the numerical tank which is shorter and does not have the deep water sections nor the broader section. The experiments were designed to yield the flow field in a steady state condition, so it is not needed to include the ramps in the numerical model.

Some of the experiments were done with the presence of an ambient current that was directed opposite to the sailing direction. An estimation of the towing tank current is made by computing the solution of the tank with the right volume flow rate. This computation needs a large spin up

	A	B	C
h [m]	0.30	0.20	0.200
ukc [m]	0.05	0.06	0.033
V_s [m/s]	0.50	0.60	0.500
U_0 [m/s]	0.00	−0.05	−0.100

Table 7.2: The conditions belonging to cases A, B and C

time. After the spin up time has passed and the current is sufficiently steady a restart file is made, which serves as the initial condition for the ship.

The linesplan of the hull that was used is not exactly known. Therefore a similar ship is scaled to the right dimensions and used as an alternative, which should not lead to major differences. The ship is also slightly smoothed so that wiggles are suppressed. The smoothing operation combined with the fact that the ship is discretely represented causes the numerical representation of the ship to be different from the exact shape. In this light not having the precise linesplan of the model ship is not the largest problem.

Since the amount of detail in the flow field that is going to be resolved is not very high, these slight deviations from the experimental conditions will not have a large impact on the outcome of the validation.

Three experiments are picked from the dataset so that something can be said about the applicable range of the computer model. In Table 7.2 the conditions under which the tests were performed are displayed. For Case C an eddy viscosity underneath the ship had to be added to keep the pressure field stable.

7.3.3 RESULTS

The computed flow fields of all cases are shown in Figure 7.1 to 7.3. In these figures the same scale for the magnitude of the vectors has been used so that they can be compared. The upper plots show the velocity vectors that were measured just above the bed during the experiments. The lower plots show the D-FLOW FM computed depth average velocities. The outline of a ship is shown to indicate the relative position of the flow field.

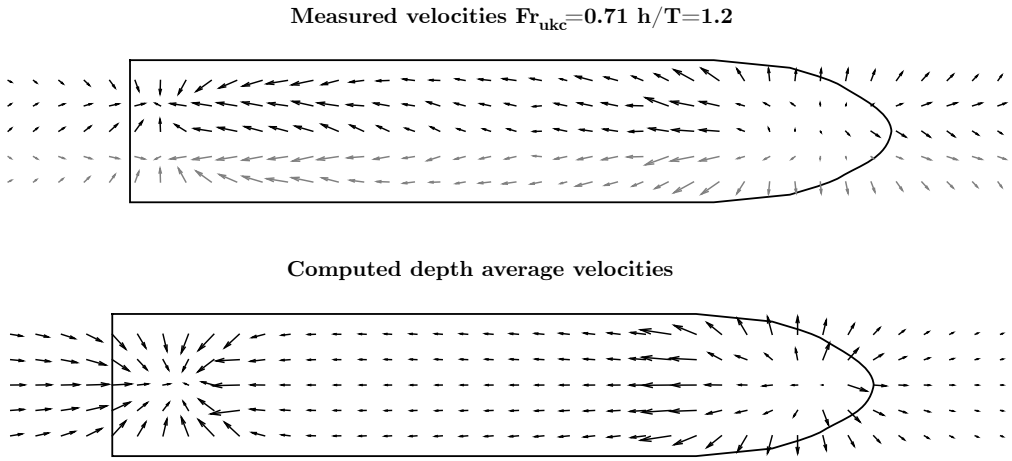

Figure 7.1: Case A: Measured and computed flow velocity beneath ship

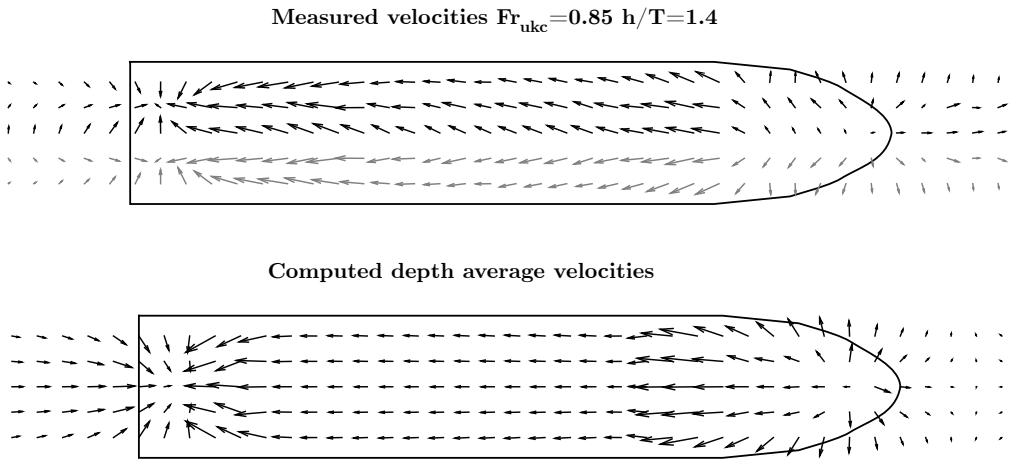

Figure 7.2: Case B: Measured and computed flow velocity beneath ship

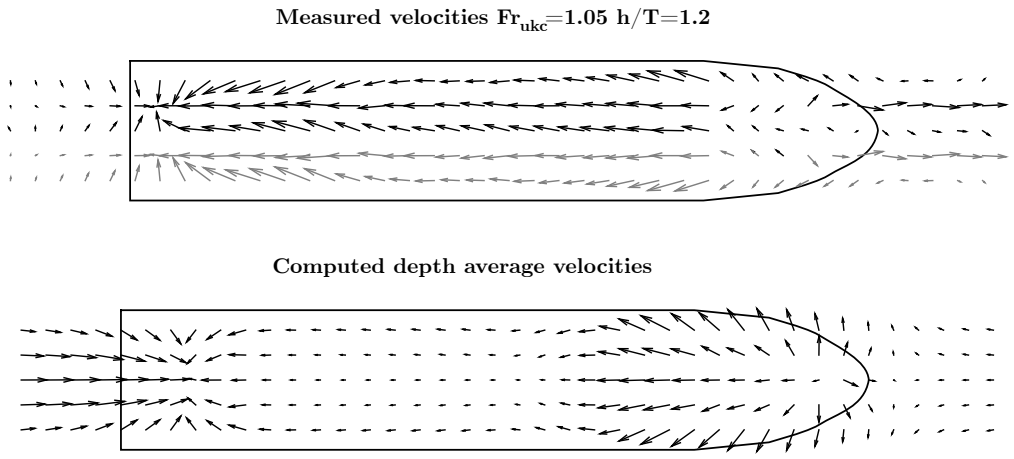

Figure 7.3: Case C: Measured and computed flow velocity beneath ship

7.3.4 DISCUSSION

In all the cases the computed solution is much more symmetric because of the ideal numerical conditions. Moreover the flow velocities near the shoulders of the ship are slightly overpredicted and the pressurised flow underneath the vessel is underpredicted. This has to do with the hull's boundary condition that is not properly enforced by the pressure field, causing the pressurised flow beneath the ship to be incorrectly modelled. Nonetheless the computed values in Figure 7.1 and 7.2 show fair resemblance to the measurements.

It should be kept in mind that D-FLOW FM computes a depth averaged solution for the flow field. The measurements however were done a few millimetres above the bed. Part of the difference between the computed value and the measurements can be attributed to this fact. This explains the difference between flow velocities behind the ship. Here the depth average is dictated by the return current that follows the movement of the hull, whereas the flow velocity near the bed is also affected by the pressurised flow coming from beneath the ship's bottom.

Figure 7.3 which belongs to Case C shows a much larger discrepancy between the computed flow field and the measured values. For this computation an eddy viscosity underneath the hull had to be applied to keep the pressure field stable. This is because local Froude numbers underneath the hull are very high, causing waves to interfere with the pressure field. An estimate of the Froude numbers underneath the hull is $Fr_{ukc} = \frac{V_s - U_0}{\sqrt{g * ukc}}$, when this number is larger than one the pressure field no longer sufficiently resembles the hull shape.

The conclusion can thus be drawn that for $Fr_{ukc} < 1$ the moving pressure field method as modelled in D-FLOW FM can provide a fair estimation of the depth average flow field underneath the ship. This depth average flow field looks similar to the velocities measured near the bed. Perhaps a better estimation can be made by relating the average velocity to the velocity near the bed, by estimating the vertical velocity profile underneath the ship for example. A numerical model with multiple layers in the vertical is a logical next step if ship induced sediment transport needs to be investigated.

When $Fr_{ukc} > 1$ the boundary condition that the ship's hull applies on the flow is no longer sufficiently well approximated by the moving pressure field. As a result the current implementation of the model cannot provide a reasonable solution to the depth averaged flow field underneath a ship sailing in those conditions. This is a modelling error that will have to be resolved to improve the accuracy and applicable range of the model. Possible ways to impose the boundary condition more strictly are applying a Preissmann slot on the grid cells beneath the ship or applying an iterative pressure to correct for wave interference. The best option would be to impose the 'hard' boundary condition on the ship, this however would require a different system of equations to be solved on a separate domain.

7.4 PRESSURE AND VELOCITY ON BED AND BANKS

7.4.1 PROBLEM DESCRIPTION

Passing ships in rivers induce flow velocities not only directly underneath them, but also on the river banks. The induced flow and waves accelerate the natural changes in morphology in these rivers which is not always desirable. To avoid unwanted changes in the river its banks need protection. Being able to simulate the far field flow and waves generated by passing vessels helps in the design of bank protection.

Another application is the assessment of forces on moored structures. When the far field waves and flow created by a passing vessel are correctly resolved those can be translated to the response of a moored vessel. This is useful for the analysis of downtime in ports for example.

7.4.2 METHOD

In this section the flow and wave field that is computed by D-FLOW FM will be compared with measurements done in a towing tank in which sloped banks were placed. The data was produced at Deltares. A model of an inland ship was towed beside long and short banks, so that the data can be used to validate the ability of D-FLOW FM to simulate transient behaviour. A more elaborate description of the experiments can be found in 6.4.

Both the experiments and the numerical calculations were done at model scale. The experimental conditions have been modelled closely in D-FLOW FM. However there are some differences between the modelled scenario and the experimental conditions. The most notable differences are briefly addressed in the following paragraphs.

The towing tank layout from Figure 6.1 was used for the experiments. The numerical model uses the same geometry except for the widened section at the end, which is primarily used for wave reduction and should not have a notable influence on the measurement section itself. Unlike what was done in Section 7.3 this time the deeper sections and ramps are modelled in D-FLOW FM so that the right transient behaviour can be captured.

The linesplan of the hull that was used is not exactly known. Therefore a similar ship was scaled to the right dimensions and used as an alternative. This combined with the smoothing operation and the fact that the ship is discretely represented causes the numerical representation of the ship to be different from the exact model used during the experiments.

	D (Mild)	E (Severe)
Fr_h [-]	0.40	0.80
h/T [-]	1.20	1.20
y_b [-]	0.14	0.14
U_0 [m/s]	0.05	0.25
Bank	Short	Long

Table 7.3: The conditions belonging to cases D and E

The experiments were done with the presence of a current with average speed U_0 that was directed opposite to the sailing direction. To model this current first the solution of the tank with the right volume flow rate was computed. This computation needs a large spin up time. After the spin up time has passed and the current is sufficient steady a restart file is made, which serves as the initial condition for the ship.

The results of two experiments will be given. One of them with rather extreme (supercritical) flow conditions and a more temperate case. Both cases have the ship sailing in the middle of the channel. The mild case has the ship sailing along a short bank. The severe case was done beside a longer bank. In Table 7.3 the experimental conditions belonging to the two test cases are displayed.

7.4.3 RESULTS

Figure 7.4 and 7.11 show the position of pressure and velocity sensors placed on bed and banks for both testcases. The sensors measured during a period of time starting at the moment when the ship's bow enters the measurement section. This means that the x-position of the bow is 0 as shown in the figure. The time period ends at $t = t_{end}$ which is when the ship leaves the measuring section.

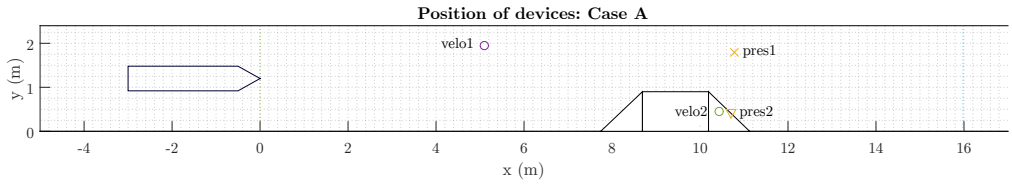

Figure 7.4: Position of measurement devices for case D

The initial conditions during the experiments cannot be exactly repeated in the numerical simulation. In reality the water in the tank is exited due to the starting of the current and from previous experiments so that low frequency oscillations will be present. Also in the initial condition computed by D-FLOW FM the flow is not completely steady. Moreover slight calibration errors and the precise depth of the pressure sensors make a difference in the absolute values that are measured. This results in a bias between the experiments and computations.

The bias can be removed by comparing the relative differences between the experimental and computational signal. To do this the average velocity and pressure measured by the sensors before

the ship starts moving is subtracted from the rest of the signal. The numerical result is also given an offset such that the signal starts at 0 at the moment that the ship starts moving (this is before $t = 0$ which is when the ship enters the measurement section at a constant speed).

In this way the bias is removed from the signals and a relative comparison can be made. The values have been non-dimensionalised by dividing both signals by the absolute maximum mean experimental value. As a result the light grey line in the graphs will not exceed plus or minus one.

Case D

Case D is the relatively mild case. The ship sails at moderate speed through a very narrow channel when it encounters a small bank structure. The measurements on the flow field are shown in Figure 7.5 to 7.10

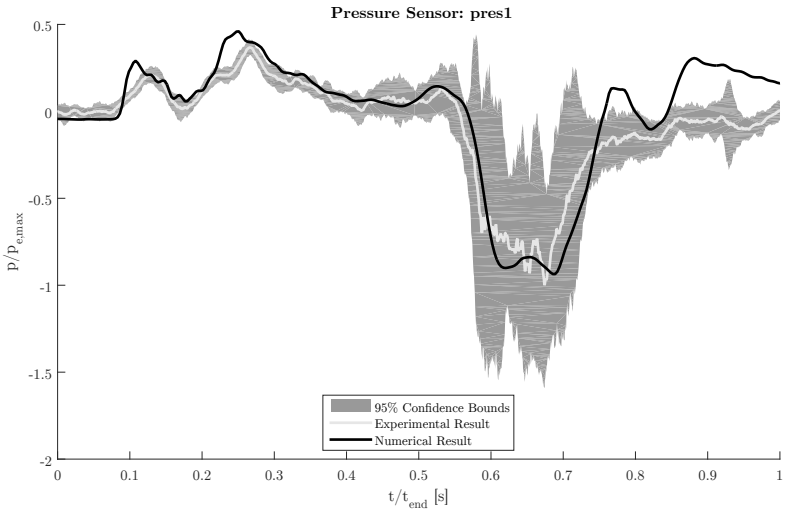

Figure 7.5: Pressure measurement on port side

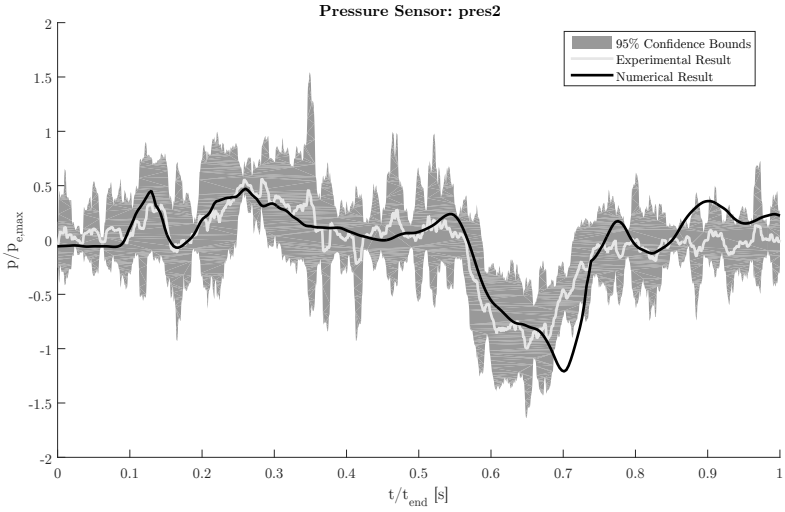

Figure 7.6: Pressure measurement on starboard side

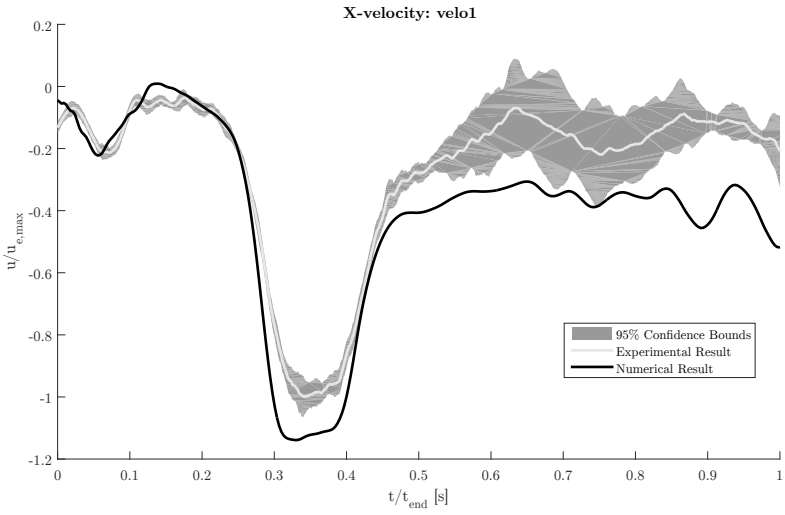

Figure 7.7: X-velocity before the bank

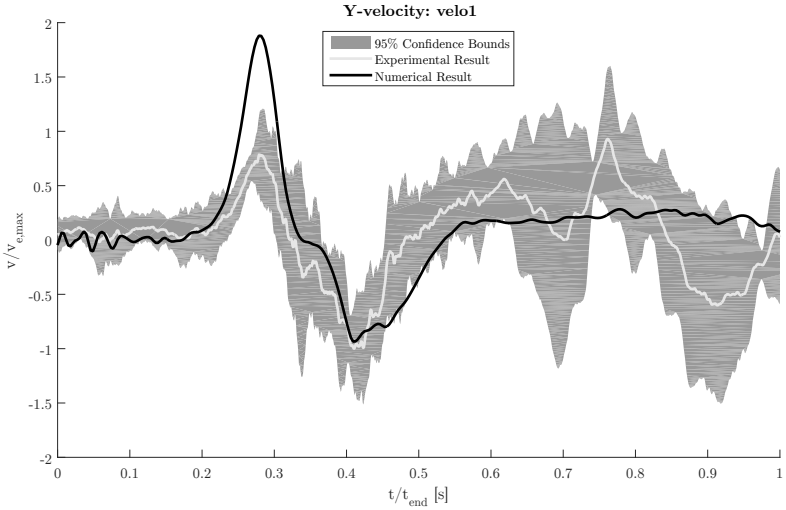

Figure 7.8: Y-velocity before the bank

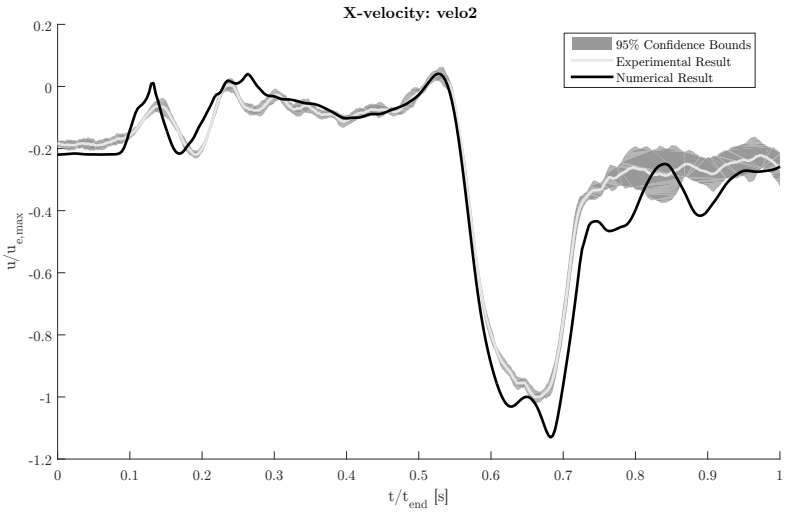

Figure 7.9: X-velocity behind the bank

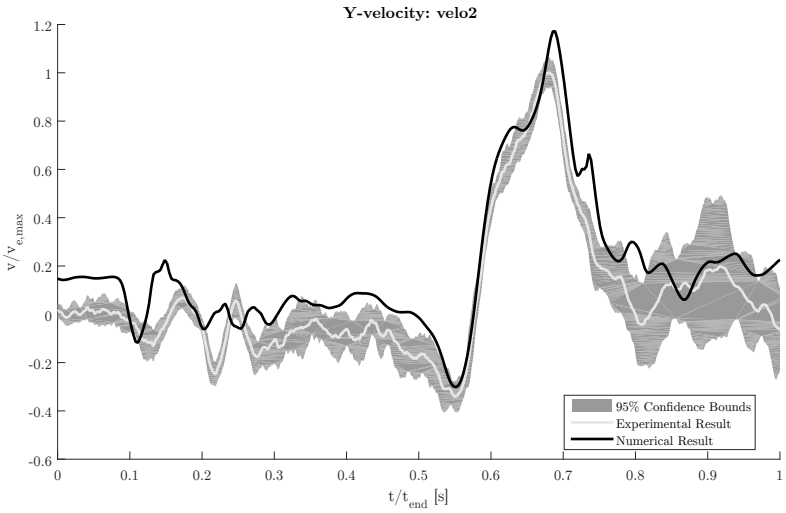

Figure 7.10: Y-velocity behind the bank

Case E

Figure 7.4 shows the position of pressure and velocity sensors placed on bed and banks for Case E. Case E is a very severe case. Due to the narrowness of the channel and high velocity the ship has surpassed Schijf's critical velocity, which means that it would not be feasible for a self propelled ship to attain this velocity. In some circumstances it might happen that when a ship suddenly enters a confined area it reaches such a state because of the momentum it still has. It is a good test case for the numerical method.

To keep the computation stable under these conditions the time step had to be reduced by a factor of three, so that the Courant condition would not be violated. A high eddy viscosity was applied underneath the hull to keep the pressure field stable.

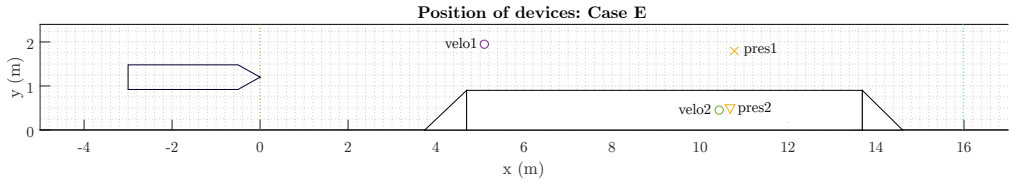

Figure 7.11: Position of measurement devices for case E

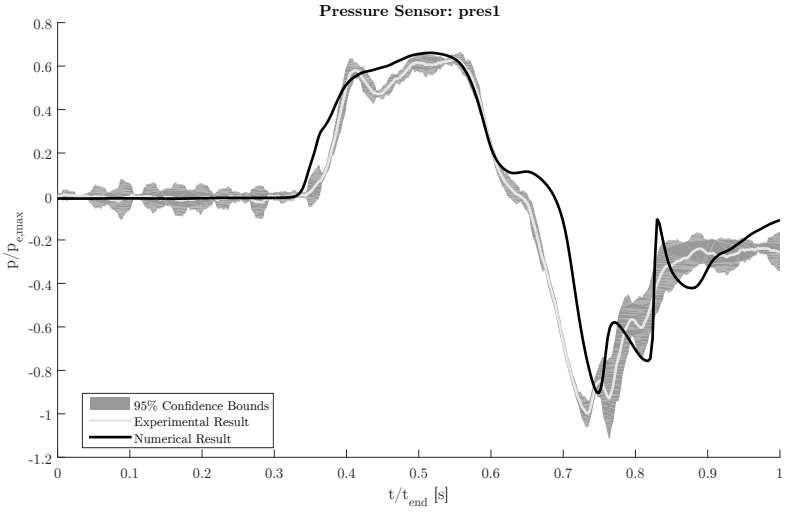

Figure 7.12: Pressure measurement on port side

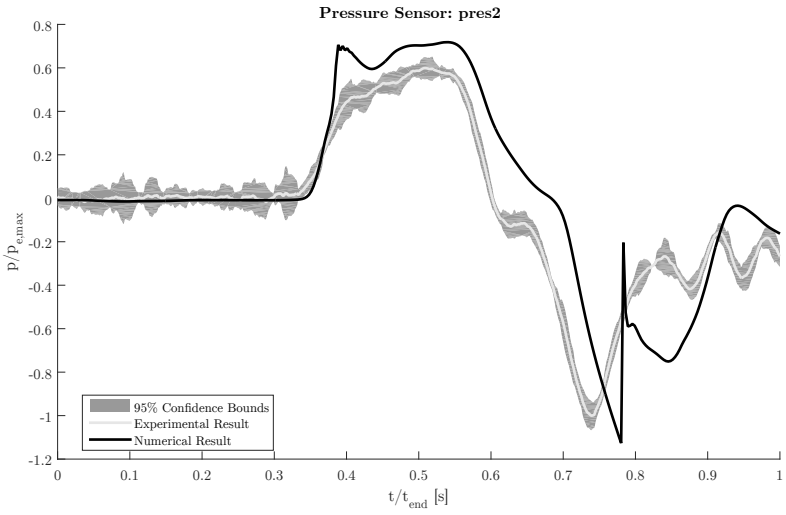

Figure 7.13: Pressure measurement on starboard side

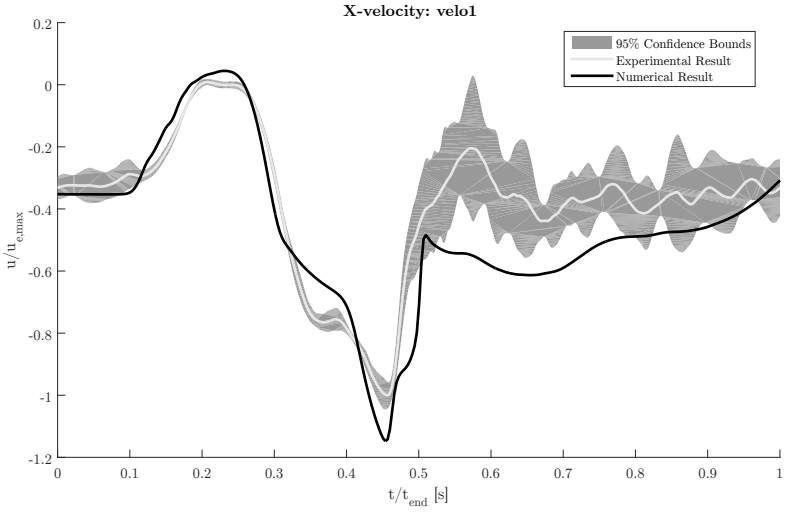

Figure 7.14: X-velocity across the beginning of the bank

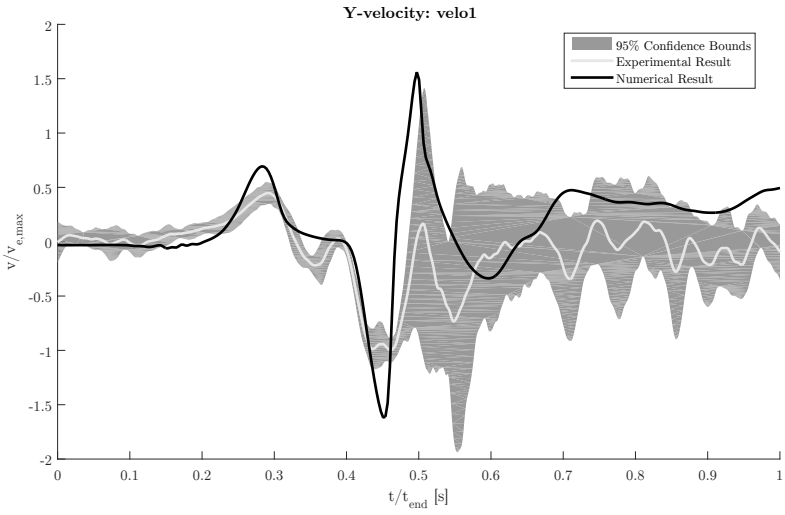

Figure 7.15: Y-velocity across the beginning of the bank

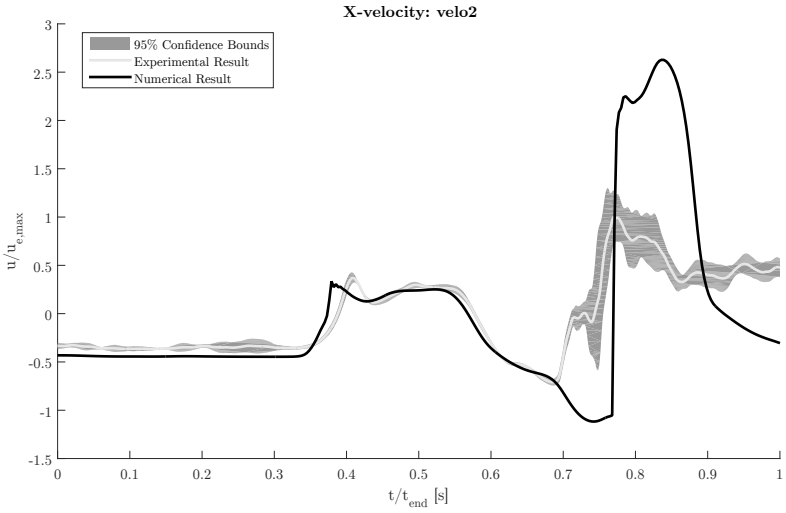

Figure 7.16: X-velocity at the end of the bank

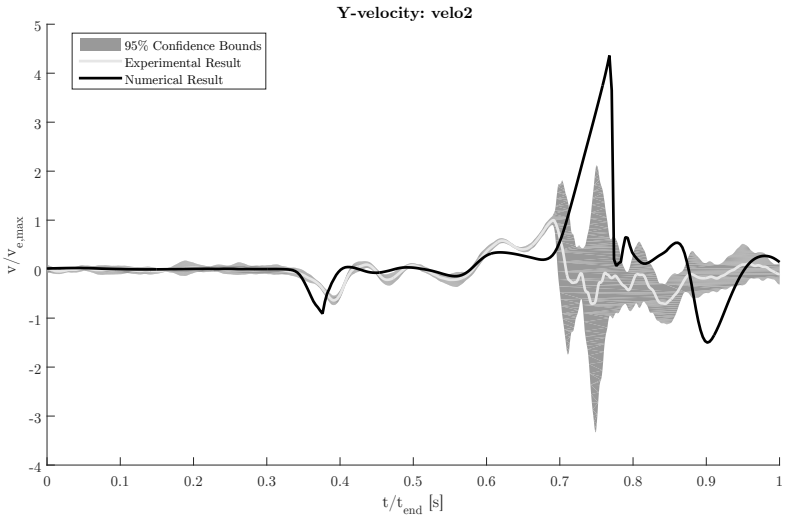

Figure 7.17: Y-velocity at the end of the bank

7.4.4 DISCUSSION

Figure 7.5 and 7.6 show that pressure differences in Case D are well represented. The acceleration phase of the vessel causes waves which form the initial bumps in the graphs. When the ship passes the Bernoulli wave that it generates also passes the pressure sensor. This water level draw down due to the passing of the ship is well resolved at both locations.

Figure 7.7 and 7.8 show the measured x- and y-velocity at $velo1$ respectively. Note once again that the numerical result is a depth average, and the velocity has been measured somewhere near the bed. This may explain why D-FLOW FM predicts a higher current directly behind the ship. The magnitude of the return current is well resolved by D-FLOW FM. The velocity in y-direction, which is caused by the fanning out effect, is predicted to be much higher than measured.

At velocity meter $velo2$ near the bank both x- and y- velocity show equally good correspondence with the experimental results.

Case E is a lot more severe and therefore more difficult to measure and to predict. At sensor $pres1$ an acceptable solution of the pressure is computed, see Figure 7.12. Resolving the pressure at the side of the bank proves to be more challenging, a discontinuity is visible in Figure 7.13 from which the numerical scheme recovers.

Both pressure sensors show a very large bow wave that was not present in Case D, but that corresponds with reality. This wave is caused by the combination of high speed and large blockage, because the shallow water wave celerity is nearly equal to the ship's speed the bow wave piles up in front of the ship. The bow wave extends over a large portion of the hull and is followed by a sharp downward peak near the stern due to the return current. The experiments show a noticeable pressure drop behind the ship corresponding to a high resistance.

Figure 7.14 and 7.15 show the measured x- and y-velocity at $velo1$ respectively. The model once again overpredicts the current behind the ship, though this could be because the answer is depth averaged. The smaller waves that appear in the experimental results cannot be represented by the numerical model. This is because the equations that are solved in D-FLOW FM cannot be used to simulate short waves. Short waves do not experience the influence of the bottom and therefore behave as though they were in deep water, which does not correspond to the mathematical assumptions.

The velocity at $velo1$ is not affected by the discontinuity that was seen in at $pres2$ which lies on the opposite side of the bank. The velocity measurement at the bank side is however heavily affected by the discontinuity, causing the computed velocity to deviate quite a lot from the real value, see Figure 7.16 and 7.17.

A further analysis showed that the reason that the discontinuity only appears on the bank side is because of the flooding/drying algorithm. During the passage of the ship in this extreme case a large portion of the bank becomes dry. D-FLOW FM tries to model this process but is not successful in doing so, since it causes the discontinuity that does not correspond to reality. Perhaps the grid size is too coarse to capture the physics behind the flooding and drying in this scenario.

In conclusion the moving pressure field method in D-FLOW FM is quite well able to solve for pressures and velocities caused by ship-induced flow in the relatively mild case. The time

dependency of the pressure and velocity correspond well to the measured signals. The magnitude of the pressure is also close to what it should be. The velocity corresponds less well but this may be attributed to the difference between depth averaged and near-bed velocity.

The most severe case has shown that D-FLOW FM is robust and is capable of providing pressure and velocity estimates even in extreme scenarios. However the region where the bank becomes dry contains a discontinuity that does not correspond to measured values. The current implementation might not be able to solve ship waves and flow near the intersection with the banks.

7.5 INTERACTION FORCE AND MOMENT

7.5.1 PROBLEM DESCRIPTION

A ship sailing in a confined waterway interacts with the nearest bank causing external forces and moments the most important of which are the sway force and yaw moment. The ability to compute these two quantities is useful in the design of entrance channels and other confined waterways. It can also be used in a manoeuvring simulator or to improve safety regulations in confined waters.

What is known about these interaction effects is that they are heavily non-linear. A suction force that is found in normal circumstances will turn into a repulsive force when the flow area between ship, bed and banks becomes small. To achieve a realistic manoeuvring simulation this change in sign should be predicted.

In this section it is assessed if the developed method in D-FLOW FM is able to predict the ship-bank interaction force and moment as a function of three parameters which indicate the severity of the ship-bank interaction problem:

- $Fr_h = \frac{u}{\sqrt{gh}}$ Froude depth number, larger is more severe
- $y_b = \frac{B}{2}\left(\frac{1}{y_{port}} + \frac{1}{y_{star}}\right)$ Inverse distance from ship to bank, larger is more severe
- h/T Under keel clearance, smaller is more severe

7.5.2 METHOD

To find out if the nature of ship-bank interaction can be replicated the computational results are compared to two trendlines, published by Vantorre et al. [35] and by Ch'ng et al. cited in [6]. These regression formulas give the sway force and yaw moment as a function of the three parameters mentioned in the previous section. The formulas are applicable to towed ships without including the effect of propulsion.

Additionally the results are compared to potential flow calculations, so that the two numerical methods can be compared to each other. The calculations done with potential flow are described in Appendix A.

The calculations that are done with D-FLOW FM are designed such that they are much like the experiments with which the trend lines were established. This can only be done for one of the trend lines. The trendlines by Vantorre et al. are used because most information was found

about those experimental conditions. The second set of trend lines from Ch'ng et al. is used for comparison.

One of the ships used in the experiments is a model of a container carrier with the following particulars:

Particular	Value
L_{pp} (m)	3.864
B (m)	0.550
T (m)	0.180
C_B (-)	0.588

A container ship with the same particulars will be used in the numerical model. It will be sailing in a rectangular channel of 7 meters wide, the same as was used in the Vantorre experiments. The range of variables that were tested during the experiments will not be exceeded, so that the validity of the trend is ensured.

Variable	Minimum	Maximum
h/T (-)	1.07	1.50
Fr_h (-)	0.00	0.33
y_b (-)	0.00	0.78

For each of the trend lines one of the listed variables is varied from its minimum to its maximum value while the other two are fixed somewhere in the middle of their range.

7.5.3 RESULTS

In Figure 7.18 to 7.23 trend lines that predict the ship-bank interaction force and moment have been plotted. In the same figure the results of a number of computations with D-FLOW FM and ROPES are displayed. This allows the comparison between experimental results, frictionless flow and the newly developed NLSW method. More information on the trend lines can be found in Section 6.3, more about the ROPES calculations in Appendix A.

Note that in the figures of this section the interaction force has not been non-dimensionalised, nor in the rest of the report. This is done because non-dimensionalisation would imply that the result is scalable. In this report it is made likely that the absolute under keel clearance is of importance to the interaction force, so that the results cannot be scaled with the standard $\frac{1}{2}\rho V^2 LT$. Moreover the Froude number plot would become difficult to interpret, since both axes would become a function of velocity. To help put the interaction effects in to context the comparison is made with a model sized container carrier of the same dimensions that sails in deep open water under a drift angle of 6 degrees. In such a case the container carrier model would experience an approximate side force of 0.5 N and moment of 1.4 Nm[1].

Figure 7.18 and 7.19 display the behaviour of sway force and yaw moment as a function of under keel clearance.

[1]This information comes from measurements on a benchmark hull form of a container carrier (KVLCC2) found in [25]

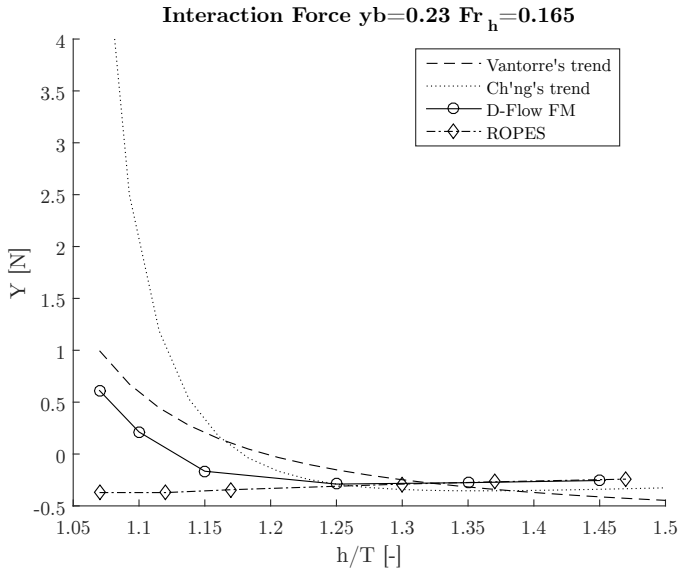

Figure 7.18: Modelling the influence of under keel clearance on sway force

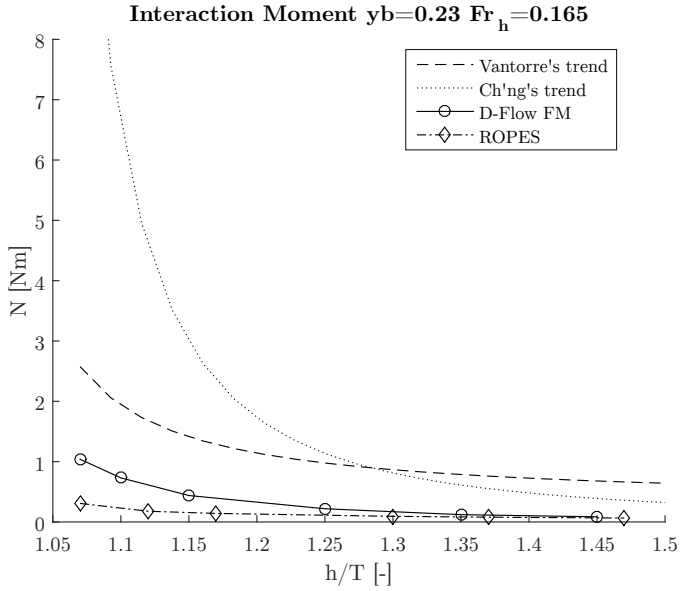

Figure 7.19: Modelling the influence of under keel clearance on yaw moment

Figure 7.20 and 7.21 show how the distance to a bank influences the interaction, the dimensionless y_b increases when a ship sails closer to a bank.

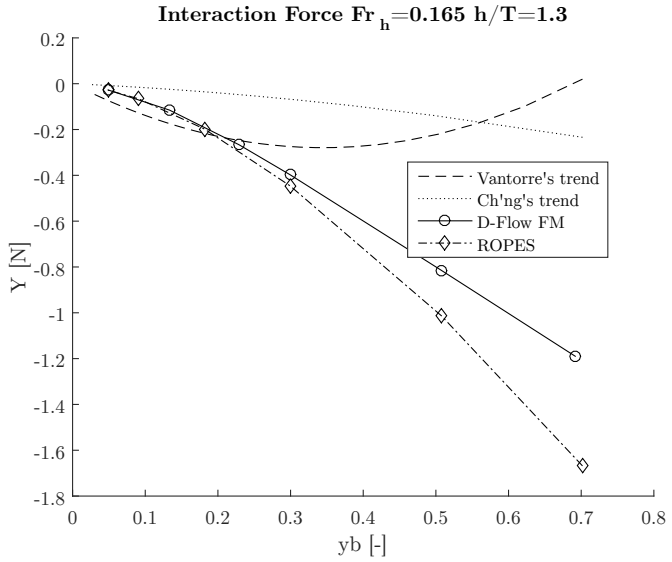

Figure 7.20: Modelling the influence of distance to bank on sway force

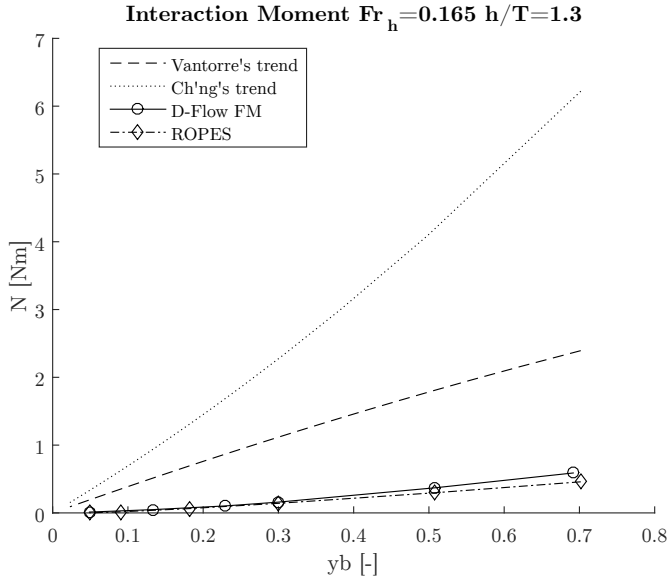

Figure 7.21: Modelling the influence of distance to bank on yaw moment

Figure 7.22 and 7.23 show the dependency on the Froude number.

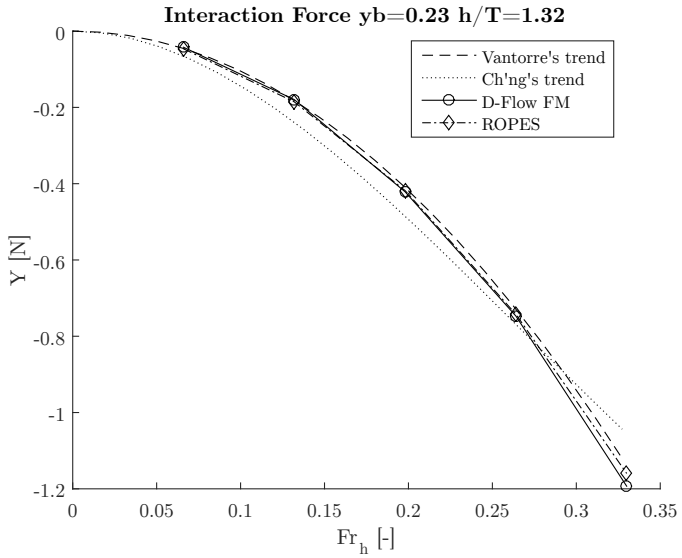

Figure 7.22: Modelling the influence of velocity on sway force

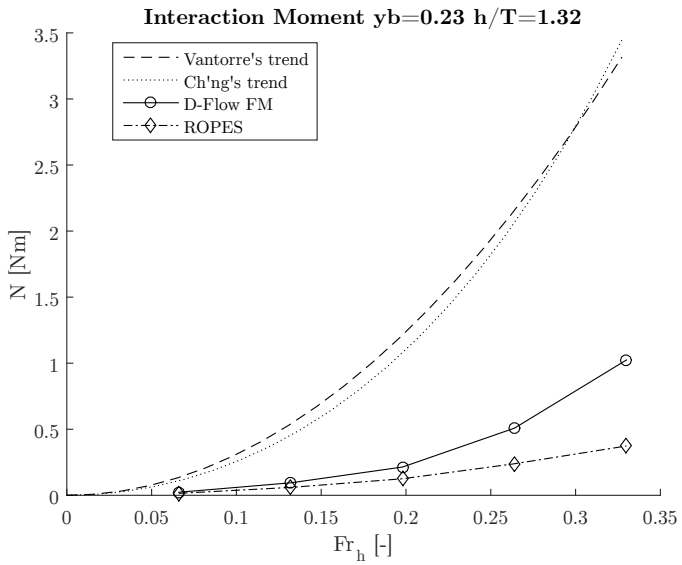

Figure 7.23: Modelling the influence of velocity on yaw moment

Figure 7.24 and 7.25 display the transient behaviour of sway force and yaw moment on a ship while it sails past a bank. The calculation for the numerical result is done in D-FLOW FM. The measurements come from Case E which is discussed in Section 7.4.3

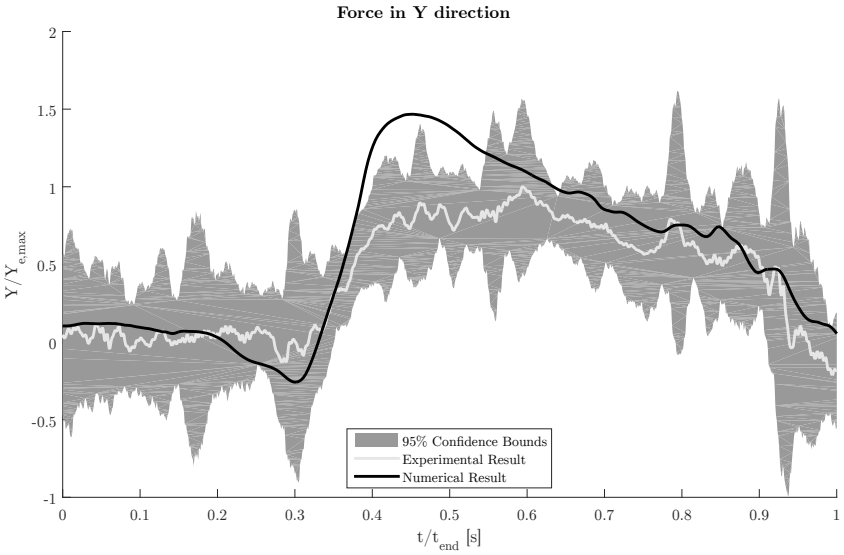

Figure 7.24: Transient behaviour of sway force during Case E

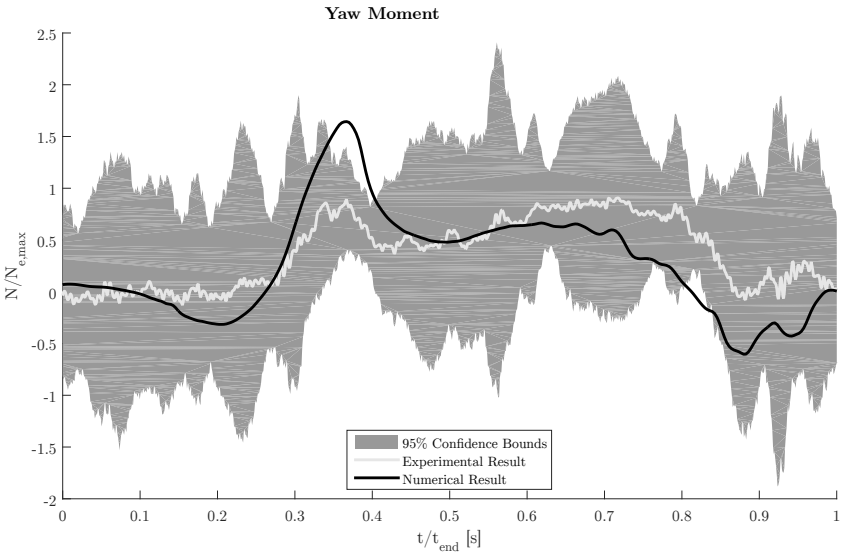

Figure 7.25: Transient behaviour of yaw moment during Case E

7.5.4 DISCUSSION

The influence of under keel clearance

In Figure 7.18 both trendlines show that when the under keel clearance of a ship becomes small the sway force changes in sign. It is also seen that the potential flow calculations with ROPES fail to describe this, indicating that a viscous or free surface effect is responsible for the change in sign.

D-FLOW FM does predict the change in sign, though later than the trendlines indicate. It does however make it likely that the right mechanism has been modelled. This mechanism is the flow blockage due to the boundary layer of the ship extending to the bottom. The way that this is modelled is described in Section 4.3.2. Although the repulsion effect is underpredicted this result shows that using simple models for viscous effects improvements can be made to the prediction of ship-bank interaction forces.

The interaction moment is heavily underpredicted by both D-FLOW FM and ROPES. This is something that is also seen when the interaction moment is plotted as a function of the other variables in Figures 7.21 and 7.23. Due to viscous effects that are modelled in D-FLOW FM the predicted moments are consistently higher than what the frictionless code predicts, though not high enough.

An attempt will be made to explain the lack of bow away moment using the working hypothesis from Section 2.1. It is seen that even when the interaction force agrees with the trends, the moment is still underpredicted. This indicates that a physical mechanism that causes a moment but not a force is wrongly modelled. This mechanism might either be the lift induced moment, or bow wave asymmetry, which possibly causes a lot larger moment than it does a force. Both of these effects cannot be predicted using ROPES which is frictionless and uses the rigid lid assumption.

The trend lines show that when the under keel clearance becomes small the bow away moment increases whereas bank suction turns into repulsion. Bank suction indicates that the flow on the bank side of the ship flows faster than on the channel side, which will also cause lift. However, because a repulsive force is found it is improbable that the increase in moment is due to lift. The most likely cause behind the discrepancy in predicted and simulated moment is therefore a modelling error related to bow wave asymmetry.

It may very well be that in addition to the error related to the bow wave there is also an error related to lift. In cases where the bow wave is not expected to be as important (deeper water), the computed yaw moment is still too small. This indicates that the locally increased friction force that is used to model the influence of side walls is too much of a simplification. Figure 4.7 shows that at the ship's vertical side walls in the middle of the ship both negative and positive vorticity is created. This indicates that modelling the friction 'on top' of the flow does not lead to good results. At the towing tank wall (bottom of the figure) only positive vorticity is found in the region next to the ship. Modelling the side walls of a ship more like the side walls of the towing tank will probably improve results.

The influence of distance to bank

In Figure 7.20 and 7.21 it is seen that both trendlines disagree on the relation between distance to bank and the interaction effect. The suction force is overpredicted by both numerical solvers. A physical mechanism that would explain the character that the numerical solvers predicts is Bernoulli wave asymmetry, see Section 2.1. As the ship sails closer to the bank the flow area between ship and bank becomes increasingly narrow. Due to the assumptions in ROPES the flow will reach large speeds in this region causing a low pressure and an unbounded increase in suction force.

In reality viscous and free surface effects will begin to play a role that limit the increase in velocity and therefore in bank suction. From the trend predicted by Vantorre it would appear that there are two competing mechanisms, one that wins at lower values of y_b causing suction, and one that wins at higher y_b causing repulsion. The first mechanism is the Bernoulli wave asymmetry, a good candidate for the latter is bow wave asymmetry. The asymmetry of the bow wave increases as the ship gets closer to the bank, which would explain both the increase in moment and force and why ROPES fails to predict it.

The influence of Froude depth number

The influence of forward speed is perhaps simplest to predict, since both D-FLOW FM and ROPES are able to predict the quadratic nature shown in Figure 7.22. The trend line by Ch'ng has squat effects contained in the dependency on velocity, which is why it deviates from the other lines.

The underprediction of the moment in Figure 7.23 could be due to a miscalculation of lift or bow wave asymmetry or a combination of both.

Transient behaviour of force and moment

A large advantage of using a time-domain numerical model to solve for ship-bank interaction effects is that a transient behaviour of interaction forces can be predicted by taking into account arbitrary changes in bank geometry. This is a lot harder to do with tabulated interaction data because those are often based on tests with steady conditions. Therefore it is interesting to see if the developed method can predict transient behaviour well.

The time dependent behaviour of the interaction moment and force predicted by D-FLOW FM shown respectively in Figure 7.24 and 7.25 agrees in shape with what was measured during the experiments. When the bow of the ship approaches the bank a small suction force and even an inward moment are found as the return current speeds up between the front of the ship and the bank. After this a large bow away moment is found which is caused by the bow cushion effect. This effect seems to be overpredicted by the numerical model. The transient effect from the sudden appearance of the bank dies down while the ship sails along it. During this time a repulsive force and a bow away moment act upon the ship. When the ship has passed the bank both the sway force and yaw moment disappear.

What is striking is that this time the repulsive force and the yaw moment are not underpredicted as they were in the trendlines. This test was however done with completely different

circumstances. Extreme velocity, super critical flow and the addition of a large $Vicushi p$ to keep the pressure field stable may all have contributed to the difference in prediction.

The bow wave in these cases is also a lot longer than it is at lower speeds, compare Figure 7.5 and 7.12. The longer bow wave can be represented better than the short one which could also explain why in this case the moment and force are not underpredicted.

In General

From the results shown it can be seen that the prediction made by D-FLOW FM follow those made by the potential flow code ROPES in the mildest regions. At low speeds, large distances from the bank and deep water viscous effects are unimportant and it appears that the developed method is just as good as ROPES is in solving those cases. When viscous effect do become important the predictions by D-FLOW FM start to deviate from the potential flow results and in those cases the predictions are always better than those done by ROPES.

By including an estimation for skin friction at small under keel clearances the trend of suction turning into repulsion can be reproduced in D-FLOW FM. This shows that including large scale viscous effects within the moving pressure field method can lead to better predictions of ship-bank interaction.

However the simulations are not satisfactory over the whole range. For example the influence of distance to bank is not predicted well. Moreover the bow away moment is almost always underpredicted by D-FLOW FM. The reason why this occurs is probably because D-FLOW FM does not represent the bow wave well because the wave is too short. For short waves the assumption of shallow water is not valid and therefore by using the shallow water equations it is impossible to resolve them. Another reason why the bow wave may not be represented well is that the boundary condition of the ship's hull cannot be strictly enforced in the current model. The bow needs to be smoothed to avoid instabilities the stagnation of flow where it meets the hull is not explicitly enforced. This 'soft' boundary condition may also be a reason behind the misrepresentation of bow wave asymmetry. This misrepresentation may very well be the modelling error that is most responsible for the inability of the developed method to predict the right bow away moment and the influence of distance to bank.

Other possible modelling errors are the incorrect modelling of lift induced moment due to the simplicity of the modelled side wall friction. Also not much attention was given to the choice of turbulent parameters, a better study of turbulence modelling may result in better simulations.

Computation times

Although the words 'real-time simulation' have appeared multiple times in this report it has thus far not been discussed how fast the model really is. The reason for this is that it greatly depends on the situation, which makes it hard to really quantify the speed of the model. The discussion on computation times will therefore not be very specific.

For the calculations done within this chapter the computation times of ROPES and D-FLOW FM were of the same order. On the CORE I7-4700MQ laptop computer that was used for these computations a typical computation was 4 times slower than real-time. Note that the computations were done at model scale. For full scale calculations computational times will hardly increase

whereas the physical time scale does. This means that for full scale computations a real-time solution is more easily obtained.

The considered scenario gives ROPES an advantage because a quay wall and flat bed can be represented as boundary conditions in the potential flow code. Conversely a varying river or harbour geometry will need to be modelled with panels which will increase computation times greatly. In such a scenario it is expected that the NLSW model will be much faster than boundary element methods.

For the NLSW model the computation time is related to the distance that is travelled by a ship, because the time step is chosen smaller when the ship increases its speed. For this reason simulations for a fast ship on the same grid are relatively slower than calculations at low speeds.

In very simple cases with a large domain a boundary element method such as ROPES may be faster than the NLSW model. But in the more complicated cases the NLSW model can be expected to be faster. Because of the relative simplicity of the NLSW model the amount of computational power required for doing real-time calculations is not unreasonable.

8 CONCLUSIONS AND RECOMMENDATIONS

The objective of the study has been to develop a method to predict ship-bank interaction. The method that was created performs well enough to be useful in the design of entrance and navigation channels. It can also be used to make initial computations on flow fields beneath ships sailing in narrow and confined waterways, which is useful in investigating ship induced erosion on river beds. The model is simple enough to be suitable for real-time computations, depending on the size of the domain, requirements on numerical accuracy and available computation power.

The developed method makes use of a two-dimensional hydrostatic non-linear shallow water (NLSW) flow model to compute the flow field in a ship-bank interaction problem. The advantage of this model is that large scale viscous effects and the effect of free surface can be included while keeping computational requirements low.

The ship is represented in the flow model by modelling its displacement with a moving pressure field. A crude estimation of skin friction based on analytical solutions of idealised flow conditions is implemented to model the flow blockage at small under keel clearances.

The method that has been developed in this thesis has passed numerical verification. To compute the interaction force and moment with sufficient numerical accuracy approximately 3400 grid cells are needed to represent the ship. The recommended time step is such that the ship crosses a grid cell in two steps at nominal speed. In Chapter 5 this resolution amounts to an estimated numerical accuracy of approximately 8 percent.

In the case used for verification viscous and free surface effects are negligible. In absence of analytical solutions the converged solution is verified by comparing it with the solution of the potential flow solver ROPES. The converged result deviates only 1.12%, proving the correctness of the modelling technique.

Comparison with experimental results indicates that the model can be used to predict near and far field velocity and pressure with acceptable accuracy. The results of measurements of the flow field during ship-bank interaction experiments have been compared to the output of the numerical model. Although no formal validation was done good correspondence was found between them.

The interaction effects predicted by the new method are equivalent to those predicted by the potential flow method in cases where free surface and viscous effects are not important to ship-bank interaction. The developed method outperforms potential flow code especially at very small under keel clearances. By taking into account the flow blockage between ship bottom and river bed the prediction of sway force has significantly improved.

Despite efforts to implement skin friction at the sides of the ship, both the NLSW model and potential flow code fail to predict the right magnitude of yaw moment. In addition to the yaw

moment it was found that other results did not always agree with experimental observations. In those cases modelling errors are most likely responsible for this discrepancy. The modelling errors that are currently present in the model are listed below:

- When local Froude numbers exceed 1 near field quantities cannot be accurately resolved because waves interfere with the moving pressure field.
- Ship forces in the sailing direction do not converge in time. As the pressure field moves through a grid it causes slight oscillations in the flow field that are related to the time step size. These oscillations show up during force calculation in the direction of sailing.
- The model underpredicts the external yaw moment in almost all cases. The way in which skin friction is currently implemented in the model is too much of a simplification to predict the right amount of lift.
- The model underpredicts the yaw moment and cannot predict the sway force when the bow cushioning effect is large (i.e. the combination of small under keel clearance and small distance to bank). Most likely the bow wave is misrepresented because it is a short wave that cannot be solved under the assumptions of shallow water flow.
- When large portions of the bank become dry due to the water level draw down caused by the ship, the flow field near the dry portion is not resolved correctly.

Even though modelling errors are present, the developed method is well usable as an alternative to time-domain potential flow codes. Since it performs better at small under keel clearances and is better suited to model complex river/harbour geometries it is expected to be a useful tool for example in the design of entrance channels.

The computed depth averaged flow field beneath a ship resembles the flow near the river bed well, it can therefore be used to make quick computations on ship induced sediment transport.

In general the model does not perform well enough to be used in a manoeuvring simulation loop, the aforementioned modelling errors limit the applicable range and the ship-bank interaction moment cannot be predicted. Moreover requirements on the grid mentioned in Chapter 5 make it impossible for a ship to navigate a domain freely without creating inconsistencies in the discretised hull shape. However if the modelling errors that were addressed in this thesis can be resolved then the applicable range can be extended. Moreover when the computational domains of ship and surroundings can be decomposed the requirements on the grid are lifted. It is therefore recommended to continue the development of the method so that in the future a coupling with a manoeuvring simulator can be achieved. Based on the findings in this thesis the following recommendations can be made regarding the further development of the NLSW model:

- Decomposing the domain of ship and river.

  One of the domains moves together with the ship whereas the other, which represents the waterway, stays fixed. There are a couple of reasons to decompose the flow field in two domains. One of them is that the grid on which the ship is discretised needs to be much finer than the grid of the surrounding river. When the ship sails through a single grid this means that the entire path that the ship takes needs to be refined to the appropriate grid size which results in unnecessary computation time.

For the best solution a ship also needs to be placed in symmetry with respect to the grid which means the grid has to be designed around the path that the ship takes, which isn't always known in advance. If the domains are decomposed the ship can have its own grid that fulfils the requirements so that the surrounding waterway grid can be chosen freely.

Another great advantage of giving the ship its own domain is that the pressure field no longer needs to move with respect to a grid which alleviates the interpolation and forcing errors that were addressed in Chapter 5.

- Creating a better approximation of the boundary condition at the ship's hull.

  It was found that at high Froude numbers the method as it is now cannot be used because the pressure field that represents the ship is counteracted by wave pressure. This problem limits the usage of the developed method.

  There are ways to make sure that the shape of the ship stays intact longer, some of those techniques are used by other authors in Section 4.1. The pressure field can be determined such that it compensates for waves. This way the indentation of the water surface stays equal to the hull shape. Another technique is to artificially make the surface area of grid cells above the ship very small. This causes the pressure to rise very quickly on those cells so that the flow beneath the ship resembles a pressurised flow. This is technique is called the Preissmann slot and is used to simulate mixed (pipe) flows with the NLSW equations[1]. The best option however, is to strictly enforce the boundary condition by prescribing a water height at the ship's location. This can only be done by solving a different set of equations on a separate domain.

- Applying a non-hydrostatic pressure correction to be able to simulate shorter waves.

  It was found that the character of ship-bank interaction when ships come increasingly close to a channel wall were not represented well in the current model. In this situation the bow-cushioning effect is expected to be important. Therefore a likely cause behind this modelling error is that the bow wave is too short to be represented accurately by the NLSW equations. However these equations can be extended with a non-hydrostatic pressure correction which makes it possible to resolve shorter waves. Further tests with such a correction could indicate if indeed the bow wave is responsible for the modelling error.

- Investigate the modelling of lift and separation.

  The increased skin friction at cells that contain the side wall of a ship appears to be too crude of an estimation to correctly model lift. If the way in which side walls bring vorticity into the flow is modelled more accurately this shall improve the prediction of the bow away moment. Moreover in this thesis only a very quick analysis of turbulence modelling was given. Because of time restrictions turbulence modelling was done with an educated guess rather than a thorough analysis. However the modelling of turbulence is expected to be of influence to the accuracy of results in the more severe interaction cases. For these cases it may be beneficial to adopt more advanced shallow water turbulence models than the Smagorinsky model.

[1] In fact, it was attempted by the development team of D-FLOW FM to adopt this technique during this thesis. But due to time constraints it did not become operational.

A POTENTIAL FLOW CALCULATIONS

A.1 INTRODUCTION

A well known method that is often applied in ship hydromechanics is to solve the Euler equations using a boundary element (panel) method. Because the velocity field in these methods can be described by a potential function, it is often referred to as potential flow. Potential flow calculations have previously been done to solve for interaction forces, which works well in situations where viscous effects are insignificant and at relatively low Froude numbers. In this chapter a time-domain potential flow model is applied to solve ship-bank interaction forces in a range of situations. The goal is to find out in which of these situations potential flow is an effective tool, and in which cases it falls short.

The severity of a ship-bank interaction problem can be expressed in the following three parameters:

- $Fr_h = \frac{u}{\sqrt{gh}}$ Froude depth number, larger is more severe
- $y_b = \frac{B}{2}\left(\frac{1}{y_{port}} + \frac{1}{y_{star}}\right)$ Inverse distance from ship to bank, larger is more severe
- h/T Under keel clearance, smaller is more severe

So it can be expected that at low Froude depth numbers, with a large distance to the bank and an under keel clearance that is not too small one can obtain a good answer with a potential flow approximation. To investigate in which situations the potential flow assumption is valid data of ship-bank interaction in temperate conditions is needed. In this chapter trendlines published by Vantorre et al. [35] and by Ch'ng et al. found in [6] are used for comparison. These regression formulas are valid at a range that starts at mild conditions and are applicable to towed ships without including the effect of propulsion.

A.2 APPROACH

The regression formulations are based on experimental results that were found for a number of specific ships, and are as such expected to be most reliable when using one of those ships for comparison. To maximise the accuracy of the regression formulation the conditions under which they were obtained are adhered to as close as possible. Because most information is available about the experimental conditions that were used to obtain the formulae presented by Vantorre et al. the test cases are designed to follow those conditions. The second set of trend lines from Ch'ng et al. is used for comparison.

One of the ships used in the experiments is a model of a container carrier with the following particulars:

Particular	Value
L_{pp} (m)	3.864
B (m)	0.550
T (m)	0.180
C_B (-)	0.588

A container ship with the same particulars will be used in the numerical model. It will be sailing in a rectangular channel of 7 meters wide, the same as was used in the Vantorre experiments. The range of variables that were tested during the experiments will not be exceeded, so that the validity of the trend is ensured.

Variable	Minimum	Maximum
h/T (-)	1.07	1.50
Fr_h (-)	0.00	0.33
y_b (-)	0.00	0.78

The numerical model that is used to replicate the trend lines is called ROPES. ROPES is a 3D time-domain potential flow model developed to predict ship-ship interaction forces in shallow and confined water. It's main purpose is to evaluate mooring loads of ships moored in ports. The model output is a record of the 6 forces and moments as a function of time. This plus the fact that shallow water and confined water can be modelled makes ROPES suitable to perform interaction calculations. The simplifications that are made to the flow are that the fluid is frictionless and free surface effects are neglected. The latter is known as double-body flow. These assumptions allow for speedy computation, making this code potentially fast enough for real-time simulation.

Three lines will be used to test the ability of ROPES to predict the influence of each of the three variables. In each of the three lines one of the variables is varied from its minimum to its maximum value, while the other pair is kept constant at a medium value. Subsequently an indication can be given under which conditions a time-domain double-body potential flow code can provide an acceptable answer to ship-bank interaction problems. Of course if ROPES is unable to make the right predictions that does not necessarily mean that potential flow methods in general are unsuitable, but it can provide a good indication.

A.3 RESULTS

A.3.1 INTERACTION FORCE

As is immediately apparent from Figure A.1 the interaction forces are hard to predict even experimentally. The trends as predicted by Vantorre and Ch'ng deviate a lot from each other, and even predict a different sign when the distance to the bank becomes small. It should be noted that it is not known how far the validity of Ch'ng's trend extends. More trust should be put into the predictions by Vantorre et al., because their range of parameters is followed. In the modelled case, for distances larger than 1 meter ROPES stays in between the two predictions. When the ship sails closer to the wall ROPES keeps predicting an increasingly larger suction force, where it is known in reality a repulsion will occur.

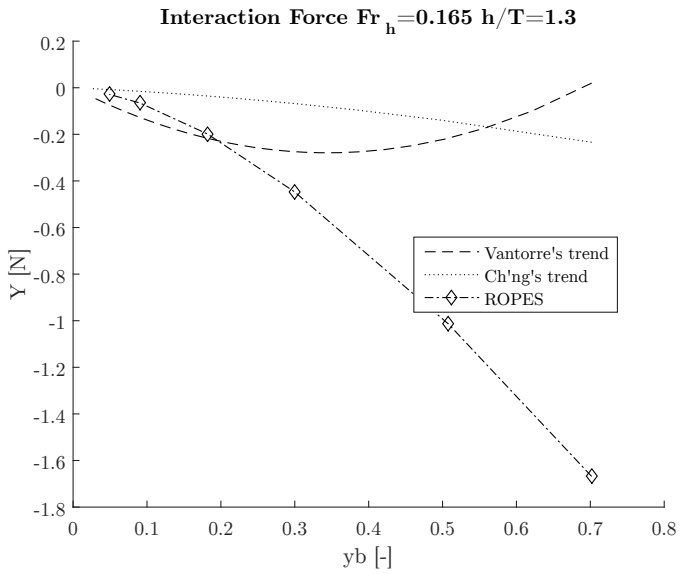

Figure A.1: Y as a function of distance to bank

The effect that an increase of Froude depth number has on the interaction force is well represented by ROPES. The fact that the predicted values follow the Vantorre line better than Ch'ng's predictions is because of squat effects. Squat is not present in the ROPES calculation because it calculates with a fixed under keel clearance. The effect that squat has on the interaction force is included through Froude number dependency in Ch'ng's formulation, so it deviates more from the computed results than Vantorre's predictions from which squat effects have been excluded. It can be excluded because it is expressed by an effective under keel clearance variable.

As the keel clearance decreases both regression formulations predict a sharp increase of interaction force. However ROPES fails to reproduce this behaviour. It can be concluded from Figure A.3 that it is not advisable to use ROPES for under keel clearances smaller than 130% of the ships draught.

A.3.2 INTERACTION MOMENT

ROPES is unable to predict an interaction moment caused by a quay wall. Figure A.4 shows that the interaction moment is heavily underpredicted. The reason behind this is that ROPES is designed to predict ship-ship interaction effects. For this kind of interaction the most important contribution comes from the time derivative of the potential which is calculated by ROPES, leading to good results such as in [22]. However the leading cause for the interaction moment in the case of a quay wall is lift. Lift is a viscous effect which is not modelled in ROPES, but should be modelled to obtain a meaningful result.

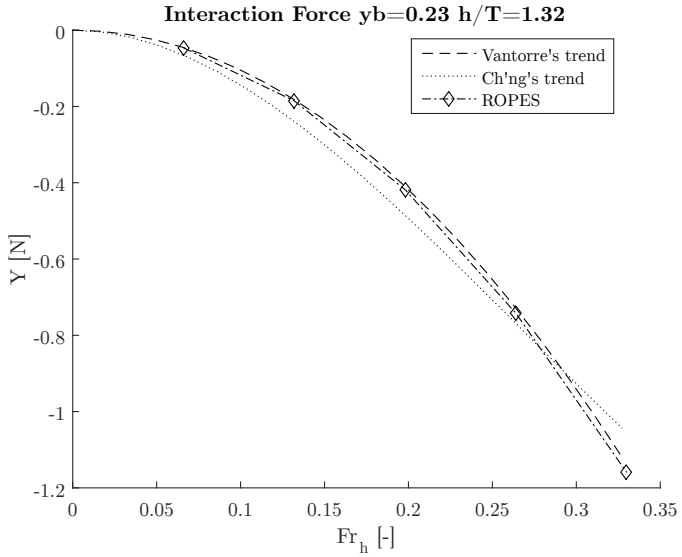

Figure A.2: Y as a function of velocity

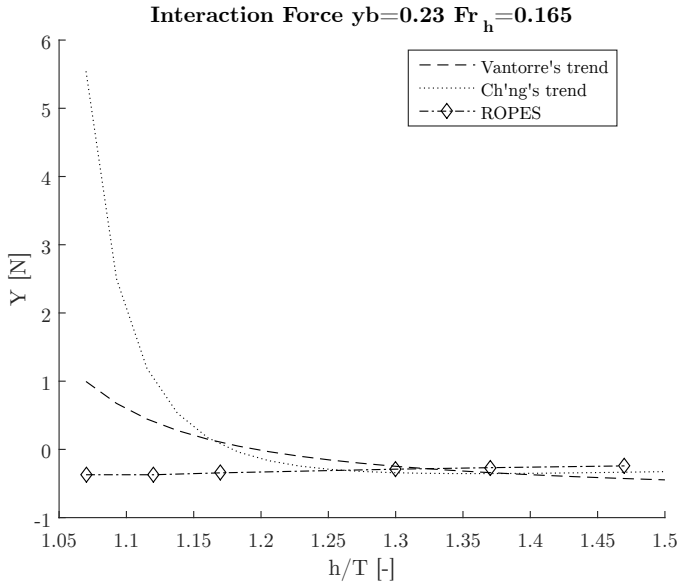

Figure A.3: Y as a function of under keel clearance

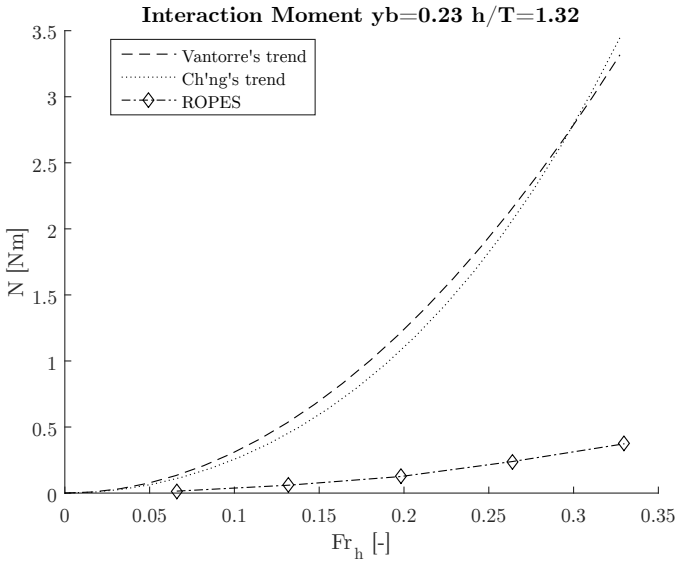

Figure A.4: N as a function of velocity

B EXPERIMENTAL RESULTS

B.1 INTRODUCTION

Model scale experiments have been carried out recently at Deltares with the purpose of investigating ship-induced sediment transport and waves. These experiments have been performed and were analysed in part by Exer [7] who tested an inland waterway ship sailing at small underkeel clearances through a narrow channel. A further analysis of data is given by de Jong. [12]. The experimental conditions include the presence of small banks in this channel, inducing hydrodynamic interaction effects between bank and ship. A part of the experimental data that has not yet been analysed are ship-bank interaction effects that were measured by force transducers in the model ship. In this section an analysis of this part of the data will be performed.

The goal of the analysis is to give further insight in the more extreme ship-bank interaction conditions. Earlier research has indicated that at critical and near critical flow conditions strongly non-linear effects start dominating, the current dataset focusses especially on these conditions. The experiments have been performed with relatively short banks ($\frac{1}{2}$ $\frac{1}{4}$ and $\frac{1}{20}$ times the ship length) so that transient effects can be investigated. Furthermore the experiments are intended as validation and or calibration material for numerical simulations. A presentation and discussion of the experimental results will be given in section B.2. A treatment of uncertainty will be given in section B.3

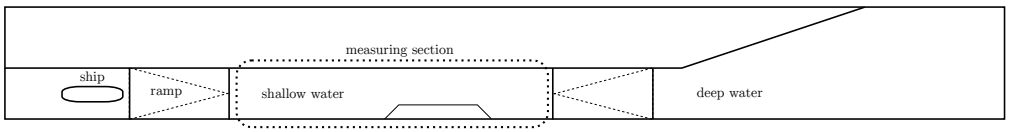

Figure B.1: Overview of the towing tank layout used in [7]

The experiments entailed towing a simplified model of an inland ship through a narrow towing tank, see Figure B.1. The ship model was rigidly connected to the towing structure. At some point during its track the ship encountered a bank adjacent to one of the tank walls. During the encounter the forces absorbed by the force meters that were mounted in the rigid connection were measured. The total amount of force and corresponding moment that was needed to keep the ship in place are the quantities of interest. They are non-dimensionalised as in Equations B.1 and B.2.

$$Y_{bank} = \frac{Y(t)}{\frac{1}{2}\rho V_{rel}^2 LT} \tag{B.1}$$

$$N_{bank} = \frac{N(t)}{\frac{1}{2}\rho V_{rel}^2 L^2 T} \tag{B.2}$$

The relative flow velocity is also measured, by measuring the flow velocity before the run starts and monitoring vessel speed during the run.

The ship is accelerated in deeper water and encounters a ramp just before and just after it encounters a bank. This will induce transient effects that will also play a role in the measured signals. Especially when the bank effects are not dominant it is hard to distinguish them from the influence of the ramps. Additionally oscillations and vibrations that originate from the rigid towing construction are a source of noise that interferes with the bank interaction effect.

B.2 FINDINGS

B.2.1 GENERAL DISCUSSION

In this section the findings from the experimental data will be summarised. There are three effects that can be investigated with the experimental conditions that have been tested:

- The influence of the Froude depth number.
- The influence of bank length.
- The influence of ship position relative to the bank.

In the other subsections these influences will be specifically treated. In this section a general discussion of the findings is done.

The tests performed to investigate bank effects at small Froude numbers are inconclusive. At these circumstances the influence of the bank is barely noticeable compared to fluctuations induced by other effects. At Froude numbers of 0.6 and 0.8 the presence of banks does clearly show up in the results. These tests surpassed the critical velocity, meaning in this context that the ship surpassed the self-propulsion limit. This is caused in part by the narrowness of the channel. At these speeds a bank repulsion force and a bow away moment are found. The maximum repulsion force develops after the midship has reached the bank. The peak in force caused by the bank is related to the length of the bank, at higher Froude numbers the influence of the bank acts over a longer distance. The measurement section was too short to see the further development of this force, it seems to die down after the entire ship has passed the bank, although at that point, the ship is already approaching deeper water.

The bank-induced moment is also indistinguishable at low Froude numbers. At the supercritical speeds a small initial bow-in moment is measured as the ship approaches the bank. A bow away moment develops as the bow passes along the bank and reaches its maximum approximately when midship aligns with the bank. As the aft ship approaches the bank the moment decreases sharply again. In the case of long banks the moment restores afterwards, in case of short banks a second peak is found after aft ship leaves the end of the bank. Further development of the moment cannot be investigated as the measurement section ends there.

B.2.2 THE INFLUENCE OF FROUDE NUMBER AND BANK LENGTH

Figures B.2 to B.4 show the ensemble averaged results of experiments. Confidence bounds have been omitted for clarity. The figures have the non-dimensionalised side force on the y-axis and position of the middle of the ship within the measurement section on the x-axis. The x-axis starts at the moment that the very front of the ship reaches the very beginning of the bank. In light grey it is indicated where the bank starts and ends. The axis ends at the point where the measurement section ends. At this point the bow of the ship reaches a ramp down to deeper water. The ship length itself is 3 meters.

The measurement section starts at a distance of 0 meters. At this distance the ship reaches shallow water and the flow starts to develop. It is therefore possible the flow has not developed fully at the first meters of the measurement section.

Because the ship has different velocities at the different Froude depth number (the depth was kept constant) the corresponding time signals have been stretched. This causes the measured force to seem much more oscillatory for the low speeds than for higher speeds. The same cut-off frequency has been used for all the signals.

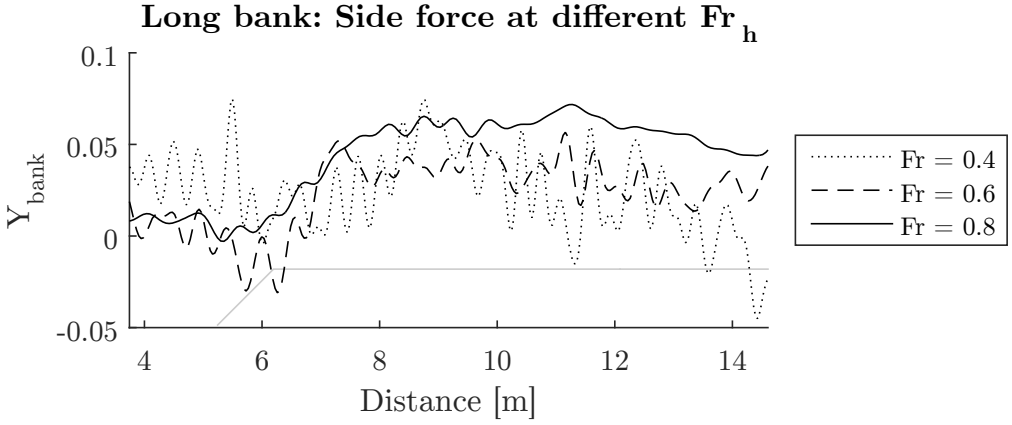

Figure B.2: Measured Y_{bank} along a long bank

In figure B.2 the results for the longest bank are shown. The lowest Froude number shows the least correlation with the bank geometry. In this case other effects than ship-bank interaction are apparently the dominating influence. This is much more so the case for the results at $Fr_h = 0.2$, these results have not been plotted because they show even less correlation with the bank and would obfuscate the other other data. It can be seen that at the highest Froude number the side force takes a longer distance to develop than at lower speeds. Once the side force develops the highest force coefficient is found for $Fr_h = 0.8$. In figure B.3 the results for a shorter bank are shown, the figure shows here that because at a high Froude number the force has no time to develop, Y_{bank} is greatest at $Fr_h = 0.6$. The same is found for all the short banks. At a distance of 15 meters where the measurement section ends the side force is still present even when the ship has already passed the bank, further development of the force cannot be investigated as the

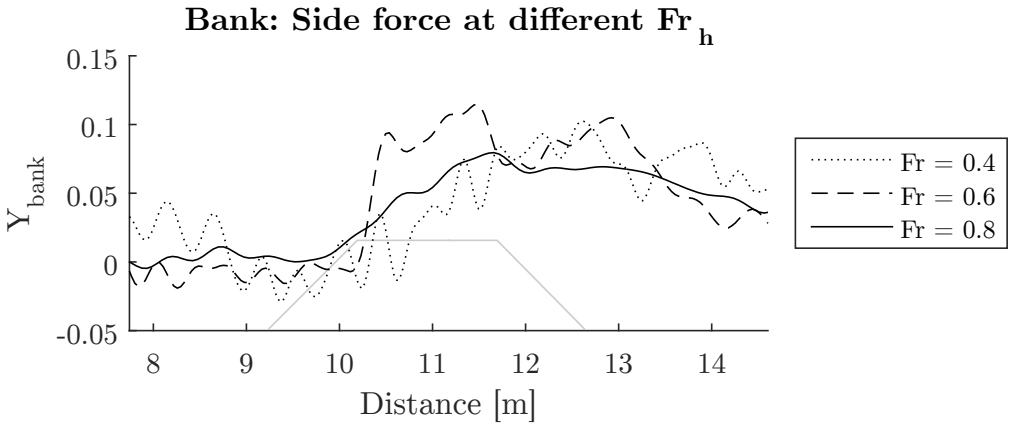

Figure B.3: Measured Y_{bank} along a bank

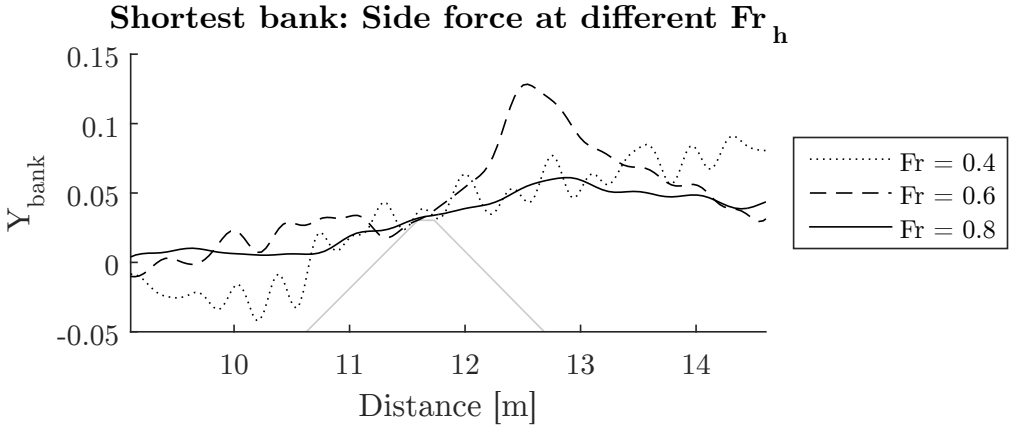

Figure B.4: Measured Y_{bank} along a short bank

measurement section ends there.

Figure B.5 and B.6 display the yaw moment that the model ship undergoes when it sails along the banks. Again for $Fr_h = 0.4$ there seems to be no clear relation between the moment and the bank geometry. There may be an initial bow-in moment when the ship nears the bank, the result is not very conclusive but since such a bow-in moment near a bank is potentially dangerous it is worth some attention. When the ship sails past the slope of the bank it experiences a peak in bow away moment. This peak may be attributed to the hydrodynamic cushioning effect mentioned in literature. The effect is transient, after it has passed the moment builds up again. This is also true for the shorter banks where a second peak builds up till the end of the measuring section.

B.2.3 THE INFLUENCE OF SHIP POSITION

All the experiments that have been done with banks have been repeated with two ship positions. One of the positions is in the centre of the towing tank, the other position is as closely to the bank

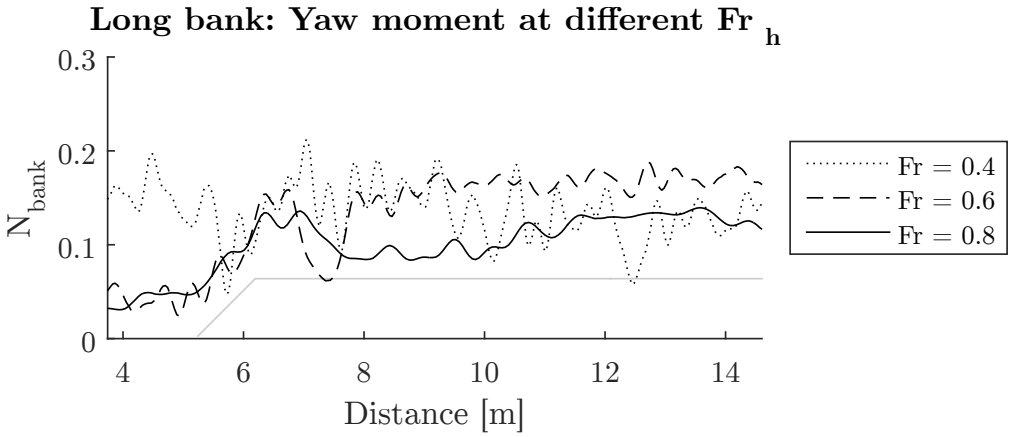

Figure B.5: Measured N_{bank} along a long bank

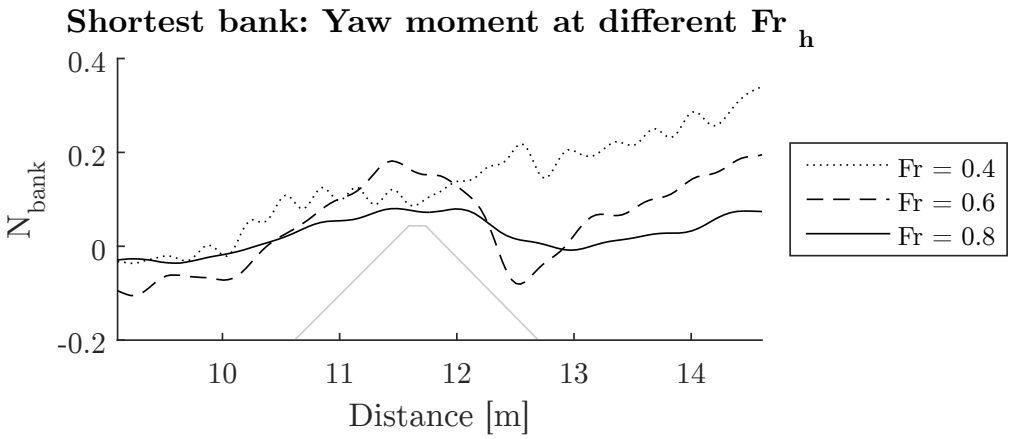

Figure B.6: Measured N_{bank} along a short bank

as possible. Figure B.7 and B.8 show the development of force along a bank for both positions. Generally the force coefficient is a little higher for the position closer to the bank, which is to be expected. However it is hard to quantify just how much more influence there is due to the fluctuating nature of the measured force.

In figure B.9 the dimensionless moments close and near the bank are plotted in otherwise the same conditions. The magnitude of the moment increases when the ship is very close to the bank, the nature of the excitation stays roughly the same. Once again it is hard to put a fair number on how much the moment has increased. Further experimentation or numerical simulation may be desired to answer this question.

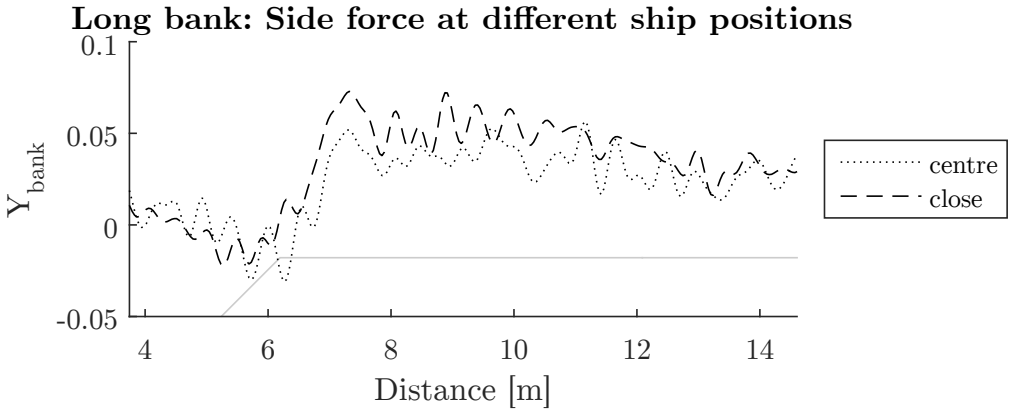

Figure B.7: Measured Y_{bank} at $Fr = 0.6$

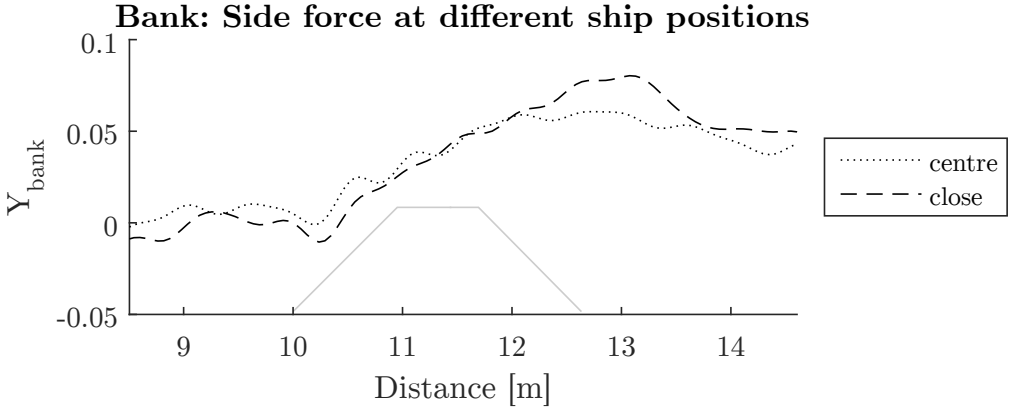

Figure B.8: Measured Y_{bank} at $Fr = 0.8$

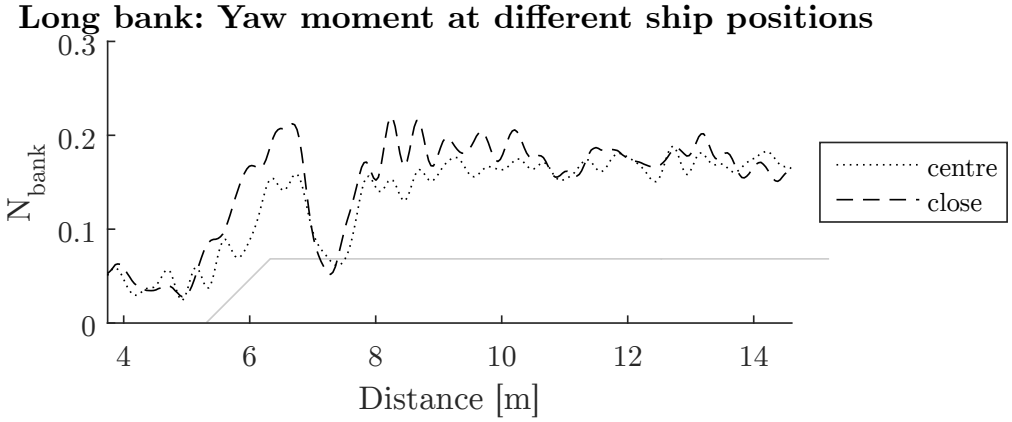

Figure B.9: Measured N_{bank} at $Fr = 0.6$

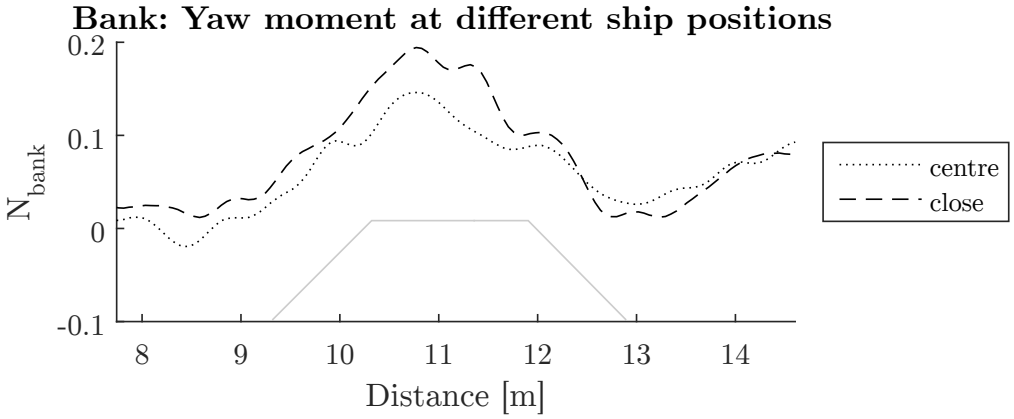

Figure B.10: Measured N_{bank} at $Fr = 0.8$

B.3 UNCERTAINTY ASSESSMENT

B.3.1 INTRODUCTION

Before any conclusions regarding the results of the experiments can be drawn, it has to be established how accurately the results of the experiments approach the values that would have been obtained in an ideal situation. For this reason an uncertainty assessment will be performed. Uncertainty knows two aspects that have to be assessed; precision and bias. The precision limit has to do with scatter, precise measurements yield the same result when repeated. The bias limit has to do with offset, a bias is the same for similar measurements, but causes a constant deviation from the true value. Very precise measurements can be inaccurate when there is a large bias. Unbiased experiments can be inaccurate when precision is poor.

B.3.2 ESTIMATING PRECISION

The preciseness of a measurement can be determined by performing the same measurement multiple times. Errors in precision can be caused by a large variety of causes, therefore assuming a Gaussian distribution of the measured values can be justified. The same conditions were repeated 4 or 6 times during the experiments of Exer. Due to water movements left over from earlier runs, mechanical oscillations, turbulence and other random effects these measurements differ from each other. In this subsection the statistical analysis used to determine a precision limit is explained.

The quantity of interest is the measured interaction force denoted as $Y_m(t)$, which is a function of time. The individual measurements $Y_{m,i}(t)$ are time-locked by aligning pulse signals at the start of each run, so that at each moment in time the ship can be assumed to have been in the same position with the same speed. Under these assumptions the real value of the interaction force $Y(t)$, defined as the force that would have been measured with an infinitely precise measuring device under ideal circumstances, can be approximated as the mean of the measured

time-series. At each of the discrete moments in time p the interaction force is now treated as its own stochastic variable Y_p, so that at all of those moments the precision can be estimated.

As indicated before those stochastic variables can be assumed to have a Gaussian distribution, however due to the small amount of samples that are available (4 to 6), the variance of these measurements can not be expected to be equal to the variance of the corresponding Gaussian distribution. To account for the uncertainty of the variance of a small sample size the t-distribution is used. The procedure to determine the precision limit is now as follows:
Estimate each Y_p as the mean of n measurements

$$Y_p = \overline{Y_{p,i}} = \frac{\sum_{i=1}^{n} Y_{p,i}}{n} \tag{B.3}$$

with an estimated sample standard deviation of

$$s_p = \sqrt{\sum_{i=1}^{n} \frac{(Y_{p,i} - \overline{Y_{p,i}})^2}{n-1}} \tag{B.4}$$

so that the standard error of the mean is

$$SE_p = \frac{s_p}{\sqrt{n}} \tag{B.5}$$

With two-sided 95% confidence bounds taken from the t-distribution with $n-1$ degrees of freedom. Most tests were repeated four times so that the double-sided confidence bounds are $\frac{3.182}{2} s_p$ either side of the mean.

B.3.3 ESTIMATING BIAS

The bias of experimental results cannot be exactly measured and has to be estimated. In this section potential sources of bias will be identified and their contribution will be discussed. The estimations of bias will be based partly on calculations, partly on physical arguments and partly on interviews with the person who conducted the experiments. His judgements will be relied on when estimating margins in the construction of the model set up.

The largest bias error will show up in the calibration of the force meters. This is because the force meters have not been calibrated, the calibration must be done in hindsight using zero measurements. The zero-measurements however, show a large amount of variance. This could be due to the ballasting procedure which were adjusted each time the draught changed. An asymmetric distribution of weights might have caused a moment upon the ship and would show up as a side force. Because of this the zero-measurements aren't used to determine the calibration constants, instead the force measured before the ship starts sailing is used. There are 4 readings for the force before the ship starts sailing and the mean of these readings is used. The bias is determined from the sample variance and t-distribution as described in the previous section. The amount of bias coming from the variance of zero measurements is by far the greatest estimable

contribution of bias. Errors in the magnitude of the variables that are used to do the non-dimensionalisation are far smaller but will be briefly addressed in the last part of this section. Within this report the problem of large bias has been dealt with by comparing the relative values of experiments and numerical results, in other words the initial value of force has been calibrated to match the initial value of the numerical solution.

Another source of error is the rotation of the ship due to resistance and side forces. This deformation took place when the ship model was towed at high speeds with a large drift angle, the model would pivot about its support and swerve back and forth in roll motion. This effect is dependant on the force and hard to account or correct for, but can be expected to cause a more significant deviation of results since the effects was visually noticeable during the experiments. Within this report only the tests that were done without a drift angle are used, for which the deformation was not a major problem.

In the following paragraphs the sources of bias that were also considered, but were found negligible are briefly addressed.

The geometrical accuracy with which the ship model was constructed was reported as 1 mm. The worst case scenario would be that the ship is 2 mm longer, 2 mm wider and and 1 mm more deep than reported. However the under keel clearance was determined very precisely, with a reported tolerance of 1 mm. The latter two inaccuracies do not accumulate. This leads to bias errors of at most 0.47% for T (depending on draught) and 0.07% or 0.13% for L and L^2 respectively when non-dimensionalising the data. This is negligible compared to the magnitude of other errors.

The flow velocity is regulated by a weir, and is measured by the measuring device that is furthest away from the influence of ship and bank before the ship starts moving. The ship speed is monitored during the run. From both measurement devices the bias (due to differences in calibration over time) is estimated from the zero-measurements, which amounts to a maximum of 0.9% of V_{rel}^2. These biases are considered negligible.

The water temperature was not measured during the experiments, however the facility is kept at a constant temperature of 20 degrees. The difference in density when the water goes up or down a degree is about 0.04%. This is also negligible.

The ship was mounted into the middle of the channel with great accuracy according to the experimenter. He was confident that the ship was mounted accurate to a millimetre. In case the forces are linear to the inverse of distance to bank as reported by earlier research this millimetre could lead to a bias of 0.11% of the total force. The experimenter reported a tolerance of 0.1 degree for the alignment of both the ship model and the force meters. This will change the measured force only very marginally.

BIBLIOGRAPHY

[1] Acevedo, M. & Mazarredo, L. "Skin Friction and Turbulence Committee" in: *Proc. 8th International Towing Tank Conference (ITTC'57), Madrid, Spain* 1957

[2] Baur, T., Weiler, O.M., & Vossen, B. van "Current forces on moored ships affected by land reclamation for new JadeWeserPort" in: *Third Chinese-German Joint Symposium on Coastal and Ocean Engineering. National Cheng Kung University, Tainan* 2006

[3] Beck, R.F. *Forces and moments on a ship moving in a canal* tech. rep. 1976

[4] Carreño, J.E., Mora, J.D., & Pérez, F.L. "A study of shallow water's effect on a ship's pivot point" in: *Ingeniería e Investigación* 32.3 (2012), pp. 27–31

[5] Chen, X.N. & Sharma, S.D. "A slender ship moving at a near-critical speed in a shallow channel" in: *Journal of Fluid Mechanics* 291 (1995), pp. 263–285

[6] Cordier, S., Hasegawa, K., Hirano, M., Petersen, J., Key-Pyo, R., Traghard, P., Triantafyllou, M., Hover, F., Vantorre, M., & Zou, Z. "The manoeuvring committee final report and recommendations to the 23rd ITTC." in: *23rd International Towing Tank Conference Proceedings, Venice.* 2002, pp. 153–234

[7] Exer, A. "Influence of non-symmetrical flow condition on a sailing vessel" MSc thesis TU Delft, Deltares, ETH Zurich, 2015

[8] Fenical, S., Kolomiets, P., Kivva, S., & Zheleznyak, M. "Numerical modeling of passing vessel impacts on berthed vessels and shoreline" in: *Coastal Engineering Conference* vol. 30 2 American Society of Civil Engineers 2006, p. 1234

[9] Fonfach, J.M.A. "Numerical study of the hydrodynamic interaction between ships in viscous and inviscid flow" MSc thesis Instituto Superior Técnico, 2010

[10] Fujino, M. "Studies on manoeurability of ships in restricted waters" in: *Selected papers from the journal of the Society of Naval Architects of Japan* 4 (1970), pp. 157–184

[11] Hammack, E.A., Smith, D.S., & Stockstill, R.L. *Modeling vessel-generated currents and bed shear stresses* tech. rep. DTIC Document, 2008

[12] Jong, J. de *Interactie gebruik vaarweg en bodemligging* tech. rep. Deltares, 2015

[13] Jong, M. de, Roelvink, D., Reijmerink, S., & Breederveld, C. "Numerical modelling of passing-ship effects in complex geometries and on shallow water" in: *Pianc Smart Rivers* 2013

[14] Kazi, S.A. "Hydrodynamic modelling of vessel-induced water motion using Delft2D-Rivers" MSc thesis IHE Delft, WL Delft Hydraulics, 1998

[15] Koster, J. *Suction effect of canal banks on ship behaviour* tech. rep. WL Delft Hydraulics, 1971

[16] Laforce, E., Vantorre, M., et al. "Experimental determination and modelling of restricted water effects on bulkcarriers" in: *Marine Simulation and Ship Manoeuvrability (The international conference MARSIM). Rotterdam* 1996

[17] Lataire, E. & Vantorre, M. "Ship-bank interaction induced by irregular bank geometries" in: *Proceedings 27th Symposium on Naval Hydrodynamics. Seoul* 2008

[18] Lataire, E., Vantorre, M., Laforce, E., Eloot, K., & Delefortrie, G. "Navigation in confined waters: influence of bank characteristics on ship-bank interaction" in: *International Conference on Marine Research and Transportation, ICMRT* 2007

[19] Lee, C.K. & Lee, S.G. "Investigation of ship maneuvering with hydrodynamic effects between ship and bank" in: *Journal of Mechanical Science and Technology* 22.6 (2008), pp. 1230–1236

[20] Pinkster Marine Hydrodynamics *User manual for Ropes 1.1* 2013

[21] Pinkster, J.A. "The influence of a free surface on passing ship effects" in: *International shipbuilding progress* 51.4 (2004), pp. 313–338

[22] Pinkster, J.A. & Bhawsinka, K. "A real-time simulation technique for ship-ship and ship-port interactions" in: *28th International Workshop on Water Waves and Floating Bodies. L'Isle sur la Sorgue, France* 2013

[23] Rijnsdorp, D.P. & Zijlema, M. "Numerical modelling of interactions between non-hydrostatic free-surface flows and a non-moving floating body" in: *IAHR World Congress* 2013

[24] Robijns, T. "Flow beneath inland navigation vessels" MSc thesis TU Delft, Delft University of Technology, 2014

[25] Rotteveel, E. "Investigation of inland ship resistance, propulsion and manoeuvring using literature study and potential flow calculations" MSc thesis TU Delft, Delft University of Technology, 2013

[26] Rozhdestvensky, K.V. "Ship motions close to a bank or in a narrow canal" PhD thesis Leningrad Shipbuilding Institue, 1981

[27] Sano, M., Yasukawa, H., & Hata, H. "Directional stability of a ship in close proximity to channel wall" in: *Journal of Marine Science and Technology* 19.4 (2014), pp. 376–393

[28] Stockstill, R., Martin, S., & Berger, R. "Hydrodynamic model of vessel-generated currents" in: *Regulated Rivers: Research & Management* 11.2 (1995), pp. 211–225

[29] Talstra, H. *Large-scale turbulence structures in shallow separating flows* TU Delft, Delft University of Technology, 2011

[30] Toxopeus, S. "Practical application of viscous-flow calculations for the simulation of manoeuvring ships" PhD thesis TU Delft, Delft University of Technology, 2011

[31] Toxopeus, S., Simonsen, C., Guilmineau, E., Visonneau, M., Xing, T., & Stern, F. "Investigation of water depth and basin wall effects on KVLCC2 in manoeuvring motion using viscous-flow calculations" in: *Journal of Marine Science and Technology* 18.4 (2013), pp. 471–496

[32] Tuck, E.O. "Hydrodynamic problems of ships in restricted waters" in: *Annual Review of Fluid Mechanics* 10.1 (1978), pp. 33–46

[33] Van Hoydonck, W., Toxopeus, S., Eloot, K., Bhawsinka, K., Queutey, P., & Visonneau, M. "Bank Effects for KVLCC2" in: *5th World Maritime Technology Conference-WMTC15* 2015

[34] Vantorre, M. et al. "Review of practical methods for assessing shallow and restricted water effects" in: *International Conference on Marine Simulation and Ship Maneuverability (MARSIM). Kanazawa, Japan* 2003

[35] Vantorre, M., Delefortrie, G., Eloot, K., & Laforce, E. "Experimental investigation of ship-bank interaction forces" in: *International Conference MARSIM* 2003

[36] Whan, G. & Rothfus, R. "Characteristics of transition flow between parallel plates" in: *AIChE Journal* 5.2 (1959), pp. 204–208

[37] Xiang, X. & Faltinsen, O. "Maneuvering of two Interacting Ships in Calm Water" in: *11th International Symposium on Practical Design of Ships and other Floating Structures.* 2010, pp. 161–171

[38] Zhou, M., Zou, Z., & Roelvink, D. "Prediction of ship-ship interactions in ports by a non-hydrostatic model" in: *Journal of Hydrodynamics, Ser. B* 27.6 (2015), pp. 824–834

[39] Zhou, X., Sutulo, S., & Soares, C.G. "Computation of ship hydrodynamic interaction forces in restricted waters using potential theory" in: *Journal of Marine Science and Application* 11.3 (2012), pp. 265–275

[40] Zhou, X., Sutulo, S., & Soares, C.G. "Simulation of hydrodynamic interaction forces acting on a ship sailing across a submerged bank or an approach channel" in: *Ocean Engineering* 103 (2015), pp. 103–113

[41] Zou, L., Larsson, L., Delefortrie, G., Lataire, E., et al. "CFD prediction and validation of ship-bank interaction in a canal" in: *2nd International conference on ship manoeuvring in shallow and confined water. Trondheim, Norway* 2011